

UNIVERSITY OF CALIFORNIA  
SANTA CRUZ

**VARIATION AND EXTINCTION: MODELS FOR ALTERNATIVE  
STRATEGIES AND CLIMATE**

A dissertation submitted in partial satisfaction  
of the requirements for the degree of

DOCTOR OF PHILOSOPHY

in

ECOLOGY AND EVOLUTIONARY BIOLOGY

by

**Carla M. Sette**

March 2020

The Dissertation of Carla M. Sette  
is approved:

---

Professor Barry Sinervo, chair

---

Professor Rita S. Mehta

---

Professor Suzanne H. Alonzo

---

Professor Daniel Friedman

---

Quentin Williams  
Acting Vice Provost and Dean of Graduate Studies

Copyright © by

Carla M. Sette

2021

## TABLE OF CONTENTS

List of figures .....	v
List of tables .....	vii
Abstract .....	viii
Acknowledgements .....	ix
General introduction .....	1
<b>Chapter 1: A game theoretic framework for assessing stability in large systems of competitors</b> .....	<b>4</b>
Introduction .....	4
Methods .....	8
<i>Estimating payoff matrices</i> .....	8
<i>Game solutions</i> .....	9
<i>Equilibrium types</i> .....	11
<i>Game classification</i> .....	12
<i>Simulations</i> .....	16
<i>Invasion pathways</i> .....	17
<i>Analysis of natural systems</i> .....	17
<i>Other analyses</i> .....	19
Results .....	20
<i>Equilibrium types</i> .....	20
<i>Apostasis, intransitivity and game stability</i> .....	23
<i>Game types</i> .....	27
<i>Ecological examples</i> .....	31
Discussion .....	33
Citations .....	47
<b>Chapter 2: An evolutionary game theory model for plastic developmental strategies of omnivory and carnivory in <i>Scaphiopus multiplicata</i></b> .....	<b>52</b>
Introduction .....	52
Methods .....	58
<i>Quantifying shrimp predation rates</i> .....	58
<i>Describing tadpole morph reaction norms</i> .....	59
<i>Selecting candidate two-strategy <math>W</math>-matrices</i> .....	59
<i>Incorporating the switcher strategy</i> .....	61
<i>Effect of temperature on time to metamorphosis and pond duration</i> .....	62

Results .....	64
<i>Quantifying shrimp predation rates</i> .....	64
<i>Describing tadpole morph reaction norms</i> .....	64
<i>Selecting candidate two-strategy W-matrices</i> .....	65
<i>Incorporating the switcher strategy</i> .....	69
<i>Effect of temperature on time to metamorphosis and pond duration</i> .....	69
Discussion .....	75
Citations .....	82
<b>Chapter 3: Thermal ecology and extinction risk of New World day geckos (Sphaerodactylidae, Squamata) under climate change</b> .....	<b>86</b>
Introduction .....	86
Methods .....	90
<i>Thermal physiology data collection</i> .....	90
<i>Ecophysiology models</i> .....	94
Results .....	101
<i>Thermal physiology data collection</i> .....	101
<i>Ecophysiology models</i> .....	102
Discussion .....	105
Citations .....	127
General synthesis .....	135
Additional citations .....	139

## LIST OF FIGURES

### **Chapter 1: A game theoretic framework for assessing stability in large systems of competitors**

1.1. Diagram of two- through four-strategy game payoff matrices and plots .....	7
1.2. Three-strategy game types classified by internal equilibrium .....	16
1.3. Simulation outcomes.....	22
1.4. Outcomes of three-strategy and three-face games .....	26
1.5. Invasion trajectories between games of different sizes .....	28
1.6. Results from empirical game theory models .....	30
1.7. Calculated payoffs for <i>Poecilia parare</i> male strategies .....	33

### **Chapter 2: An evolutionary game theory model for plastic developmental strategies of omnivory and carnivory in *Scaphiopus multiplicata***

2.1. <i>Spea multiplicata</i> range .....	54
2.2. Fitted tadpole reaction norms to shrimp-to-tadpole density .....	65
2.3. Proportion of carnivores at a range of shrimp-to-tadpole ratios .....	68
2.4. Plot of days to omnivore metamorphosis under different environmental temperatures .....	70
2.5. Boxplot of average precipitation and average daily temperature by month for 1970-2000 and 2061-2080 .....	72
2.6. Average time for Class A containers to empty evaporatively for 1970-2000 and 2061-2080 .....	74

**Chapter 3: Thermal ecology and extinction risk of New World day geckos (Sphaerodactylidae, Squamata) under climate change**

3.1. Localities for 2013-15 field sampling .....	89
3.2. Occurrence records for seven species of sphaerodactyline gecko .....	96
3.3. Thermal performance curves for sphaerodactyline geckos .....	103
3.4. Yearly average monthly $T_{\min}$ and $T_{\max}$ from microclim and WorldClim 1970-2000 and 2070 projections.....	104
3.5. Species distribution model for <i>C. amazonicus</i> .....	114
3.6. Species distribution model for <i>G. albogularis</i> .....	114
3.7. Species distribution model for <i>G. humeralis</i> .....	116
3.8. Species distribution model for <i>S. argus</i> .....	116
3.9. Species distribution model for <i>S. elegans</i> .....	118
3.10. Species distribution model for <i>S. macrodactylus</i> .....	118
3.11. Species distribution model for <i>S. nicholsi</i> .....	120

## LIST OF TABLES

### **Chapter 1: A game theoretic framework for assessing stability in large systems of competitors**

1.1. ESS and non-ESS Nash Sink equilibria outcomes by game size .....	27
1.2. Percentages of expected and simulated game outcomes and face games .....	44
1.3. Table with p-values from various statistical analyses .....	46

### **Chapter 3: Thermal ecology and extinction risk of New World day geckos (Sphaerodactylidae, Squamata) under climate change**

3.1. List of sphaerodactyline species and field measurements taken .....	92
3.2. Thermal physiology parameters of sphaerodactyline geckos .....	100
3.3. P-values for Tukey multiple comparisons of means for $T_{pref}$ .....	122
3.4. P-values for Tukey multiple comparisons of means for $CT_{min}$ and $CT_{max}$ .....	122
3.5. AIC values for thermal performance curve (TPC) model fits .....	122
3.6. Fitted coefficients for equations 3.1, 3.7, 3.8, 3.9 .....	124
3.7. Yearly average thermal physiological parameters across all occurrence sites for predicted persistent and extirpated populations .....	126

## ABSTRACT

### **Variation and Extinction: Models for Alternative Strategies and Climate**

by

Carla M. Sette

The merging of empirical tests and theoretical models allows us to make sense of complex biological concepts. This thesis explores questions of biological variation (both within and between species) and its persistence through evolutionary time scales primarily through the development of mechanistic models. The first chapter uses a game theory framework to describe drivers of persistence in systems of alternative strategies, and presents a new framework to describe competition within large systems. The second chapter describes the plastic system of developmental polyphenisms in the Mexican spadefoot toads, *Scaphiopus multiplicata* using a game theory framework. The possibility that anthropogenic climate change will alter selection on developmental polyphenisms is explored. The third chapter uses a mechanistic ecophysiology-based model to explore extinction risk in seven species of tropical New World day geckos (Sphaerodactylidae, Squamata). These studies highlight the importance of incorporating empirical data in modeling. Given anthropogenic changes to climate and habitat availability, ecosystem resilience of particular concern to conservationists. We need tools to predict how species losses will affect eventual equilibrium outcomes – whether ecosystems will survive in a recognizable state, or whether the loss of key species can affect larger-scale stability.

## ACKNOWLEDGEMENTS

My research and time at UCSC has granted me the most amazing naturalist opportunities; I've bagged an elephant seal pup, spent months in the Amazon, watched seagulls dive into the wake of a boat at sunset, and gotten my first dozen tick bites. I've also cried more in the last year than during any other period of my adult life. Completing this thesis was the most challenging, fascinating, and at times demoralizing accomplishment I've ever undertaken. It simply would not have been possible without the support and the steady presence of my parents, Ron and Josie Sette – they fed me and housed me much better than I could have done on my own and listened to my frustrations, even when they couldn't identify with them.

During this time, I have made some of the most delightful, brilliant, supportive friends one could ever ask for, and for the sake of brevity, I will praise them less than they deserve. I want to give particular thanks to Theadora Block, Cara Thow, and Kelley Voss, who listened to all my complaints and edited all my professional emails, and who were always sweet to me during my rough patches. Another expression of gratitude to Pauline Blaimont, who kept my spirits high with a constant supply of wild green memes, and Sarah Kienle, who texted me weekly words of encouragement from Texas. Finally, I have to acknowledge the sweetest social distancing companion anyone could hope for, my delightfully frenetic cat, Lemmy.

My advisor, Barry Sinervo, passed away suddenly mere days before my thesis defense. He died far too soon. Over the years, I have heard many people describe him as “a force of nature,” and this was truly apt. He was a research powerhouse and an endless storm of ideas. He was also my biggest cheerleader and the biggest believer in the value of my research. It has been very difficult completing my thesis, knowing he’s not there to see me over the finish line. I’m not alone in missing him terribly – his scientific insights, his odd sense of humor, and his infectious enthusiasm for lizards. I also want to express my gratitude to my thesis committee, Professors Rita S. Mehta, Suzanne H. Alonzo, Daniel Friedman. They provided thoughtful feedback on a tight schedule and stepped in to offer their support after Barry’s passing.

I want to acknowledge my collaborators on the *Scaphiopus project*, Matthew Kustra, Haley Ohms, and Regina Spranger. They were great fun to work with, and the source of several key insights. My work for my ecophysiology chapter took me all over the Americas. Without my collaborators, I would have been lost in the jungle (and would still be, today)! My entire third chapter wouldn’t have been possible without Professors Jack Sites, Martha Calderon, Angela M. Ortega León, Omar Torres Carvajal, Guarino Colli, Teresa Avila Pires, Patricia Burrowes, Richard Thomas, and Jason Rohr, who opened their labs, facilitated my travel, arranged field assistants, and shared their knowledge with me. This work also could not have been completed without the student collaborators and volunteers – they gave their time generously and caught dozens of lizards for the sake of science. Also a *big* thanks to

Gabriel Caetano, who patiently explained species distribution modeling steps to me at least twice and whose code saved the day at a tricky step in my analyses.

Finally, science builds upon the work that has been done before. Every study I cite has felt like a gift – an answer to a question I wasn't clever enough to ask myself. To the researchers who I cite (and snagged data from), a big thank you! My graduate studies were funded at various times by the Cota Robles and ARCS Fellowships, which was a massive financial relief, given the state of graduate funding, generally.

To those I mention here and to those I may have forgotten, you have all my thanks!

## GENERAL INTRODUCTION

Variation within populations is an essential condition for evolution (Darwin and Wallace 1858). Conversely, the expectation of evolution by natural selection is that selection will reduce that variation over time. Nevertheless, we recognize vast variation within and among lifeforms. An essential unanswered question is how do evolutionary processes maintain variation, both within and between species?

Biologists have similarly struggled with the apparent dichotomy that although large systems of competitors lead to mathematical instability (May 1972), a high degree of species diversity correlates with ecosystem stability. It has been a challenge to reconcile these contradictory observations, in part due to the different scales between ecosystem observations and models (McCann 2000).

Temperature and climate are some of the strongest forces influencing species abundance and distribution, i.e. ecology (Brown et al. 2004). Anthropogenic climate change threatens to disrupt (and has already altered) ecosystem norms globally. Shifts in phenology, geographic distribution, and interactions across trophic levels have already been recorded in many species (Parmesan 2006). Widespread extinctions as climate conditions exceed species' physiological thresholds have been predicted across taxa (Sinervo et al. 2010; Pinsky et al. 2019). The knock-on effects of these changes are nearly impossible to predict at the ecosystem level due to the difficulty of predicting ecosystem stability from changes in individual species' persistence.

Empirical analysis of large systems of species or strategies is needed to work out the broader forces which drive these patterns. Computational modeling provides a way to understand complex systems, such as ecosystem interactions, through the construction of plausible simplifications. Progress is made through the merging of empirical tests and theoretical models (Pielou 1981). The three chapters in this thesis are united by a computational approach to understanding questions of biological variation and its persistence through evolutionary time scales. I utilized published and field-collected data to develop primarily mechanistic models of species and trait persistence. Each chapter centers on a different selective mechanism – competition, developmental plasticity, and physiological constraints.

In **Chapter 1**, “A game theoretic framework for assessing stability in large systems of competitors,” I identified mathematical and ecological properties that contribute to stability in a system of competitors. I utilized an evolutionary game theory framework to assess the relationship between system stability and number of competitive types. I applied these analyses to a number of empirically quantified competitive outcomes in systems of alternative strategies, including the largest known biological system of alternative strategies, the Amazonian Para molly, *Poecilia parae* (Bourne et al. 2003). Finally, I expanded existing frameworks to describe systems of alternative strategies to encompass competition within larger systems, such as ecosystem-level interactions.

In **Chapter 2**, “An evolutionary game theory model for plastic developmental strategies of omnivory and carnivory in *Scaphiopus multiplicata*,” I applied the

evolutionary game theory framework from Chapter 1 to a system of plastic, rather than fixed, competitive types. Mexican spadefoot toads, *Scaphiopus multiplicata*, have two developmental polyphenisms which are comprised of phenotypically distinct morphs like alternative strategies, but arise from the same genotype. I modeled morph determination in *S. multiplicata* based on empirical data. I addressed challenges in describing fitness outcomes in plastic systems where lifetime reproductive fitness may not be a practical endpoint to compare the relative fitness of plastic traits. Additionally, I also explored the possibility of climate-driven changes to morph competitive ability due to anthropogenic climate change.

**Chapter 3**, “Thermal ecology and extinction risk of New World day geckos (Sphaerodactylidae, Squamata) under climate change” describes extinction risk in spherodactyline geckos due to predicted changes in temperature and climate based on species’ ranges and ecophysiology. Tropical ectotherms are predicted to have particular vulnerability to changes in environmental temperature (Tewksbury et al. 2008; Huey et al. 2009; Sinervo et al. 2010). Spherodactyline geckos provide a good model system for small tropical ectotherms as inhabit a broad range of habitats and elevations throughout the New World tropics. I used a mechanistic ecophysiology-based model to predict climate-driven extinctions in seven species of spherodactyline geckos. I identified abiotic factors linked to species persistence, as well as several species at risk due to climate change.

# A game theoretic framework for assessing stability in large systems of competitors

## Introduction

Biologists struggle to explain how variation among individuals in populations are maintained over evolutionary time, when the expectation is that natural selection will reduce variation in populations. Systems of alternative strategies are an often used as model system in the study of natural variation because they exist as an evolutionary stable state (ESS) or Nash Equilibrium (NE) in which each strategy has equal fitness. Alternative strategies are an extreme example of variation where discontinuous behavioral and morphological traits serve the same functional end. Alternative strategies are most conspicuous when they occur within individuals of the same species and sex. Systems of two and three alternative strategies have evolved in diverse taxa from yeast to elephant seals (reviewed in (Sinervo and Calsbeek 2006; Taborsky et al. 2008; Friedman and Sinervo 2016; Sinervo 2021). The same mechanisms maintaining alternative strategies may be present in larger competitive systems and competitive interactions between species, such as in food webs.

The biological system with the largest number of documented discrete strategies is the five-strategy mating system of the Amazonian freshwater fish, the Paramecium molly, *Poecilia parae*. Males exhibit five polymorphisms with different morphology and reproductive behavior based on haploid inheritance of a sex-linked trait (Lindholm et al. 2004). Paramecium males engage in courtship and territorial behaviors; immaculata males are smaller and specialize in sneaked copulations; and the three

colors of melanzoa male – blue, red, and yellow – engage in both courtship and sneaking behaviors with different success rates. If we extend our current thinking on alternative strategies to include ecological interactions among species, systems of five or more competitors is not unrealistic (Buss and Jackson 1979; Kraft et al. 2008; Coyte et al. 2015), particularly when considering intraguild competition (Sinervo 2021).

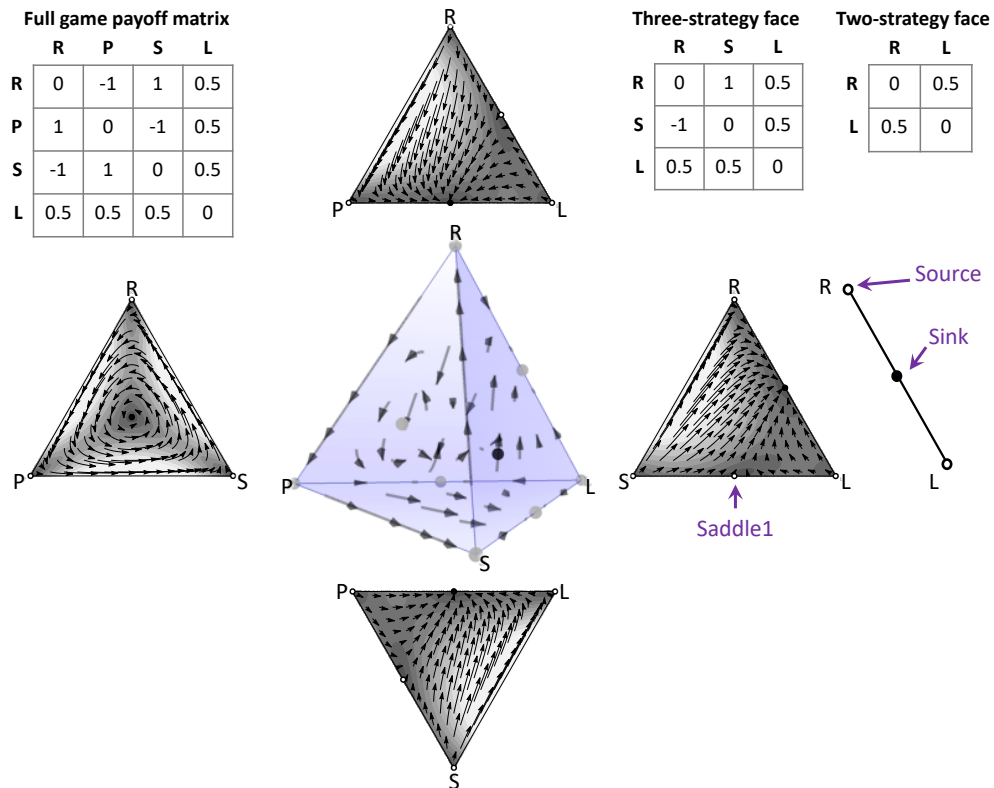
The best-described system of alternative reproductive strategies is the side-blotched lizard, *Uta stansburiana*. Both males and females of this species exhibit behavioral polymorphisms that are identifiable by color whose intrasexual competitive strategies intersect through sexual selection and mate choice. Males exhibit three polymorphisms: orange-throated territorial despots, blue-throated cooperative mate-guarders, and yellow-throated female mimics which interact in a rock-paper-scissors-like intransitive (cyclical) hierarchy. Females exhibit two polymorphisms; orange females lay fewer large eggs and yellow females lay many smaller eggs. Each is favored under different population densities and generate density and frequency cycles of r- vs. K-strategists (Sinervo et al. 2000; Alonzo and Sinervo 2001). Frequency manipulations of *Uta stansburiana* span decades (Sinervo et al. 2000; Bleay et al. 2007; Friedman and Sinervo 2016) and have elucidated the causes of frequency- and density-dependent selection on male and female sexual strategies (Sinervo and Lively 1996; Sinervo et al. 2000; Sinervo 2001), female mate choice (Alonzo and Sinervo 2001), evolution of sex ratios (Alonzo and Sinervo 2007), greenbeard social interactions among male and female strategies (Sinervo and

Clobert 2003; Sinervo et al. 2006), and the loss of strategies across large geographic ranges in response to climatic variation (Corl et al. 2010; Friedman et al. 2017). Evolutionary game theory has been an invaluable tool in explaining the various behavioral and ecological dynamics within this system. However, relatively few systems of two or three strategies have been described in a mathematic (as opposed to qualitative) framework.

A game theoretic approach to explaining evolutionary outcomes is highly flexible – one does not need to have intimate understanding of life history tradeoffs between competing strategies, only phenotypic fitness. Reproductive success, changes in demography, and experimental competitive trials can all be used to parameterize models, making these methods adaptable to many study systems and questions (Brown 2016). The mathematical properties of competitive systems with two and three competitive strategies have been well studied in mathematical, economic, and biological frameworks (Zeeman 1980; Smith 1982; Bomze 1983; Friedman and Sinervo 2016). Two-strategy systems have a limited number of possible outcomes: there may be a stable equilibrium internal to the system, known as a Sink and also an ESS, an unstable internal equilibrium, known as a Source, or one strategy may dominate and go to fixation. With each added strategy, the graphical dimensions of the game also increase by one (Fig. 1.1), and game classification becomes more complex. Systems with three or more strategies therefore have more equilibrium types, including Saddles. They may additionally have equilibria that lie on faces (any edge-game with reduce dimensionality) of the system's state space,

where at least one strategy in the system has a population of zero. A system of three strategies or more may have multiple equilibria: internal, on faces, or at vertices.

Figure 1.1. Four-strategy (3D) game plotted with constituent three-strategy face games (2D), and RL two-strategy face game (1D). Payoff matrices for the full four-strategy game, RSL three-strategy and RL two-strategy faces are shown. Examples of Source, Saddle1, and Sink equilibria are identified.



Applying these mathematical methods to larger systems, such as what we observe in *Poecilia*, greatly increases model complexity. Few studies model ecological interactions of more than three competitors in a mathematical framework, and those that do typically apply spatial constraints (Avelino et al. 2012; Juul et al. 2013; Kang et al. 2013) or assume competitive intransitivity as the basis for stability (Laird and Schamp 2009; Allesina and Levine 2011). These assumptions can lead to

underestimates of the prevalence of larger competitive systems persisting in admixture. Thus, it is important to develop methods for simplifying and describing higher-dimension systems if we hope to extend these methods to understanding systems of competitors at the ecosystem level.

In this study, I utilize evolutionary game theory to assess the mathematical and ecological properties of stable systems of competitors. I simulated systems of two to five strategies, and solve for the equilibria. I then classified games by their equilibrium outcome and other properties. I compared the properties of stable and unstable games. I used these simulated games to develop a framework for describing competitive systems with more than three strategies. I utilized previously published experimental data to model the largest known naturally-occurring system of alternative strategies, *Poecilia parae* morphs. Finally, I applied the analytical framework I developed to several naturally-occurring systems of three alternative strategies and the *Poecilia parae* model to assess whether the features of stable simulated systems appear in naturally-occurring systems of alternative tactics.

## **Methods**

### *Estimating payoff matrices*

The fitness of a strategy (i) in competition with another strategy (j) can be represented as an element of a payoff matrix ( $w_{ij}$ ) where positive values indicate direct benefit to the target competitor, negative values indicate loss of fitness, and 0 is a neutral outcome in continuous time. These elements, when aggregated into a *payoff*

*matrix*, have one row (i) for each invasion (rare) strategy and one column (j) for each common strategy. Values along the right-facing diagonal represent competition against one's own type (own-response) (Fig. 1.1).

The relative values of competitive outcomes in the payoff matrix can be used to describe game dynamics. If a strategy's own-response has the lowest fitness of all the payoffs in that row, it is described as *apostatic*. Apostatic strategies are disadvantaged because the likelihood of low-fitness interactions with own-type grows as the strategy becomes common in a population. Apostasis gives a complementary advantage to off-diagonal strategies when they are rarer in the population (Sinervo and Calsbeek 2006; Friedman and Sinervo 2016). When a strategy's own-response has the highest fitness, it is *anti-apostatic*. This is analogous to the Allee effect in ecology, which is density-dependent, and gives an advantage to strategies that are common in a population. Finally, *intransitivity* refers to systems of strategies with cyclical hierarchy, such as rock-paper-scissors. A game is intransitive when each strategy in the system is the best response (gains the highest fitness) to exactly one other strategy in the system.

### *Game solutions*

I used the R 3.5.0 (R Core Team 2018) to develop a series of functions to solve for the equilibrium of haploid, continuous time (rather than discrete) replicator systems of alternative strategies. I used frequency-dependent, continuous replicator dynamic modeling methods from Friedman and Sinervo 2016. The frequencies or

shares ( $s$ ) of all strategies in the population should sum to 1; the state space for each competitive system is comprised of all possible combinations of shares that satisfy this criteria. The fitness of a single strategy ( $w_i$ ) is described as the sum of all competitive outcomes between that strategy and each strategy in the population, weighted by the frequencies henceforth referred to as shares of each strategy ( $i, s_i$ ).

$$w_i(s) = \sum_{j=1}^n w_{ij}s_j \quad i = 1, \dots, n \quad (1)$$

The shares of each strategy will increase or decrease over time ( $t$ ), based on the difference between the fitness of that strategy and the average fitness of all strategies in the population ( $\bar{w}$ ).

$$\dot{s}_i(t) = (w_i - \bar{w})s_i(t) \quad i = 1, \dots, n \quad (2)$$

The equilibrium, or internal stable state ( $s^*$ ), of the population can be calculated from the resulting series of ordinary differential equations. First, I calculate equations for lines of equal fitness for pairs of strategies by subtracting values of each row of the  $W$ -matrix from the previous row (looping top-to-bottom) (solutions in Friedman and Sinervo 2016). Next, I calculate the eigenvalues for that series of equations. If a zero eigenvalue exists, its corresponding eigenvector describes the population frequencies where those lines of equal fitness intersect. The eigenvector may need to be scaled to sum to 1 (unity) by dividing all the values of the vector by the sum of the eigenvector elements. If no zero eigenvalue exists for the system, then it lacks an internal stable state.

### *Equilibrium types*

Internal stable states must additionally be classified, since the dynamic behavior around a stable state may differ, driving a population towards or away from that stable state, or both, depending on the direction of approach. Only a stable state which is globally asymptotically stable will lead to the persistence of all strategies through evolutionary time. I classified stable states using the eigenvalue technique described in Friedman and Sinervo 2016. An  $n \times n$  Jacobian matrix is calculated  $Dw_i(s^*) = \partial w_i(s^*)/\partial s_j$ , then scaled by multiplying by a projection matrix  $P_0 = I - \frac{1}{n} \mathbf{1}_{n \times n}$ . The eigenvalues for this matrix,  $J = P_0 Dw_i(s^*)$ , are calculated and sorted by their real parts from largest to smallest (Sandholm 2010).

Positive eigenvalues represent trajectories moving away from an equilibrium point, while negative eigenvalues represent trajectories moving toward an equilibrium point. Equilibria are Sinks if all the eigenvalues have a negative real part; populations with different starting frequencies will shift to the equilibrium frequency over time. Equilibria are Sources if all the eigenvalues have a positive real part; populations at this equilibrium frequency will remain stable, but populations at other frequencies will move away from the equilibrium frequency, potentially losing strategies. Finally, Saddle equilibria have both positive and negative real parts; population outcomes depend on starting frequencies relative to the equilibrium point. Five-strategy systems have three separate types of Saddle points because they have more dimensions (and eigenvalues), which I classified by the number of positive eigenvalues they have (Saddle1, Saddle2, Saddle3). To simplify comparisons, games with more negative

eigenvalues will be described as more “Sink-like” and games with more positive eigenvalues will be described as more “Source-like.”

An internal Sink equilibrium which is the only Sink in the state space is a global steady state, a mixed evolutionary stable state (ESS). However, if another Sink is present on a face or vertex, it is a local steady state, or non-ESS Nash equilibrium, hereafter referred to as “Nash equilibrium” or NE. For the purpose of distinction, I classify games with no internal equilibrium as None, though these games may have equilibria on faces or vertices. A game with a single strategy which reaches fixation is described as dominated.

### *Game classification*

When classifying systems of three strategies, I took into account the dynamics on the faces and vertices of the state space in addition to the type of internal equilibrium (Table 1.1). To my knowledge, systems of four and five strategies haven't been classified in any systematic way. Defining four- and five-strategy games following the same convention as three-strategy games results in exponentially more categories of games, since the number of potential equilibrium types, number of face-game dimensions, and number of face games all increase with each added strategy. Because I was primarily interested in the possibility of evolving higher-order games from games with fewer competitive types, I have chosen to define four- and five-strategy games in terms of their equilibria and component three-strategy face games.

I focused on games with internal Sinks, because these dynamics sustain multiple strategies (Fig. 1.2). There are five classes of games with internal Sinks, distinguished by the number of Saddle1 equilibria on the system's faces and the vertices. True RPS systems (RPS0) (defined in Friedman and Sinervo 2016) are fully intransitive and have Saddle1s on all vertices. There is an interesting subset of RPS0 games that are NE, because population trajectories form stable orbits around the equilibrium point, rather than move toward the attractor over time. RPS1 has a Saddle1 on one face, while the corresponding vertex is a Source. RPS2 has two Saddle1s on its faces. An RPS2 with a Nash internal equilibrium (RPS2-N) also exists, with a Saddle1 on one vertex, a Sink at another vertex, and two Saddle1s on the opposite face (Zeeman 1980; Bomze 1983). RPS3 has Saddle1s on all three-faces, and all strategies are apostatic. Equivalent games with Source equilibria exist, with Sinks at the vertices, rather than Sources. Seven types of Saddle1 games and 14 types of games with no internal equilibria can be defined, but this added complexity does not help elucidate ecological patterns, so I did not include those here (Bomze 1983).

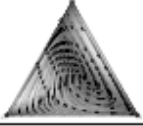
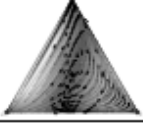
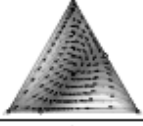
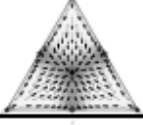
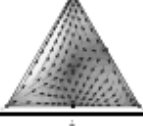
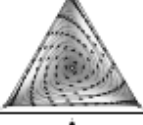
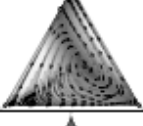
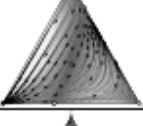
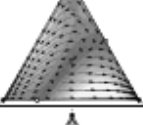
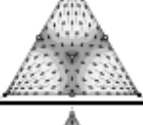
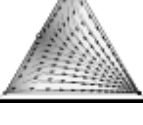
I also classified two types of two-strategy games that interest biologists because they both describe competition between cooperating and non-cooperating strategies: Prisoner's Dilemma, which is dominated by the non-cooperating strategy, and Snowdrift, which is dominated by the cooperative strategy. In both Prisoner's Dilemma and Snowdrift games, competitors have the option to cooperate (C) with one another toward a shared goal, or to behave selfishly or "defect" (D), forcing the cost of competition onto the other competitor. These games both have narrowly

defined conditions for cooperation and non-cooperation (Doebeli and Hauert 2005; Friedman and Sinervo 2016). The outcome of these games depends on the relative fitness of each of the four possible competitive interactions in the payoff matrix. In Prisoner's dilemma games, the defect strategy dominates the cooperate strategy, driven by the following relationship between the values in the payoff matrix:  $DC > CC > DD > CD$ . In Snowdrift, the cooperate strategy outperforms defection, however it can be invaded by rare defectors:  $DC > CC > CD > DD$ . An additional condition must be added to the Prisoner's Dilemma and Snowdrift games to ensure that mutual cooperation has a higher payoff than either outcome with a single defector, and both cases have a higher payoff than mutual defection:  $CC > \frac{1}{2}(CD + DC) > DD$  (Friedman and Sinervo 2016).

### *Simulations*

I randomly generated 1,000,000 payoff matrices with uniformly distributed values bounded  $[-1, 1]$  for systems with two to five strategies. I calculated equilibria and classified games as described above. I also counted the number of apostatic and anti-apostatic nodes in each payoff matrix and classified qualifying games as intransitive. For games with more than two strategies, I classified internal, face, and vertex equilibria. I assessed face equilibria two ways: as components of a larger game in which populations of strategies not represented on that face are zero and as independent games.

Figure 1.2. Three-strategy game types classified by internal equilibrium: Sink, Saddle1, Source, and None.

Internal Eq.	Name	Example	Edges			Vertices		
Sink	RPS0		None	None	None	Saddle1	Saddle1	Saddle1
	RPS1		None	None	Saddle1	Saddle1	Saddle1	Source
	RPS2-NE		None	Saddle1	Saddle1	Saddle1	Sink	Source
	RPS2		None	Saddle1	Saddle1	Saddle1	Source	Source
	RPS3		Saddle1	Saddle1	Saddle1	Source	Source	Source
Saddle1	Saddle1		7 possible combinations of edge / vertex equilibria					
Source	anti-RPS0		None	None	None	Saddle1	Saddle1	Saddle1
	anti-RPS1		None	None	Saddle1	Saddle1	Saddle1	Sink
	anti-RPS2-NE		None	Saddle1	Saddle1	Saddle1	Source	Sink
	anti-RPS2		None	Saddle1	Saddle1	Saddle1	Sink	Sink
	anti-RPS3		Saddle1	Saddle1	Saddle1	Sink	Sink	Sink
None	None		14 possible combinations of edge / vertex equilibria					

### *Invasion pathways*

The most parsimonious explanation for the existence of larger systems of competitors is that new strategies invade existing, smaller stable systems, rather than evolve simultaneously. Therefore, a stable invasion pathway would consist of a stable system of  $n$  competitors before the addition of a novel strategy, a pathway for the new strategy to invade, and a stable system of  $n+1$  competitors after invasion. I assess games for the presence of invasion pathways by looking for faces with Sink equilibria when assessed as independent games and Saddle equilibria (a trajectory off the face into the interior of the higher-dimension state space) when assessed as face games. By this reasoning, a complete invasion pathway from 2 strategies to 5 strategies would consist of a 5-strategy system with an internal Sink and these dynamics on at least one 4-face, then that 4-face must have the same dynamics on one of its 3-faces, and one of those 3-faces must have the same dynamics on one of its 2-faces.

### *Analysis of natural systems*

I applied the above analytical framework to several naturally-occurring systems of three alternative strategies in order to assess whether these games share the same features as stable simulated systems. Because two-strategy systems have simple dynamics, and no naturally-occurring four-strategy systems have been experimentally described, I focused on three-strategy systems. I also develop a model for morph competition in *Poecilia parae*.

I used published data (Hurtado-Gonzales and Uy 2009, 2010) to estimate the payoff matrix for *Poecilia parae*, partitioning fitness into various phases of selection. I generated a mating payoff matrix using average copulation rates for each strategy in pairwise competition, and by adding the rates of successful courtship and sneaked copulations for each male strategy for average copulation rates against own-type competitors, and (Hurtado-Gonzales and Uy 2009, 2010). I generated a sperm competition payoff matrix by calculating the ratio of log-transformed average sperm loads for each pair of male strategies (Hurtado-Gonzales et al. 2010). I calculated a payoff matrix for the baseline game by using the Hadamard product (multiply matrices element-wise, *sensu* (Sinervo et al. 2007; Friedman et al. 2017) of the first two payoff matrices (Fig. 1.7). The baseline game has a Sink on the immaculata-*parae*-red face. Because blue males' reproductive success was likely underestimated in pairwise experiments in the lab (Hurtado-Gonzales 2014), I performed a breakpoint analysis to estimate the value required to add to blue mating payoffs to generate a stable four-strategy face. Finally, because yellow was underperforming in the model, yellow payoffs in competition against immaculata (yellow is most aggressive toward immaculata sneakers) were increased until a five-strategy equilibrium was reached.

I used the game theoretic framework described above to re-analyze several previously-quantified three-strategy competitive systems in order to compare results from the simulations to naturally-occurring games. These included the mating systems of the side-blotched lizard, *Uta stansburiana* (references above), the blue gilled sunfish, *Lepomis macrochirus* (Neff et al. 2003; Sinervo and Calsbeek 2006),

the marine isopod, *Paracerceis sculpta* (Shuster and Wade 1991; Sinervo and Calsbeek 2006), the female damselfly, *Ischnura elegans*, and male avoidance strategies (Svensson et al. 2005; Sinervo and Calsbeek 2006). I also assessed stability in a system of plant competitors consisting of a nitrogen-stealing parasitic plant, *Rhinanthus minor*, its host grass species with no parasitic defenses, and its host forb species with defenses against parasitic plants (Cameron et al. 2009). Competitive fitness (dry biomass ratios) was compared under high and low nitrogen conditions.

#### *Other analyses*

Simulation outcomes were validated statistically. The relative proportions of each equilibrium outcome can be predicted by calculating the expected frequency of combinations of eigenvalues for each number of competitors. Differences in frequency of outcomes between game sizes and equilibrium types were determined by equal proportions tests with a 95% confidence level. I also tested whether traits expected to contribute to stability of competitive systems differ among game outcome types. Student's t-test was used to compare the degree of apostasis or anti-apostasis between groups. All p-values are  $> 0.05$  unless otherwise stated (for all p-values, see Table 1.3). I used linear models to compare whether the number of negative eigenvalues defining each equilibrium type predicted the proportion of intransitive games and average number of apostatic nodes for each game size. I used binomial generalized linear models to test whether apostasis contributes to intransitivity for games with three to five strategies. I calculated average interaction strength for each

equilibrium type as the average absolute value of all the W matrices. I also recorded the presence of evolutionary stable pathways to build larger systems of strategies from smaller systems. Faces have a trajectory off the face into the interior of the higher-dimensional state space when they have Sink equilibria when assessed as independent games and Saddle equilibria when assessed as face games, indicating the potential for the additional strategy to invade, even as a rare mutant.

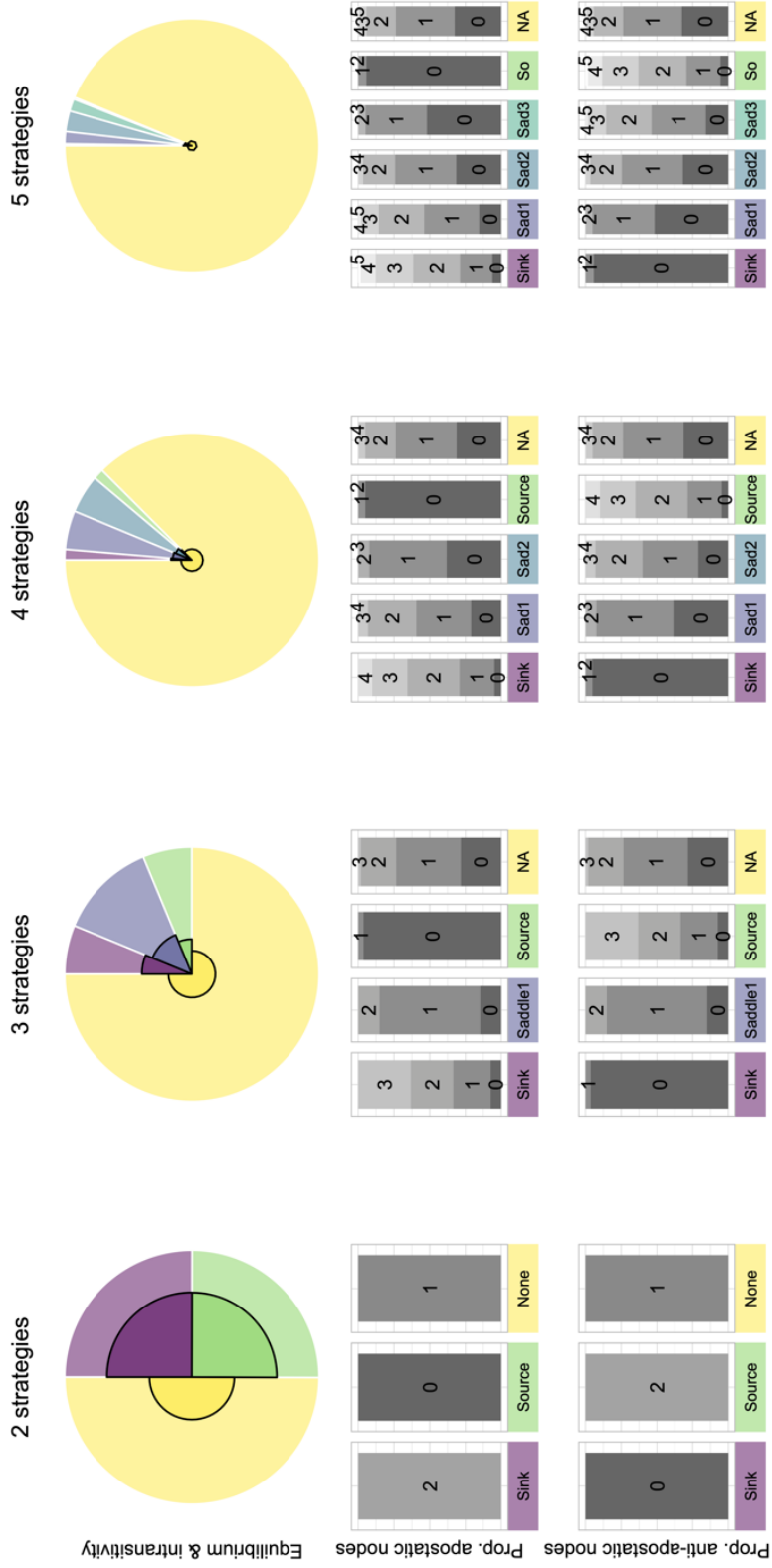
## Results

### *Equilibrium types*

In simulations for two- to five-strategy games, the most frequent outcome was the absence of any internal equilibrium, indicating systems in which at least one randomly-generated strategy is lost. In two-strategy systems, internal equilibria occurred in 50% of games. The proportion of games with internal equilibria approximately decreased by half with each additional strategy added ( $p = 0.70$ ) (Fig. 1.3). The reverse is true when assessing face games of any system: for faces, the proportion of stable games doubles with every strategy excluded (Table 1.2). The average interaction strength for every equilibrium type for every size game was 0.50, and each had a standard deviation of 0.289.

The frequency of each internal equilibrium type can be calculated as the probability of obtaining the necessary combination of positive and negative eigenvalues from the Jacobian matrix (Table 1.2). Therefore, Sinks and Sources are always the least frequent equilibrium types. Equilibrium outcomes defined by

Figure 1.3. Simulation outcomes. Top row: proportion of internal equilibrium types (and intransitive games) by equilibrium type. Middle row: proportion of apostatic node counts by equilibrium type. Bottom row: proportion of anti-apostatic node counts by equilibrium type.



inverse-eigenvalue decomposition occur in equal proportions: Sinks and Sources of all game sizes, Saddle1 and Saddle2 equilibria in four-strategy systems, and Saddle1 and Saddle3 equilibria in five-strategy systems (p-values, Table 1.3). In the simulations, four-strategy Source, Sink, Saddle1, and Saddle2 outcomes and five-strategy Source, Sink and Saddle2 occur with significantly different frequency than expected through probability of eigenvalue combinations (equal proportions test, *all*:  $p < 0.01$ , Table 1.3). The equilibria calculated for face games of larger systems are the same when those strategies are assessed as independent games. The equilibrium type may differ when a system of strategies is assessed as an independent game and as a face of a larger game, since the latter adds one or more dimensions to the system. When the face games of larger systems (e.g. five-strategy, four-face) are assessed as independent games, the proportion of each equilibrium type is the same as randomly generated systems of the same size (equal proportions test, *all*:  $p > 0.05$ ).

#### *Apostasis, intransitivity and game stability*

Games with no internal equilibrium have equal average numbers of apostatic and anti-apostatic nodes, as do games with equilibrium outcomes defined as having the same number of positive and negative eigenvalues (i.e. three-strategy Saddle1s and five-strategy Saddle2s) (Fig. 1.2). More “Sink-like” games have higher average numbers of apostatic nodes, and more “Source-like” games have a higher average number of anti-apostatic nodes (linear regression, 3-5s:  $p < 0.01$ , Table 1.3). The equilibria calculated for face games of larger systems are the same when those). For

all game sizes, Sinks have the same average number of apostatic nodes as Sources have anti-apostatic nodes (Student's t-test, *all*:  $p > 0.05$ , Table 1.3). A similar pattern can be observed between Saddle equilibria with opposite eigenvalue signs.

Two-strategy games and two-faces have equal proportions of intransitive Sink and Source outcomes. In games and faces with more than 2 strategies, the proportion of intransitive games is higher in more "Sink-like" games (Fig. 1.3). This pattern is weakly predicted by the number of negative eigenvalues defining each equilibrium type (linear regression,  $3s$ ,  $4s(3)$ ,  $5s$ ,  $5s(4)$ ,  $5s(3)$ :  $p < 0.01$ ,  $4s$ :  $p = 0.02$ ). Intransitivity is not significantly predicted by the number of apostatic nodes at any game size (generalized linear regression: *all*:  $p > 0.05$ , Table 1.3).

Games with three or more strategies may have interior Sink equilibria that are global ESS or are otherwise NE, differentiated by the presence of additional Sink equilibria on the faces of the state space. In the simulations, mixed ESS's are much more common than NE (Table 1.1). Games with mixed ESS's are more likely to be intransitive than games with NE ( $3-5s$ :  $p < 0.01$ ). Among Sinks, only games with NE have anti-apostatic nodes. Games with mixed ESS's have a higher average degree of apostasis than games with NE ( $3-5s$ :  $p < 0.01$ ) and no anti-apostatic nodes. Games with NE never have more than half anti-apostatic nodes (Table 1.1).

Figure 1.4. Proportion of three-face outcome types in five-strategy games and four-strategy games, and all outcomes of three-strategy games.

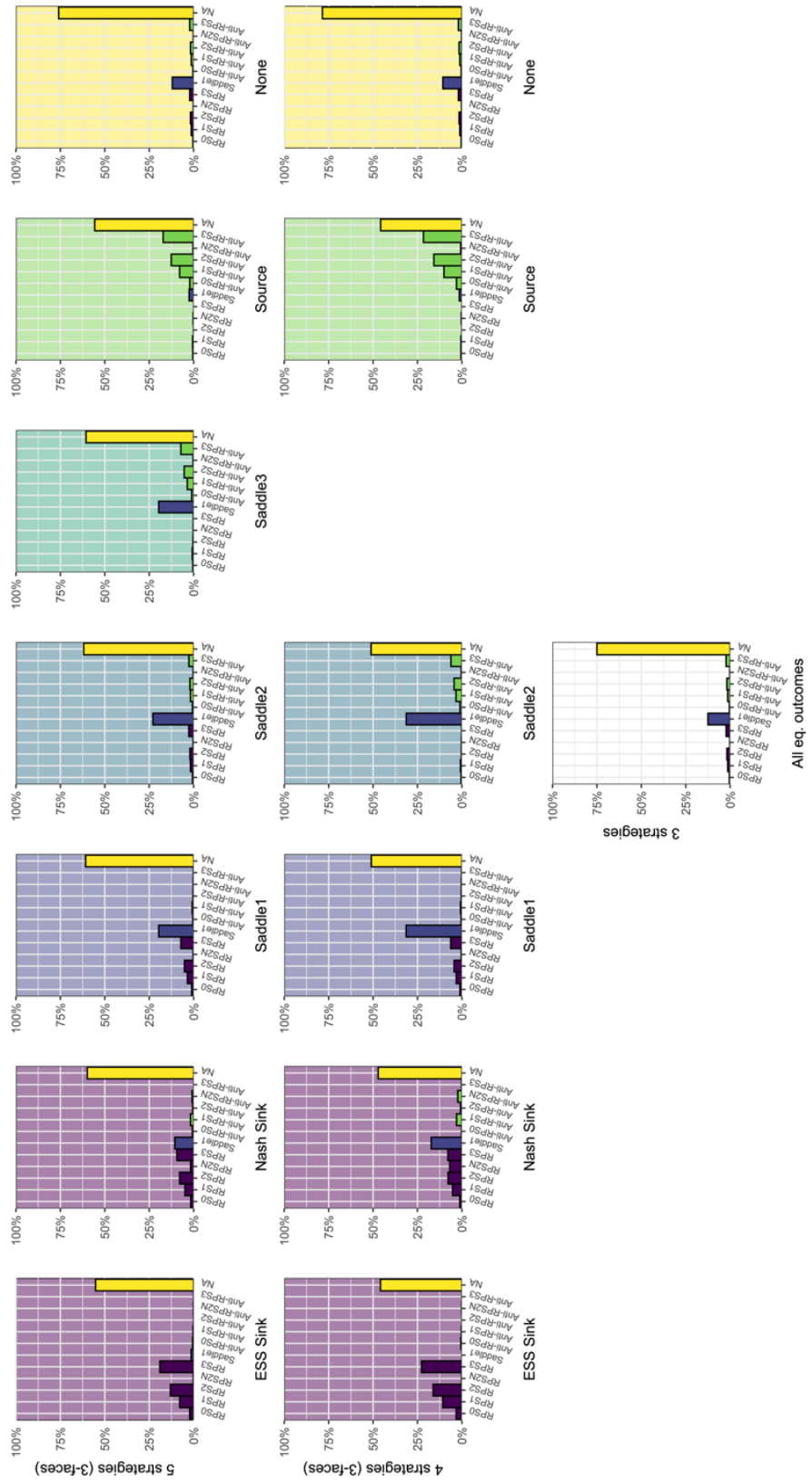


Table 1.1. ESS and non-ESS Nash Sink equilibria outcomes by game size. Apostatic and anti-apostatic nodes are reported as mean number of nodes, with the range parenthetical.

	5 strategies		4 strategies		3 strategies	
	ESS	Nash	ESS	Nash	ESS	Nash
Total % Sink eq.	0.25%		1.35%		6.23%	
% of Sinks	85.43%	14.57%	91.65%	8.35%	96.35%	3.65%
% Intransitive	7.26%	3.85%	16.98%	10.39%	40.04%	18.99%
Apostatic nodes	2.26 (0-5)	1.67 (0-4)	2.16 (0-4)	1.46 (0-3)	1.99 (0-3)	1
Anti-apostatic nodes	0	0.40 (0-2)	0	0.60 (0-2)	0	1

### Game types

Two-strategy games can be classified as Prisoner's Dilemma (PD) or Snowdrift (SD) games if they fit certain criteria. PD games make up 8.28% of all two-strategy games and 16.58% of games without internal equilibria. SD games make up 8.33% of all games and 33.28% of Sink games. Using a more rigorous definition of these games based on two criteria (defined above and in Cameron et al. 2009), the proportion of both PD and SD games is reduced by half (equal proportions test, PD:  $p = 0.54$ , SD:  $p = 0.46$ ). SD and PD games also occur in equal proportions (equal proportions test, *relaxed*:  $p = 0.21$ , *rigorous*:  $p = 0.95$ ). PD and SD games are not common face game types of most three-strategy systems. 81.38% of RPS0 games and 47.06% of RPS1 games have PD faces, though the other three-strategy equilibrium outcomes most commonly have no PD or SD faces. Notably, though 57.45% of RPS2-N games have no PD or SD faces, 41.36% of games have one SD face, the most of any three-strategy outcome.

Three-strategy games have 31 different combinations of internal, face, and vertex equilibria, four-strategy games have 3,822 different combinations, and five-

strategy games have 250,729 different combinations of internal, face, and vertex equilibria. For clarity, I define larger games by the equilibrium types of their component three-faces, when assessed as independent games (Fig. 1.2). The most common constituent three-face type for all game outcomes is no internal equilibrium (Fig. 1.4). For most other game outcomes, the second most abundant three-face type is Saddle1. However, for mixed ESS games, the next most abundant three-faces are RPS3 and RPS2, which are also the most common Sink outcomes for three-strategy games. Sink four- and five-strategy games have a higher proportion of Sink three-faces than occur in randomly-generated three-strategy games (equal proportions test,  $4(3) \text{ \& } 5(3)$ :  $p < 0.01$ , Table 1.3).

Figure 1.5. Invasion trajectories between games of different sizes. The purple trace shows the pathway new strategies must take to invade existing systems of two or more strategies.

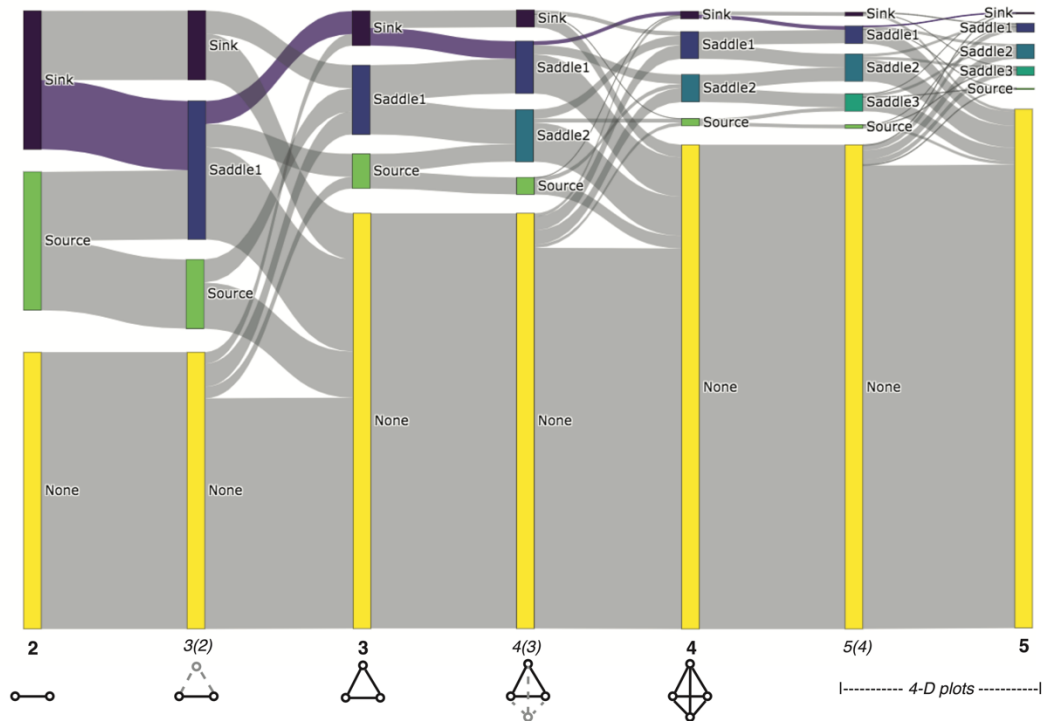
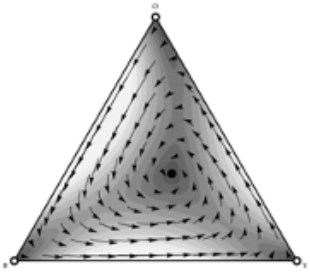
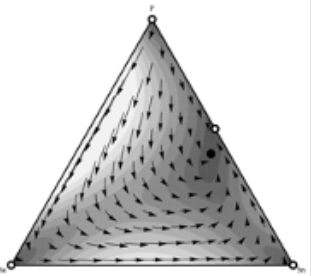
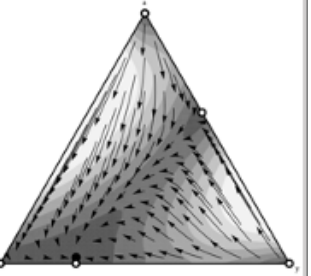
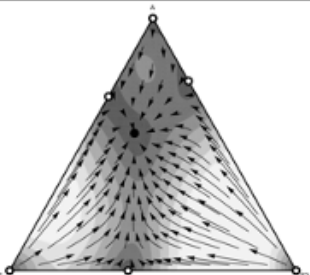
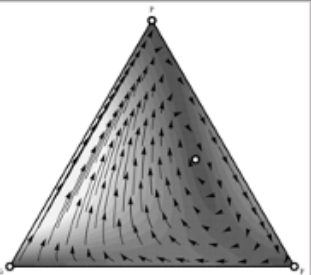
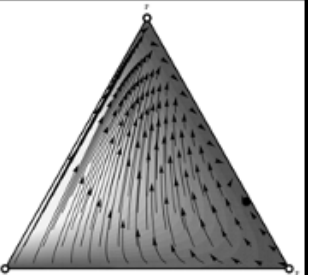


Figure 1.6. Results from empirical game theory models. Strategies are plotted anti-clockwise from the top.

Species	Side-blotched lizard males ( <i>Uta stansburiana</i> )	Bluegill sunfish males ( <i>Lepomis macrochirus</i> )	Marine isopod males ( <i>Paracerceis sculpta</i> )									
Strategies	Orange - territorial	Parental	$\alpha$ - territorial									
	Blue - mate-guarding, cooperative	Satellite	$\beta$ - female mimic									
	Yellow - sneaker (female mimic)	Sneaker	$\gamma$ - cryptic									
Payoffs												
		O	B	Y		P	Sa	Sn		$\alpha$	$\beta$	$\gamma$
	O	0	-0.49	0.80	P	0	-0.41	0.51	$\alpha$	0	-0.500	2.442
	B	0.93	0	-0.42	Sa	0.92	0	-0.41	$\beta$	1.832	0	0.811
Y	-0.09	0.78	0	Sn	0.41	0.51	0	$\gamma$	1.603	0.287	0	
Plot												
Sink type	RPS0	RPS1	RPS2									
Intransitive?	yes	yes	no									
Apostatic strategies	none	Parental	$\alpha$ & $\beta$									
Anti-apostatic strategies	none	none	none									
Data source	Sinervo and Lively 1996; Friedman and Sinervo 2016	Neff et al. 2003; Friedman and Sinervo 2016	Shuster and Wade 1991; Sinervo and Calsbeek 2006									
Species	Blue-tailed damselfly females ( <i>Ischnura elegans</i> )	Parasitic plant ( <i>Rhinanthus minor</i> ) & grass & forb hosts, HIGH NITROGEN	Parasitic plant ( <i>Rhinanthus minor</i> ) & grass & forb hosts, LOW NITROGEN									
Strategies	Androchrome - male mimic	Parasitic plant	Parasitic plant									
	Infuscans coloration	Grasses	Grasses									
	Infuscans-obsolete coloration	Forbs	Forbs									
Payoffs												
		A	I	IO		P	G	F		P	G	F
	A	-0.693	0.976	1.053	P	1.00	3.06	0.33	P	1.00	5.43	0.96
	I	0.057	-0.693	1.538	G	0.69	1.00	1.25	G	0.50	1.00	1.25
IO	-0.116	0.877	-0.693	F	1.00	0.80	1.00	F	1.18	0.80	1.00	
Plot												
Sink type	RPS3	Anti-RPS0 (Source)	RPS0									
Intransitive?	no	yes	yes									
Apostatic strategies	ALL	none	none									
Anti-apostatic strategies	none	none	none									
Data source	Svensson et al. 2005; Sinervo and Calsbeek 2006	Cameron et al. 2009										

Mixed ESS's have the highest proportion of Sink three-faces, followed by NE games (equal proportions tests:  $p < 0.01$ , Table 1.3). Nash Sinks have a higher proportion of Saddle1 and Source faces than do mixed ESS's (4(3) & 5(3):  $p < 0.01$ , Table 1.3). Each three-face RPS type occurs in Sinks in the same proportion as the Anti-RPS face type occurs in Sources for both four- and five-player games (*all*:  $p > 0.05$ , Table 1.3), except for five-player RPS1 and Anti-RPS1 in the simulations ( $p = 0.05$ ). Source games have the highest proportion of Source three-faces of any equilibrium type, and Saddle games of all types also have the highest proportion of Saddle1 three-faces (equal proportions tests:  $p < 0.01$ , Table 1.3). RPS0 games have 0 trajectories since there are no saddle points on the 2-faces, RPS1 and RPS2-N games have 1, RPS2 games have 2, and RPS3 games have 3. The number of complete invasion trajectories from two strategies upwards decreases as more strategies are present in the system (Fig. 1.5).

### *Ecological examples*

I assessed experimentally-generated payoff matrices from a variety of previously-quantified ecological systems using the framework established above. The side-blotched lizards, blue gilled sunfish marine isopods, and female damselflies systems have been thoroughly described previously within a game theoretic framework (Cameron et al. 2009), so I revisit them only briefly here (Fig 1.6). I examined one game of each Sink equilibrium type. I also explored a three-species system of plant competitors consisting of the parasitic plant, *Rhinanthus minor*, and

its host grass and forb species (Cameron et al. 2009) under two sets of experimental conditions that affect the equilibrium of the system.

Side-blotched lizard, bluegill sunfish, and the grass-forb-parasite system of plant competitors are all intransitive systems. Male bluegill sunfish males and marine isopods, and female blue-tailed damselflies all have apostatic strategies; none of the systems have anti-apostatic strategies. No PD- or SD-type games were detected among the two-faces of these games. Interaction strengths in the grass-forb-parasite system were experimentally tested under low- and high-nitrogen treatments. Payoffs for grass and parasite and forb and parasite pairs were calculated as average dry plant biomass from growth experiments while the payoffs for grasses and forbs were estimated from apparent competitive ability. Under the high-nitrogen treatment, the system has an anti-RPS0 Source equilibrium, driven by two anti-apostatic nodes in the parasite-forb face game (Fig. 1.6, bottom column 2). Under low-nitrogen treatment, the system has an RPS0 Sink, which was reflected in their converged non-spatial model (Fig. 1.6, bottom column 3).

The base payoff matrix for male Para molly derived from experimental copulation rates for each morph and sperm competition is shown in Fig. 1.7. The base matrix has a Sink equilibrium on the immaculata-parae-red face, as well as five separate two-faces with Saddle equilibria. Increasing the average copulation rate for blue males in all competitive encounters by 0.29 generates in a Saddle1 equilibrium on the immaculata-parae-blue-red face and additional Saddle equilibria on the immaculata-parae-blue, immaculata-blue-red, and blue-red-yellow faces. Because the

yellow strategy has a lower average fitness than the other strategies, we increased the fitness of yellow when in competition with immaculata, based on observed rates of aggression of yellow directed towards immaculata (Hurtado-Gonzales and Uy 2010). A multiplier of 2.97 or higher results in a system with a five-strategy Saddle1 equilibrium, Saddle2s on the immaculata-parae-blue-red and immaculata-parae-blue-yellow four-faces, as well as Saddles on the immaculata-parae-blue and blue-red-yellow three-faces and Sinks on the immaculata-parae-red and immaculata-blue-red three-faces.

Figure 1.7. Calculated payoffs for *Poecilia parare* immaculata, parae, blue, red, and yellow male strategies. Adjustments to experimentally-determined payoffs are indicated in ***bold italics***.

Copulatory success						Sperm competition						Y vs I adjustment							
	I	P	B	R	Y		I	P	B	R	Y		I	P	B	R	Y		
I	0.16	0.50	0.80	0.60	0.00	x	I	1.00	1.24	1.15	1.08	1.13	x	I	1	1	1	1	1
P	0.80	0.49	0.80	1.00	0.70		P	0.81	1.00	0.93	0.87	0.91		P	1	1	1	1	1
B	<b><i>0.20+0.29</i></b>	<b><i>0.10+0.29</i></b>	<b><i>0.54+0.29</i></b>	<b><i>0.50+0.29</i></b>	<b><i>0.00+0.29</i></b>		B	0.87	1.07	1.00	0.94	0.98		B	1	1	1	1	1
R	1.20	0.40	0.60	0.17	0.78		R	0.92	1.14	1.06	1.00	1.04		R	1	1	1	1	1
Y	0.40	0.30	0.60	0.88	0.50		Y	0.89	1.10	1.02	0.96	1.00		Y	<b><i>2.97</i></b>	1	1	1	1

Estimated payoff matrix					
	I	P	B	R	Y
I	0.16	0.62	0.92	0.65	0.00
P	0.65	0.49	0.74	0.87	0.64
B	0.43	0.42	0.83	0.74	0.28
R	1.11	0.46	0.64	0.17	0.81
Y	1.06	0.33	0.61	0.85	0.50

## Discussion

A large number of two- and three-strategy systems of alternate mating strategies have been described, but examples of larger systems are sparse (Taborsky et al. 2008). *Xiphophorus multilineatus* has four size classes of males, differing in

body size and mating behavior (Kingston et al. 2003; Tudor and Morris 2011). Another potential system of four male strategies exists in the lizard species *Gonatodes rozei*, however the mating behavior of this species has not yet been studied (Rivero-Blanco and Schargel 2012). The Para molly (*Poecilia parae*) is the only single-population system of five strategies I have found described. Although mating systems are easily-identified systems for study, it is necessary to move beyond mating systems as model systems if we wish to understand the processes that maintain larger stable systems in nature. A new framework is needed to bridge the apparent gap between studies on mechanisms of stability at smaller scales, and modelling systems at the ecosystem scale. One such system occurs among co-occurring salamanders in Northern California: *Taricha torosa* are toxic and have aposematic coloration (A) to deter predators, *Ensatina eschscholtzii xanthoptica* are non-toxic Batesian mimics (B) of *Taricha*, and *Ensatina eschscholtzii eschscholtzii* are cryptic (C) (inconspicuous) and non-toxic. Predators may inexperienced (naïve, N) with regards to these three prey types or responsive (R) to species' cues based on prior experience (Kuchta et al. 2008; Friedman and Sinervo 2016; Sinervo 2021). The resulting two-population game has five total strategies and is depicted in four dimensions, the same as the Para molly system. Considerably larger systems of co-occurring competing species are also known (Buss and Jackson 1979; Kraft et al. 2008; Coyte et al. 2015).

Analysis of face games of larger systems suggests a possible bridge between within-species and ecosystem-level scales. Face games in this study are analogous to

the “block” structures which are hypothesized to stabilize larger competitive systems (May 1972; Allesina and Tang 2012; Bairey et al. 2016; Levine et al. 2017). Because the equilibria of face games remain unchanged when assessed individually or as components of larger games, we can build accurate models of complex systems by empirically assessing face subsets of strategies. At the ecosystem level, systems may consist of stable blocks of strategies with strong interactions, which are connected by weaker interactions. Intraguild competition is likely to be stronger than interguild competition given that “niches” of individuals within a species overlap more strongly than individuals between species. This approach may also be the key to reconciling niche models with neutral theory models of community ecology, however as long as empirical studies focus on smaller systems of competitors, evidence for this link will remain largely theoretical (Chave 2004).

The likelihood of stability decreases with each additional strategy added, thus smaller systems (blocks) of competitors are more likely to occur in nature than more complex systems. Stable games are more likely to have stable faces than other equilibrium types, but they do not arise from a subset of games with smaller interaction strengths. Sinks have the same average interaction strength as every other equilibrium type in the simulations and have a standard deviation consistent with uniform probability density resulting from the random generation of payoff matrices. My findings on game size and stability are consistent with prior assertions that larger systems may be inherently less stable than smaller ones, but contradict assertions that

weak competitive interactions may allow larger competitive systems to remain stable (May 1972; McCann 2000).

I was not able to calculate a stable Sink equilibrium for the Para molly system of five male strategies based on the raw data in the laboratory. To arrive at an equilibrium for the full system, I had to apply assumptions about blue males' mating success in their natural habitat vs. laboratory conditions and yellow's competitive advantage against immaculata due to male-male aggression. Blue males' reproductive success has likely been underestimated in the base mating rate payoff matrix, because the visual environment during mating experiments does not match the visual environment in the wild (Hurtado-Gonzales 2014). Furthermore, blue males school with own-type and this may reflect a coordinated strategy (G. Bourne, pers. comm.). This behavior is beyond the ability of pairwise experiments to capture, thus larger-scale frequency experiments are required. Predation likely plays an important role in reducing the overall fitness of conspicuous male morphs (Hurtado-Gonzales et al. 2010), however realistic predation rates in the wild are needed to accurately model this aspect of male fitness. Nonetheless, there are still insights we can glean from this system as it is currently modeled. For example, increasing the mating success of the blue strategy by as little as 0.06 makes the blue-red-yellow face intransitive; it is likely that these strategies form an intransitive RPS0 face in the complete game. As the model became more stable when parameters were added, more equilibria appeared on the faces of the system. This matches the results of the randomly-generated simulations; games with stable equilibria had more face equilibria.

While empirical studies on pairwise interactions have been sufficient to quantify competitive interactions in three-strategy systems, this may not be sufficient to accurately assess payoffs in larger systems, particularly if anti-apostasis, positive frequency-dependence, is present. Frequency manipulation experiments are often necessary to understand dynamics in systems of alternative strategies (Sinervo and Basolo 1996). Frequency manipulations on the side-blotched lizard have revealed the paternity game is an RPS0 with an internal NE driving frequency fluctuations among the three strategies (Bleay et al. 2007). Tracking population frequencies over many years reveals that these cycles are maintained in orbits around the mixed NE but are also perturbed by climate fluctuations that push the game toward edge games with two stable strategies (Friedman et al. 2017). Manipulations of the frequency of kin vs. non-kin males in nest sites reveal that blue males exhibit greenbeard recognition of mutualistic behavior due to a shared phenotypic trait (blue throat, cooperative mate guarding) (Sinervo and Clobert 2003; Sinervo et al. 2006). In addition to the three male strategies, female strategies include mate choice and sex ratio (Alonzo and Sinervo 2001, 2007) as well as egg size as a driver of female r- and K-strategies, which was also revealed through frequency manipulations (Sinervo et al. 2000). Similar frequency manipulations of Para molly males in mesocosm experiments will likely be required to fully describe the competitive dynamics among male strategies.

Structuring our understanding of larger systems around the dynamics of smaller faces of those systems also allows us to assess the possible evolutionary history of larger systems. I apply the assumption that larger systems of strategies

evolve from smaller stable systems of strategies that experience the invasion of new mutant strategy off a Saddle face of the larger system (Fig. 1.5). It is possible to use this same structured approach to assess the effect that loss of a strategy or multiple strategies will have on the system as a whole – whether the system will reach a stable equilibrium at a smaller number of competitors or collapse into a system dominated by a single strategy. These dynamics are particularly important in multi-species ecosystem interactions, where resilience to perturbation (particularly anthropogenic) is of great concern to conservationists (McCann 2000).

With the exception of the pure-paternity game of side-blotched lizards (Bleay et al. 2007), the three-strategy games I examined all have potential invasion pathways off at least one two-strategy face. This assessment is based on the assumption that competitive interactions are not themselves evolving through character displacement. Existing strategies can shift in competitive strength, both upon the invasion of a novel strategy or the loss of an existing one. While the paternity game of side-blotched lizards shown here does not exhibit any invasion trajectories nor face equilibria, the game computed from life-time reproductive success indicates yellow is susceptible to loss from its strategy performing well under warm climates, but poorly in cool environments (Friedman et al. 2017). Yellow has been lost from eight populations located in cooler climates across the species' range (Corl et al. 2010). We see these same invasion dynamics at a phylogenetic time scale. Rodent species evolve mating systems with RPS dynamics that transition at the species level among promiscuous, polygynous, and monogamous strategies along predictable invasion trajectories

(Sinervo et al. 2020). Several species of *Xiphophorus* swordtail fish, the ancestral clade to *Poecilia*, exhibit male polymorphism in body size (Ryan et al. 1992; Schroeder and Oiten 1999) or coloration (Moretz 2005; Borowsky 2010), suggesting that male polymorphism may be ancestral to *Poecilia*. Several of these polymorphisms, including *Xiphophorus multilineatus*, are Y-linked traits, like *Poecilia parae* (Ryan et al. 1992; Schroeder and Oiten 1999; Kingston et al. 2003).

I show that while intransitivity is more common in stable systems, it is not necessary for stability. In fact, the majority of stable games in the simulations are not intransitive, which is consistent with findings by (Laird and Schamp 2009; Levine et al. 2017). RPS0 games are intransitive by definition and thus considered true intransitive RPS systems (Friedman and Sinervo 2016). However, RPS1-3 games may or may not be intransitive. I find stable non-intransitive systems in nature such as male marine isopods and female damselflies. Bluegill sunfish male strategies are technically intransitive, but a Saddle1 equilibrium on the parental-sneak face alters these dynamics. Empirical studies on alternative tactics (Laird and Schamp 2006; Szolnoki et al. 2014) as well as theoretical studies (Allesina and Levine 2011) often focus on intransitive competitive systems. Intransitivity can be stabilizing, but focusing on intransitivity as the basis for stability can lead to incorrect conclusions, such as the assertions in Allesina and Levine (2011) that no single theoretical patch can support an even number of species, and that stable five-strategy systems are more common than four-strategy systems.

Apostasis, or negative frequency-dependence, also contributes to the presence of Sinks within a system of competitors, such as the stable non-intransitive systems described above. Among the simulations, many games with internal Sinks have both apostatic and anti-apostatic nodes (and some nodes which are neither). One can easily imagine how negative frequency-dependence can maintain systems of strategies; each strategy's fitness decreases as its frequency increases, preventing any strategy from becoming dominant. Bluegill sunfish's parental strategy, marine isopods' territorial and female mimic strategies, and all female damselfly strategies are all apostatic RPS systems. For despotic (parental/territorial) strategies, increased frequency can lead to lower fitness due to an increase in the rate of aggressive encounters. Marine isopods' female mimicry and cryptic strategies and all female blue-tailed damselfly strategies rely on evading detection, so high frequency could lead to higher detection through development of a search image (Lindström et al. 2001; Rowe et al. 2004).

Conversely anti-apostasis contributes to the presence of Sources. The presence of positive frequency-dependence is a hallmark of cooperation, which increases fitness at higher strategy frequencies, and possibly Allee effects. Consistent with these findings, cooperation destabilizes competitive systems, while competition is stabilizing (Nowak and Sigmund 2004; Doebeli and Hauert 2005). None of the systems I looked at have positive frequency-dependent nodes in the full games, though some were present on two-strategy faces. The side-blotched lizard's mate-guarding strategy is cooperative (Sinervo et al. 2006); however, that cooperative interaction is not strong enough to be anti-apostatic. I likewise didn't detect SD or PD

games in any real-world competitive systems, likely because both of these scenarios are very narrowly-defined (see Supplement). Spatial population structure may be central to maintaining cooperative strategies, as even spatial PD games, cooperative strategies can persist if they are able to cluster together in space such as in the cooperative mate-guarding strategy of side-blotched lizards (Sinervo and Clobert 2003; Sinervo et al. 2006). Parental-type bluegill sunfish males also aggregate and share parental care (Neff et al. 2003). This analytical approach was able to shed new insights into the parasite-grass-forb competitive system (Cameron et al. 2009). The original study calculated payoff matrices for the high- and low-nitrogen treatments but used time series simulations, rather than a game theoretic framework for analysis. Their simulations for the high-nitrogen treatment had vastly different outcomes, sensitive to the starting frequencies of each plant type. My analysis clarifies that this is due to the presence of an anti-RPS0 Source equilibrium in the system. Cameron et al. (2009) identified the parasite-forb interaction as causing the biggest impact between the high-nitrogen and low-nitrogen simulations.

In addition to intransitivity and apostasis, other forces, such as fluctuating environmental conditions, for instance climate, can also stabilize systems of competitors (Chesson and Huntly 1997; Friedman et al. 2017). I modeled admixed populations, but spatial population structure can also maintain strategies both theoretically (Avelino et al. 2012; Juul et al. 2013; Kang et al. 2013) and experimentally (Kerr et al. 2002). Behavioral selection of local neighborhoods allows morphs which may have low fitness in an admixed population to select a more

favorable competitive environment. These models have haploid inheritance of strategies, but in models which account for more complex genetic inheritance additional characteristics such as plasticity and genic dominance play a role in the stability of game theoretic models (McCann 2000; Sinervo 2001, 2021; Friedman and Sinervo 2016; Moulherat et al. 2017). Game theory is an extremely useful approach to understanding competition, as it relies on the competitive outcomes among phenotypes. While these can be mechanistically modeled, with game theory it is not necessary to quantify the underlying ontogenetic tradeoffs that differentiate competing strategies or species. The game theory can also be applied to any competitive system, evolutionary or ecological, and models can be modified to include density-dependence, spatial dynamics, and other environmental perturbations (Friedman et al. 2017).

Ecologists need more empirical studies and experimental manipulations (Schluter 1994; Sinervo and Basolo 1996) on larger competitive systems to truly understand the mechanisms that arise in nature to maintain complex systems of interactions. Models can be built up from subsets of strategies to simplify the experimental process. Conversely, independently assessing stability of subsets of strategies within large systems can give insights into the evolutionary-ecological dynamics present. I provide a new framework for describing systems too large to visualize graphically, as well as tools to assess how subsets of competitors may contribute to overall system stability that can be generalized to even higher dimensions.

Table 1.2. Percentages of expected and simulated Sink, Saddle, and Source game outcomes of full two, three, four, and five-strategy games, and percentages two-, three-, and four-strategy face games of larger systems.

	2 strategies		3 strategies		4 strategies			5 strategies						
	Sink	Source	Sink	Saddle1	Source	Sink	Saddle1	Saddle2	Source	Sink	Saddle1	Saddle2	Saddle3	Source
Full games	Expected	25.00	25.00	12.50	6.250	6.250	4.688	4.688	1.563	1.563	2.344	1.563	1.563	0.3906
	Simulated	25.04	25.03	12.52	6.247	6.231	4.925	4.890	1.348	4.925	4.890	1.333	1.333	0.25
Face games	5-strategy faces	24.99	24.99	12.50	6.242	6.245	4.901	4.935	1.333	4.901	4.935	1.323		
	4-strategy faces	25.02	25.02	12.50	6.271	6.268								
	3-strategy faces	24.96	24.97											

Table 1.3. Table with p-values from various statistical analyses: equal proportions test comparing frequency of equilibrium outcomes within and between game types, student's t-tests comparing degree of apostasis and anti-apostasis, linear and generalized linear models comparing degree of apostasis and intransitivity. P-values <0.01 are highlighted in yellow.

			2	3	4	5	ALL	
			strategies	strategies	strategies	strategies		
Equal proportions test, p-values	Proportion of games with Sink eq.	Sinks decrease by 1/2, full games Sinks decrease by 1/2, face games		0.4982	0.7578	0.9979	0.6954	
	Expected vs. actual eq. outcomes	Sink	0.5512	0.5726	< 0.01	< 0.01		
		Saddle1		0.6690	< 0.01	0.3913		
		Saddle2			< 0.01	< 0.01		
		Saddle3				0.8732		
		Source	0.6800	0.9200	< 0.01	< 0.01		
	No eq.	0.3800	0.9700	0.9300	0.9900			
	Eq. outcomes w/ equivalent eigenvalues	Sink vs. Source	0.8511	0.6420	0.3563	0.5258		
		Saddle1 vs. Saddle2			0.2452			
		Saddle1 vs. Saddle3				0.3065		
Full vs. face games with same # of strategies	Sink	0.1713	0.2230	0.2386				
	Saddle1		0.8690	0.3040				
	Saddle2			0.0589				
	Source	0.2740	0.1205	0.4236				
	No eq.	< 0.01	0.1713	0.9024				
Prop. of 3-faces	ESS vs. Nash, Sinks			< 0.01	< 0.01			
	ESS vs. Nash, Saddle1			< 0.01	< 0.01			
	ESS vs. Nash, Sources			< 0.01	< 0.01			
	Full 3-player games vs. 3-faces, Sinks			< 0.01	< 0.01			
Student's t-test, p-values	Apostatic vs. anti-apostatic nodes by eq. outcome	Sinks apostatic vs. Sources anti-apostatic		0.7770	0.1940	0.5436		
		Sources apostatic vs. Sinks anti-apostatic		0.5172	0.7077	0.9854		
		Saddle1 apostatic vs. Saddle2 anti-apostatic			0.2318			
		Saddle2 apostatic vs. Saddle1 anti-apostatic			0.3995			
		Saddle1 apostatic vs. Saddle3 anti-apostatic				0.7863		
		Saddle3 apostatic vs. Saddle1 anti-apostatic				0.9043		
	Degree apostasis	ESS vs. Nash		< 0.01	< 0.01	< 0.01		
	Linear models, slopes & p-values	Avg. apostasis vs. # of negative eigenvalues	Full games: slope (p-value)		0.9594 (< 0.01)	0.6721 (< 0.01)	0.5166 (< 0.01)	
		Avg. anti-apostasis vs. # of negative eigenvalues	Full games: slope (p-value)		0.9605 (< 0.01)	0.6763 (< 0.01)	0.5124 (< 0.01)	
Intransitivity vs. # of negative eigenvalues		Full games: slope (p-value)		0.0583 (< 0.01)	0.0169 (0.0164)	4.471e-3 (< 0.01)		
		3-faces: slope (p-value)			0.0354 (< 0.01)	0.0233 (< 0.01)		
	4-faces: slope (p-value)				0.0101 (< 0.01)			
GLM	Intransitivity vs. # of apostatic nodes	Full games: slope (p-value)	0.0035 (0.301)	0.0046 (0.121)	-0.0015 (0.578)	-0.0013 (0.606)		

## Citations

- Allesina, S., and J. M. Levine. 2011. A competitive network theory of species diversity. *Proceedings of the National Academy of Sciences of the United States of America* 108:5638–5642.
- Allesina, S., and S. Tang. 2012. Stability criteria for complex ecosystems. *Nature* 483:205–208.
- Alonzo, S. H., and B. Sinervo. 2001. Mate choice games, context-dependent good genes, and genetic cycles in the side-blotched lizard, *Uta stansburiana*. *Behavioral Ecology and Sociobiology* 49:176–186.
- Alonzo, S. H., and B. Sinervo. 2007. The effect of sexually antagonistic selection on adaptive sex ratio allocation. *Evolutionary Ecology Research* 9:1097–1117.
- Avelino, P. P., D. Bazeia, L. Losano, and J. Menezes. 2012. Von Neumann's and related scaling laws in rock-paper-scissors-type games. *Physical Review E - Statistical, Nonlinear, and Soft Matter Physics* 86:4–8.
- Bairey, E., E. D. Kelsic, and R. Kishony. 2016. High-order species interactions shape ecosystem diversity. *Nature Communications* 7:1–7.
- Bleay, C., T. Comendant, and B. Sinervo. 2007. An experimental test of frequency-dependent selection on male mating strategy in the field. *Proceedings of the Royal Society B: Biological Sciences* 274:2019–2025.
- Bomze, I. M. 1983. Lotka-Volterra equation and replicator dynamics: A two-dimensional classification. *Biological Cybernetics* 48:201–211.
- Borowsky, R. 2010. Tailspots of *Xiphophorus* and the evolution of conspicuous polymorphism. *Society for the Study of Evolution* 35:345–358.
- Brown, J. S. 2016. Why Darwin would have loved evolutionary game theory. *Proceedings of the Royal Society B: Biological Sciences* 283.
- Buss, L. W., and J. B. C. Jackson. 1979. Competitive networks: Nontransitive competitive relationships in cryptic coral reef environments. *The American Naturalist* 113:223–234.
- Cameron, D. D., A. White, and J. Antonovics. 2009. Parasite-grass-forb interactions and rock-paper-scissor dynamics: Predicting the effects of the parasitic plant *Rhinanthus minor* on host plant communities. *Journal of Ecology* 97:1311–1319.
- Chave, J. 2004. Neutral theory and community ecology. *Ecology Letters* 7:241–253.

- Chesson, P., and N. Huntly. 1997. The roles of harsh and fluctuating conditions in the dynamics of ecological communities. *The American Naturalist* 150:519–553.
- Corl, A., A. R. Davis, S. R. Kuchta, and B. Sinervo. 2010. Selective loss of polymorphic mating types is associated with rapid phenotypic evolution during morphic speciation. *Proceedings of the National Academy of Sciences of the United States of America* 107:4254–4259.
- Coyte, K. Z., J. Schluter, and K. R. Foster. 2015. The ecology of the microbiome: Networks, competition, and stability. *Science* 350:663–666.
- Doebeli, M., and C. Hauert. 2005. Models of cooperation based on the Prisoner's Dilemma and the Snowdrift game. *Ecology Letters* 8:748–766.
- Friedman, D., J. Magnani, D. Paranjpe, and B. Sinervo. 2017. Evolutionary games, climate and the generation of diversity. *PLoS ONE* 12:1–14.
- Friedman, D., and B. Sinervo. 2016. Evolutionary Games in Natural, Social, and Virtual Worlds. *Evolutionary Games in Natural, Social, and Virtual Worlds*.
- Hurtado-Gonzales, J. L. 2014. The maintenance of male color polymorphism in *Poecilia parae*.
- Hurtado-Gonzales, J. L., D. T. Baldassarre, and J. A. C. Uy. 2010. Interaction between female mating preferences and predation may explain the maintenance of rare males in the pentamorphic fish *Poecilia parae*. *Journal of Evolutionary Biology* 23:1293–1301.
- Hurtado-Gonzales, J. L., and J. A. C. Uy. 2009. Alternative mating strategies may favour the persistence of a genetically based colour polymorphism in a pentamorphic fish. *Animal Behaviour* 77:1187–1194.
- . 2010. Intrasexual competition facilitates the evolution of alternative mating strategies in a colour polymorphic fish. *BMC Evolutionary Biology* 10:391.
- Juul, J., K. Sneppen, and J. Mathiesen. 2013. Labyrinthine clustering in a spatial rock-paper-scissors ecosystem. *Physical Review E - Statistical, Nonlinear, and Soft Matter Physics* 87:3–6.
- Kang, Y., Q. Pan, X. Wang, and M. He. 2013. A golden point rule in rock-paper-scissors-lizard-spock game. *Physica A: Statistical Mechanics and its Applications* 392:2652–2659.
- Kerr, B., M. A. Riley, M. W. Feldman, and B. J. M. Bohannan. 2002. Local dispersal promotes biodiversity in a real-life game of rock – paper – scissors 418:171–174.

- Kingston, J. I., G. G. Rosenthal, and M. J. Ryan. 2003. The role of sexual selection in maintaining a colour polymorphism in the pygmy swordtail, *Xiphophorus pygmaeus*. *Animal Behaviour* 65:735–743.
- Kraft, N. J. B., R. Valencia, and D. D. Ackerly. 2008. Functional traits and niche-based tree community assembly in an Amazonian forest. *Science* 322:580–582.
- Kuchta, S. R., A. H. Krakauer, and B. Sinervo. 2008. Why does the Yellow-eyed Ensatina have yellow eyes? Batesian mimicry of Pacific newts (genus *Taricha*) by the salamander *Ensatina eschscholtzii xanthoptica*. *Evolution* 62:984–990.
- Laird, R. A., and B. S. Schamp. 2006. Competitive intransitivity promotes species coexistence. *American Naturalist* 168:182–193.
- . 2009. Species coexistence, intransitivity, and topological variation in competitive tournaments. *Journal of Theoretical Biology* 256:90–95.
- Levine, J. M., J. Bascompte, P. B. Adler, and S. Allesina. 2017. Beyond pairwise mechanisms of species coexistence in complex communities. *Nature* 546:56–64.
- Lindholm, A. K., R. Brooks, and F. Breden. 2004. Extreme polymorphism in a Y-linked sexually selected trait. *Heredity* 92:156–162.
- Lindström, L., R. v. Alatalo, A. Lyytinen, and J. Mappes. 2001. Predator experience on cryptic prey affects the survival of conspicuous aposematic prey. *Proceedings of the Royal Society B: Biological Sciences* 268:357–361.
- May, R. M. 1972. Will a large complex system be stable? *Nature* 238:413–414.
- McCann, K. S. 2000. The diversity–stability debate. *Nature* 405:228–233.
- Moretz, J. A. 2005. Aggression and fighting ability are correlated in the swordtail fish *Xiphophorus cortezi*: The advantage of being barless. *Behavioral Ecology and Sociobiology* 59:51–57.
- Moulherat, S., A. Chaine, A. Mangin, F. Aubret, B. Sinervo, and J. Clobert. 2017. The roles of plasticity versus dominance in maintaining polymorphism in mating strategies. *Scientific Reports* 7:1–10.
- Neff, B. D., P. Fu, and M. R. Gross. 2003. Sperm investment and alternative mating tactics in bluegill sunfish (*Lepomis macrochirus*). *Behavioral Ecology* 14:634–641.
- Nowak, M. A., and K. Sigmund. 2004. Evolutionary dynamics of biological games. *Science* 303:793–799.

- Rivero-Blanco, C., and W. E. Schargel. 2012. A strikingly polychromatic new species of *Gonatodes* (Squamata: Sphaerodactylidae) from northern Venezuela. *Zootaxa* 66–78.
- Rowe, C., L. Lindström, and A. Lyytinen. 2004. The importance of pattern similarity between Müllerian mimics in predator avoidance learning. *Proceedings of the Royal Society B: Biological Sciences* 271:407–413.
- Ryan, M. J., C. M. Pease, M. R. Morris, S. The, A. Naturalist, N. Jan, J. Ryan, et al. 1992. A genetic polymorphism in the swordtail *Xiphophorus nigrensis*: Testing the prediction of equal fitnesses. *The American Naturalist* 139:21–31.
- Sandholm, W. H. 2010. Population games and evolutionary dynamics. (K. Binmore, ed.) *Economic Learning and Social Evolution*. The MIT Press.
- Schluter, D. 1994. Experimental evidence that competition promotes divergence in adaptive radiation. *Science* 266:798–801.
- Schroeder, J. H., and I. S. Oiten. 1999. Courtship and female choice behavior in the male-polymorphic high-backed pygmy swordtail, *Xiphophorus multilineatus*. *Naturwissenschaften* 86:251–269.
- Shuster, S. M., and M. J. Wade. 1991. Equal mating success among male reproductive strategies in a marine isopod. *Nature* 350:608–610.
- Sinervo, B. 2001. Runaway social games, genetic cycles driven by alternative male and female strategies, and the origin of morphs. *Genetica* 112–113:417–434.
- . 2021. *Behavioral Genetics to Evolution*. TopHat Publishing.
- Sinervo, B., and A. L. Basolo. 1996. Testing Adaptation Using Phenotypic Manipulations. Pages 149–185 *in* *Adaptation*. Academic Press.
- Sinervo, B., and R. Calsbeek. 2006. The developmental, physiological, neural, and genetical causes and consequences of frequency-dependent selection in the wild. *Annual Review of Ecology, Evolution, and Systematics* 37:581–610.
- Sinervo, B., A. Chaine, J. Clobert, R. Calsbeek, L. Hazard, L. Lancaster, A. G. Mcadam, et al. 2006. Self-recognition, color signals, and cycles of greenbeard mutualism and altruism. *PNAS* 103:7372–7377.
- Sinervo, B., A. S. Chaine, and D. B. Miles. 2020. Social games and genic selection drive mammalian mating system evolution and speciation. *American Naturalist* 195:247–274.

Sinervo, B., and J. Clobert. 2003. Morphs, dispersal behavior, genetic similarity, and the evolution of cooperation. *Science* 300:1949–1951.

Sinervo, B., B. Heulin, Y. Surget-Groba, J. Clobert, D. B. Miles, A. Corl, A. Chaine, et al. 2007. Models of density-dependent genic selection and a new rock-paper-scissors social system. *American Naturalist* 170:663–680.

Sinervo, B., and C. Lively. 1996. The rock-paper-scissors game and the evolution of alternative male strategies. *Nature* 380:240–243.

Sinervo, B., E. Svensson, and T. Comendant. 2000. Density cycles and an offspring quantity and quality game driven by natural selection. *Nature* 406:985–988.

Smith, J. M. 1982. *Evolution and the Theory of Games*. Cambridge University Press, Cambridge, United Kingdom.

Svensson, E. I., J. Abbott, and R. Härdling. 2005. Female polymorphism, frequency dependence, and rapid evolutionary dynamics in natural populations. *American Naturalist* 165:567–576.

Szolnoki, A., M. Mobilia, L. L. Jiang, B. Szczesny, A. M. Rucklidge, and M. Perc. 2014. Cyclic dominance in evolutionary games: A review. *Journal of the Royal Society Interface* 11:1–20.

Taborsky, M., R. F. Oliveira, and H. J. Brockmann. 2008. The evolution of alternative reproductive tactics. *Alternative Reproductive Tactics: An Integrative Approach*.

Tudor, M. S., and M. R. Morris. 2011. Frequencies of alternative mating strategies influence female mate preference in the swordtail *Xiphophorus multilineatus*. *Animal Behaviour* 82:1313–1318.

Zeeman, E. C. 1980. *Population dynamics from game theory. Global theory of dynamical systems*. Springer, Berlin, Heidelberg.

# **An evolutionary game theory model for plastic developmental strategies of omnivory and carnivory in *Scaphiopus multiplicata***

## **Introduction**

Phenotypic plasticity is a form of biological variation wherein multiple phenotypes may arise from a single genotype, depending on environmental conditions. The potential for plastic variation resides within a single individual, rather than a population. Phenotypically plastic traits may be continuous or discrete. Polyphenisms are a subset of plastic traits which, like alternative strategies, are comprised of discontinuous morphs that may vary behaviorally as well as physiologically (Taborsky et al. 2008). Plasticity is found in nearly every taxon, including inducible chemical defenses in algae and plants, feeding morphs in amphibian tadpoles, sequential hermaphroditism in various invertebrates and fish, and caste differences in eusocial insects (Pomeroy 1981; Charnov 1982; Policansky 1982; Schlichting 1986; Padilla and Savedo 2013; Lackey et al. 2019; Yang and Pospisilik 2019).

The evolution of plasticity is a topic of some controversy due to alternate views on the level at which selection acts. Plasticity is alternately considered trait that is itself under selection (de Jong 2005), or the result of selection favoring different phenotypes under different environmental conditions (West-Eberhard 1989; van Tienderen 1991; Via 1993). I take the latter view, that plasticity evolves under environmental variation, which gives rise to variable selective pressure on trait values

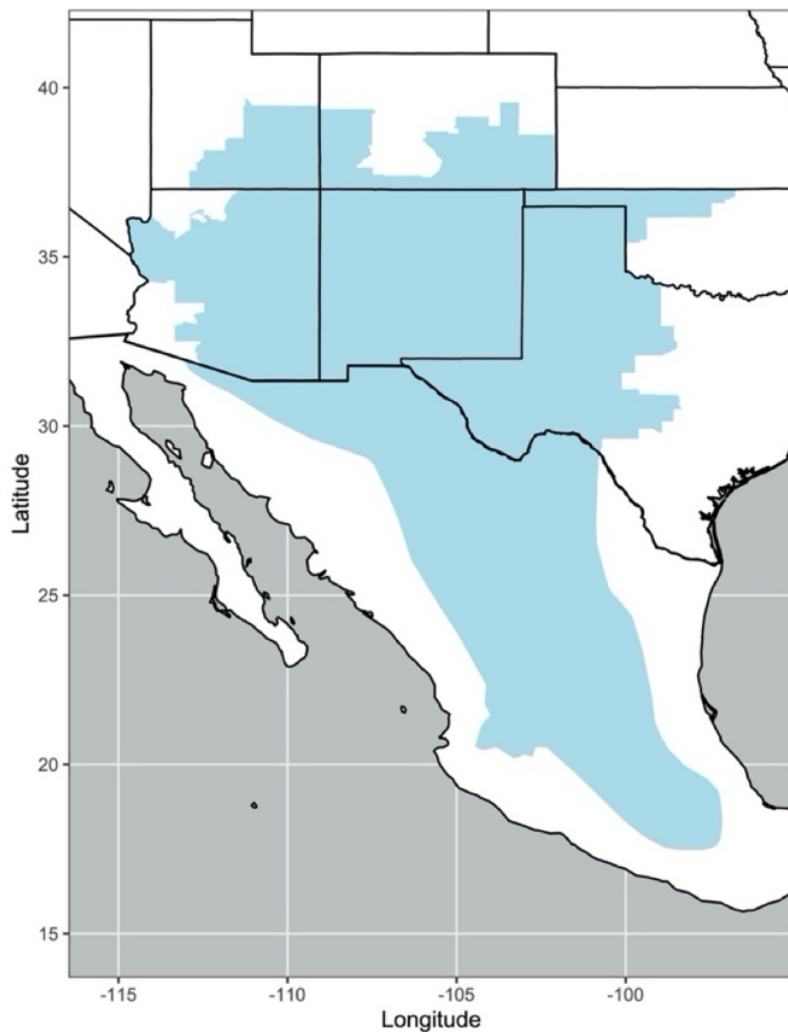
(Via 1993). This selection shapes the reaction norm - the range of phenotypes produced contingently in response to environmental cues. There is additional debate whether due to selection, plastic traits may become fixed at a particular value through genetic assimilation, erasing the reaction norm, or whether the potential for plasticity is maintained, though environmental conditions may not reveal all potential phenotypes (Pigliucci et al. 2006; Levis et al. 2018; Levis and Pfennig 2019). Testing these varying hypotheses empirically can be extremely challenging, however, as a multiple biotic and abiotic factors can simultaneously influence phenotypic expression. Models are a powerful tool in understanding the factors acting on evolution of plasticity (Friedman and Sinervo 2016).

Polyphenisms can be modeled using an evolutionary game theory framework. However, unlike genetically determined alternative strategies, polyphenisms are frequently associated with non-reproductive life phases and may be reversible (West-Eberhard 1989). Because these traits may not have a direct link to fecundity, parameterizing game theoretic models is more challenging. Fitness variation due to environmental pressures occurs within a generation for plastic traits as well as between generations, and may impact survivorship, fecundity, or both. The goal of this study was to model the biotic and abiotic factors which influence fitness in a species with plastic developmental morphs.

Plasticity has been extensively studied in spadefoot toads in the genus *Spea*, which have multiple developmental morphs which respond to resource levels in their environment (Pfennig 1992a; Levis and Pfennig 2019), and particularly in the

Mexican spadefoot toad, *Spea multiplicata* (previously *Scaphiopus multiplicatus*). *S. multiplicata* lives in the Chihuahuan Desert in the southern US and Mexico (Fig 2.1). They reproduce in ephemeral ponds and man-made structures such as cattle tanks during the Spring and Summer after rain (Pomeroy 1981; Stebbins 2003). Eggs are laid within one day of pond filling and hatch into tadpoles within 42 hours (Pfennig et al. 1991).

Figure 2.1. *Spea multiplicata* range in blue (Santos-Barrera et al. 2010) in the Southern United States and Mexico.



Spadefoot tadpoles have high mortality rates (Creusere and Whitford 1976) – as many as 10% of ponds may dry before any tadpoles are able to metamorphose (Pfennig 1990a), and even in high-resource environments as many as 50% of tadpoles may fail to metamorphose before pond drying (Pfennig et al. 1991). Because pond duration is so strong a selective force during development, spadefoot tadpoles have evolved resource polyphenisms: omnivore and carnivore morphs whose specialized diets provide tradeoffs between increasing fat storage and shortening time to metamorphosis (Pfennig 1992a). Slow-drying ponds favor omnivores, which take a minimum of 17 days to develop and build larger fat stores, while quickly-drying ponds favor carnivores, which develop in 12 days and grow to a larger average body length with smaller fat deposits (Pomeroy 1981; Pfennig 1990a). As both temperature and precipitation levels shift globally due to climate change (Pomeroy 1981), *S. multiplicata* tadpoles may experience large shifts in survivorship and selection on the morph reaction norm may change.

All *S. multiplicata* tadpoles begin life as omnivores, eating a diet that primarily consists of detritus and algae (Pomeroy 1981). Morphs can be distinguished 2-4 days after hatching (Pomeroy 1981; Pfennig 1990a, 1992a; Levis et al. 2015). Tadpoles that eat enough anostracan shrimp, known as fairy shrimp, or other tadpoles and obtain thyroid hormones through their diet transform into the carnivorous morph with enlarged jaw muscles and shortened intestines (Pomeroy 1981; Pfennig 1990a, 1992a; Levis et al. 2015). The reaction norm for *S. multiplicata* describes the proportion of carnivore morphs in a population depending on fairy shrimp density;

ponds with few fairy shrimp may have no carnivores (Pfennig 1990a). Only one naturally-occurring population of all carnivores has been reported, and that was a small water tank described as having an “unusually dense” population of fairy shrimp (Pomeroy 1981). It is possible for carnivore morphs to revert to back to omnivore physiology (Pfennig 1992b), constituting a third “switcher” strategy. The switcher strategy likely exhibits state-dependent costly plasticity (Friedman and Sinervo 2016). I am not aware of any studies on *S. multiplicata* that have attempted to quantify the proportion of switcher morphs in unmanipulated populations, nor the cost of reverting from carnivore back to omnivore morphology.

Tadpoles primarily compete for food with other individual of the same morphotype, leading to negative frequency-dependence (Pfennig 1992b). Carnivores also exhibit territorial behavior and occasionally cannibalism towards conspecifics (Pomeroy 1981; Pfennig and Frankino 1997). On the other hand, intraspecific predation by carnivores is reduced while omnivores aggregate into feeding schools, potentially providing a fitness benefit to omnivores at higher frequencies (Pfennig 1990a). Both morphs also experience density-dependent fitness; inadequate resource levels result in smaller body size (both length and mass) and longer time to metamorphosis for both carnivore and omnivore morphs (Pfennig 1990a). After metamorphosis, mass is the primary predictor of survivorship for juvenile toads (Pfennig 1990a). Omnivores are resource-limited by detritus quality, which varies between ponds, but has never been explicitly quantified (Bomze 1983). Carnivores are limited by shrimp abundance, and this may reduce body size and increase time to

metamorphosis as well as trigger a shift to the switcher strategy. Pfennig (1992) proposed a game theory model of morph determination based on the Lotka-Volterra competition model (Bomze 1983), though he does not estimate parameter values for his model. The equilibrium frequency in Pfennig's model incorporates morph frequency and resource values as factors, but not population density.

In this study, I used a game theory to model the biotic and abiotic drivers of fitness in *S. multiplicata*. I utilized published data on *S. multiplicata* morphs to model developmental morph fitness (Pomeroy 1981; Pfennig 1990a, 1990b, 1992b, 1992a; Pfennig et al. 1991; Buchholz and Hayes 2000). Because the tadpole life stage is non-reproductive, comparisons of morph fitness had to be partitioned into two model phases: morph determination and survivorship. First I modeled the reaction norm for morph determination, based on fairy shrimp abundance. I then developed an evolutionary game theory model describing *S. multiplicata* omnivore and carnivore frequency based on the reaction norm for carnivore determination. Factors such as resource limitation during development, developmental rate, and pond duration affect metamorph survivorship, and therefore morph fitness. Because, there is limited empirical data on these aspects of tadpole fitness, I was not able to model all aspects of this system. I described the effects of temperature on time to metamorphosis for omnivores and on pond duration across *S. multiplicata*'s range. These models are a step closer to fully describing the factors that maintain plasticity in *S. multiplicata*, and understanding selection on *S. multiplicata* polymorphisms under future climate regimes.

## Methods

### *Quantifying shrimp predation rates*

Carnivore tadpoles are the primary predators of fairy shrimp, but omnivores do consume shrimp at low rates (Pomeroy 1981). It is necessary to account for shrimp predation that took place in the time between morph determination and experimental sampling in the data used to predict carnivore abundance. A model was fitted to experimental data describing the average shrimp density under manipulated frequencies of omnivore and carnivore morphs in cordoned sections of a pond (Pfennig 1992*b*). Tadpole predation and mortality occurred naturally during this experiment. Tadpole density was not reported, so the average field-observed tadpole density ( $0.54 \pm 0.91$  tadpoles/L) (Pfennig et al. 1991) was used to estimate starting shrimp-per-tadpole density. The estimated shrimp-per-tadpole density (SPT) for this pond (25.93 shrimp/tadpole) falls plausibly within the range reported for natural ponds in the same study (0-31.39 shrimp/tadpole). The WebPlotDigitizer tool (Rohatgi 2020) was used to extract data from published figures. The rate of shrimp consumption by carnivores was fit using the nls function in R (R Core Team 2014) with the default Gauss-Newton algorithm. Models describing different potential impacts of omnivores relative to carnivores were compared. Carnivore predation rates were weighted by either the shrimp handling time ratio of omnivores to carnivores (6/21), gut content ratio (37.5/84.9) (Pomeroy 1981), or both to predict omnivore predation rates. The model with the lowest AIC was selected.

### *Describing tadpole morph reaction norms*

The proportion of carnivores in a population increases as a function of shrimp abundance (Fig. 2.2). I was unable to find any study that reports both shrimp density and tadpole density alongside the proportion of carnivores in a population for *S. multiplicata* (nor the quantity of shrimp needed to induce morphological changes in a single tadpole). The best data available is Pomeroy (1981), which reports shrimp density and the proportion of carnivores during seven breeding events. Density of shrimp and the proportion of carnivores were measured on day 3-13 after oviposition, and the proportion of carnivores was also averaged across three or four sampling dates. For ponds initially measured after day four, I back-calculated the starting shrimp density for day four, the start of morph differentiation, using the shrimp predation rate model. The average field-observed tadpole density ( $0.54 \pm 0.91$  tadpoles/L) was then used to calculate the shrimp/tadpole density for each pond on day four after oviposition. I fit both a linear model as well as a power model using the `nls` function in R to predict the average proportion of carnivores in the population from shrimp-per-tadpole density data at the start of morph differentiation.

### *Selecting candidate two-strategy W-matrices*

I developed a two-strategy game theoretic model to describe the competitive system of omnivore and carnivore *S. multiplicata* developmental morphs. Based on the ecology of *S. multiplicata* morphs, I restricted the ranges of values for payoffs for each pair of strategies ( $W_{ij}$ ) in potential payoff matrices ( $W$ ) describing this system.

Because carnivores exhibit strong negative frequency-dependence due to competition for food (Pfennig 1992a), I fixed the payoff for carnivores in competition with other carnivores at  $W_{CC} = -1$ . Omnivores potentially exhibit negative frequency-dependence driven by food limitation (Pfennig 1992b; Friedman and Sinervo 2016), but they also may exhibit positive frequency-dependence, as they form feeding aggregations to protect themselves from cannibalism (Pomeroy 1981). Therefore, I allowed a range of possible values  $W_{OO} = [-1,1]$ . The potential ranges of payoffs for omnivores and carnivores in competition reflect the fact that carnivore morphs outperform omnivores when fairy shrimp are present as a food source (Pomeroy 1981), thus ( $W_{OC} = [-1,0]$ ,  $W_{CO} = [0,1]$ ). Finally, because the proportion of carnivores in a population is linearly predicted by the shrimp-per-tadpole density at day four, I set  $W_{OC} = -W_{CO}$  so that the proportion of carnivores in a population would vary from 0% to 100% linearly with a slope of 1, based on the value of  $W_{CO}$ .

A set of candidate payoff matrices was generated by assembling every potential combination of payoffs for each strategy  $W_{ij}$ , iterating values by 0.01 within their potential ranges. For a fixed value of  $W_{OO} = 0$ , reflecting neutral competition among omnivores, I predicted  $W_{OC}$  and  $W_{CO}$  from the shrimp-per-tadpole density on day four using the tadpole reaction norm linear model. Finally, I adjusted the model so that populations would have 0% carnivores when shrimp are absent at any value of  $W_{OO}$  by modifying the  $W_{OC}$  and  $W_{CO}$  payoffs. Payoff matrices were tested for the presence of an internal Sink equilibrium under continuous time replicator dynamics

across all possible ranges of shrimp-to-tadpole densities and payoffs (Friedman and Sinervo 2016).

### *Incorporating the switcher strategy*

Tadpoles are able to revert from carnivore morph back to omnivore morph (Pfennig 1992a), however no studies have attempted to quantify the proportion of switcher morphs in the wild. Following population manipulations in cordoned sections of a pond, excess carnivores switched to omnivores at a steady rate over time (Pfennig 1992b). Because this relationship is linear, it is reasonable to assume that on average, switchers spend 50% of their development as carnivores and 50% as omnivores. Therefore, I calculated the payoff for the switcher strategy as the average payoff for omnivores and carnivores. The morphological changes switchers undergo presumably come with a metabolic cost (Friedman and Sinervo 2016), so a fitness penalty ( $p = [-1,0]$ ) was applied to the payoffs for the switcher strategy. The payoff for switchers' own-type competition ( $W_{SS}$ ) was calculated as the average of payoffs for  $W_{OO}$ ,  $W_{OC}$ ,  $W_{CO}$ , and  $W_{CC}$  both with and without the fitness penalty. I also tested whether omnivores and carnivores competing against the switcher strategy might experience a corresponding fitness advantage.

I tested for an internal stable state in three-strategy games across the range of possible shrimp-to-tadpole densities, calculating payoffs to switchers including a fitness cost, to switchers' own-type competition with and without a fitness cost, and

to competitors of switchers with and without a fitness benefit. The payoffs for omnivores and carnivores remained the same.

*Effect of temperature on time to metamorphosis and pond duration*

At the equilibrium frequencies supplied by the game theory model, each morph has equal average fitness at metamorphosis. However, many tadpoles never reach metamorphosis (Pfennig et al. 1991). Carnivores can metamorphose in as little as 12 days, while omnivores take a minimum of 17 days, however, in a desert environment, pond drying time can have a big impact on morph fitness (Pomeroy 1981; Pfennig 1990a). Smaller body mass at metamorphosis lowers survivorship, therefore resource limitation during development affects the overall fitness of *S. multiplicata* morphs (Pomeroy 1981; Pfennig et al. 1991). Unfortunately, there is little empirical data describing the effects of tadpole density and resource limitation on time to metamorphosis or size at metamorphosis. I analyzed the contribution of environmental temperature on both the speed of tadpole development and the rate of pond drying.

As ectotherms, tadpoles' developmental rate responds to environmental temperature (Angilletta et al. 2002). Warmer temperatures may speed tadpole development, but they will also speed pond drying. Buchholz and Hayes (2000) describe the time to metamorphosis of omnivore *S. multiplicata* fed rabbit chow ad libitum and grown under different temperature regimes. I fit a linear model to predict the number of Gosner stages of development that omnivore tadpoles experience per

day, based on average environmental temperature. Tadpoles undergo 46 Gosner stages during development, the 46<sup>th</sup> stage being metamorphosis (Gosner 1960). *S. multiplicata* must complete metamorphosis before their natal ponds dry.

Pond duration is challenging to estimate since most evapotranspiration models have factors that are not easily predicted for future climate scenarios (Pyke 2004; Sabziparvar et al. 2010; Harwell 2012). I used the Hamon method because it requires only saturation vapor density (*SVD*), calculated from average daily air temperature, and hours of daylight (*D*) at a given site (Hamon 1960; Harwell 2012). This measurement estimates daily evaporation in fill inches for Class A containers (cylindrical metal containers of a fixed size) and is used as a proxy for natural reservoirs. A site-specific multiplier, the pan coefficient, can be used to adjust the Hamon estimates to predict evaporation from naturally-occurring ponds (Harwell 2012).

$$\frac{evap}{day} = (0.55) \times \left(\frac{D}{12}\right)^2 \left(\frac{SVD}{100}\right) \quad (2.1)$$

Daylength was calculated using the function `daylengthFUN` in the R package `Mappinguari` (Caetano et al. 2019). Average daily temperatures were obtained using WorldClim average daily temperature rasters (10x10 km, 5 arcmin resolution) for the near past (WorldClim v2.1 1970-2000) and by averaging maximum and minimum daily temperature rasters for future climate predictions under the CMIP6 BCC-CSM2-MR ssp585 scenario (WorldClim v2.1 2061-2080) ([worldclim.org](http://worldclim.org)). I used the Hamon equation to compare the time to complete evaporation for Class A containers

during both climatic time frames, based on average daily temperatures for the six months with the highest rainfall, May-October.

Student's t-test was used to test whether climatic variables differ significantly between time frames. I used an equal proportions test to compare the proportion of raster cells within *S. multiplicata*'s range where the average duration of Class A containers for May-October falls within the following bins: under 12 days, 12-17 days, 17-45 days, and above 45 days under the near past and future climate scenarios. The longest time recorded for tadpole metamorphosis is around 45 days, under resource-limited conditions (Pomeroy 1981).

## Results

### *Quantifying shrimp predation rates*

The estimated starting experimental shrimp-per-tadpole density (SPT) was 25.93 in the experimental ponds. The best model of shrimp predation weights the impact of omnivores compared to carnivores by both the shrimp handling time and gut content ratios for fairy shrimp.

$$SPT = 25.93 \times e^{[-0.2077 \times Time] \times \left( p_C + \left( \frac{6}{21} \right) \left( \frac{37.5}{84.9} \right) \times p_O \right)} \quad (2.2)$$

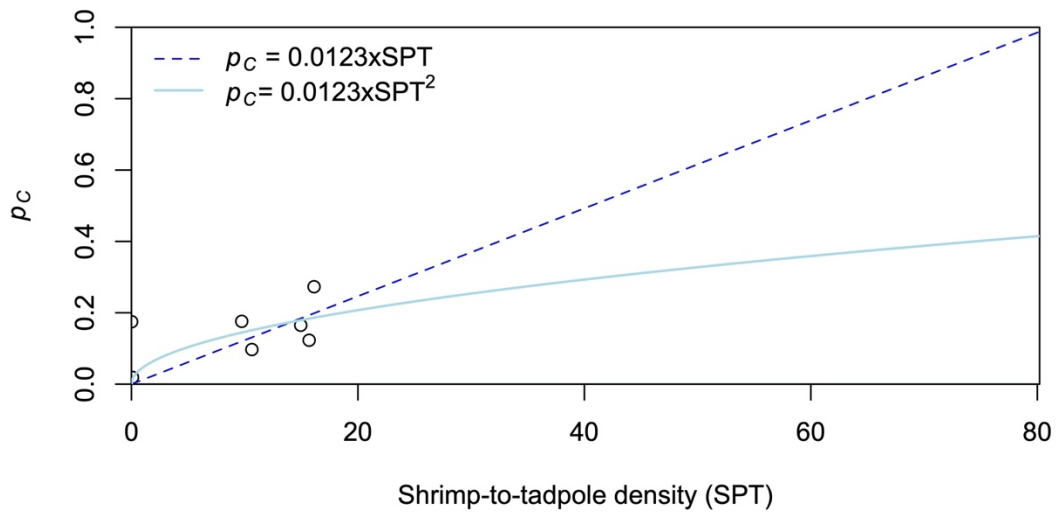
### *Describing tadpole morph reaction norms*

For both the power and linear models, the population has 100% omnivores at shrimp-to-tadpole densities of zero. For the linear model, the population has 100% carnivores at a shrimp-to-tadpole density of 81.2. For the power model, the shrimp-

to-tadpole density required for a population to have 100% carnivores is considerably higher than the linear model (Fig. 2.2). Because populations with 100% carnivores have been seen in nature, albeit under unusually high abundance of shrimp (Pomeroy 1981), I used the linear model in subsequent modeling steps. The linear model that best describes the tadpole reaction norm based on the starting shrimp-to-tadpole density is:

$$p_C = 0.0123 \times SPT \quad (2.3)$$

Figure 2.2. Fitted tadpole reaction norms to shrimp-to-tadpole density. Dashed line shows linear model and solid line shows power model. Open circles show experimental populations from Pomeroy (1981).



### *Selecting candidate two-strategy W-matrices*

Using the linear tadpole reaction norm to define  $W_{OC}$  and  $W_{CO}$ , only  $W_{OO} = 0$  results in 0-100% carnivores at equilibrium across the range of plausible values for shrimp-to-tadpole density (0-81.2 SPT).

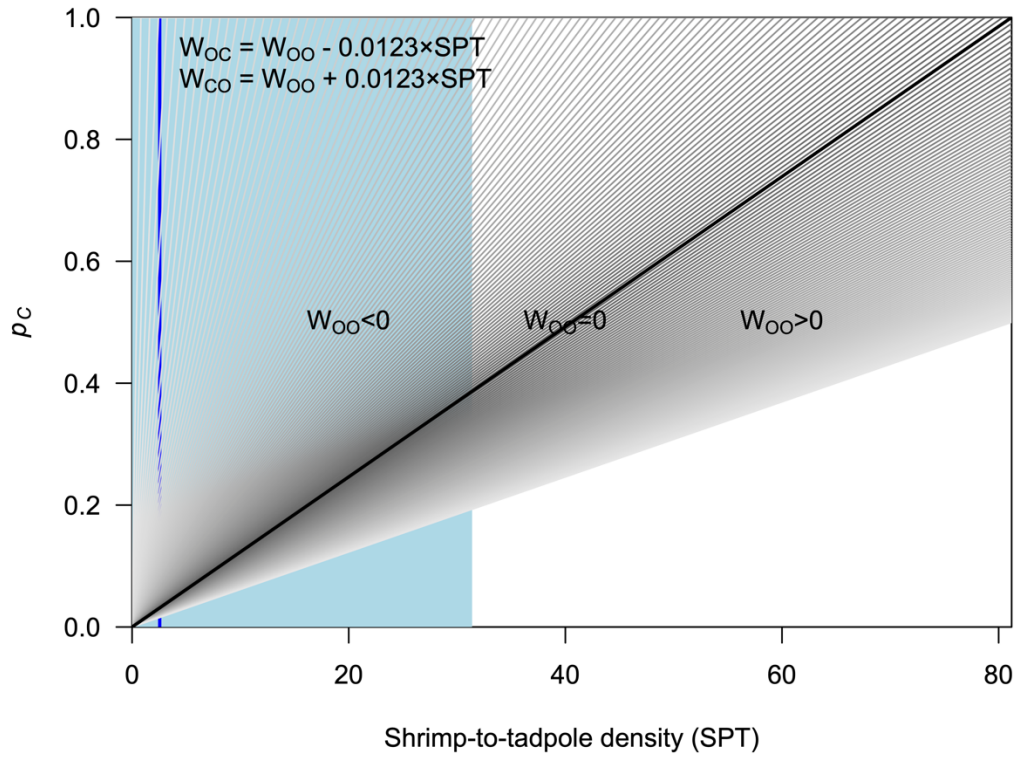
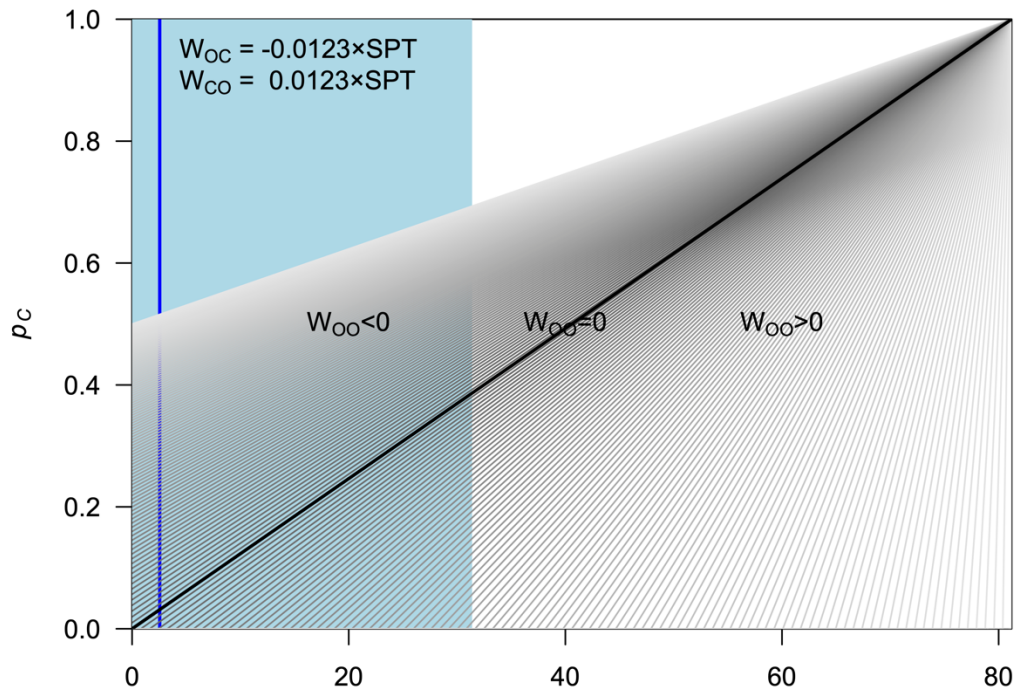
$$W = \begin{array}{c|cc} & \text{O} & \text{C} \\ \hline \text{O} & 0 & -0.012 \cdot SPT \\ \hline \text{C} & 0.0123 \cdot SPT & -1 \end{array} \quad (2.4)$$

Under this model, when omnivores experience food-limitation ( $W_{OO} < 0$ ), populations will always have some carnivores, even in the absence of shrimp (Fig. 2.3, top panel). Adjusting the tadpole reaction norm equation by setting the intercept to  $W_{OO}$  changes the equilibrium dynamics of the model.

$$W = \begin{array}{c|cc} & \text{O} & \text{C} \\ \hline \text{O} & [-1,1] &  $W_{OO} - (0.0123 \cdot SPT)$  \\ \hline \text{C} &  $W_{OO} + (0.0123 \cdot SPT)$  & -1 \end{array} \quad (2.5)$$

In the new model, the proportion of carnivores is zero at all values of  $W_{OO}$  when no shrimp are present. Populations in which omnivores experience stronger competition (have smaller values of  $W_{OO}$ ) reach 100% carnivores at lower shrimp-to-tadpole densities (Fig. 2.3, bottom panel). The value of  $W_{OO}$  will vary by pond and should scale to detritus nutritional value-to-tadpole density in a manner similar to shrimp-to-tadpole density. The payoffs  $W_{OO}$ ,  $W_{OC}$  and  $W_{CO}$  reflect both frequency- and density-dependence, while the payoff  $W_{CC}$  reflects strong negative frequency-dependence.

Figure 2.3. Graphs show the proportion of carnivores at equilibrium at a range of shrimp-to-tadpole ratios for populations with different values of  $W_{00} \in [-1,1]$ . Top panel shows the equilibrium frequency of carnivores calculated using the tadpole reaction norm equation with intercept of 0. Bottom panel shows the equilibrium frequency of carnivores calculated using the adjusted tadpole reaction norm equation with intercept of  $W_{00}$ . The blue rectangles indicate the range of shrimp-to-tadpole densities and the dark blue lines shows the mean observed in the field in Pfennig et al. 1991.



### *Incorporating the switcher strategy*

I tested games both with and without a fitness advantage to strategies in competition against switchers, and with and without a fitness penalty for switchers competing against switchers. No magnitude of fitness penalty [-1,0] to switchers in competition against omnivores or carnivores resulted in a stable 3-strategy game at any shrimp-to-tadpole density nor in any combinations of fitness penalty and benefit tested. The switcher strategy was unable to invade the two-strategy system in any scenario.

### *Effect of temperature on time to metamorphosis and pond duration*

Omnivores' development responds linearly to environmental temperature (T):

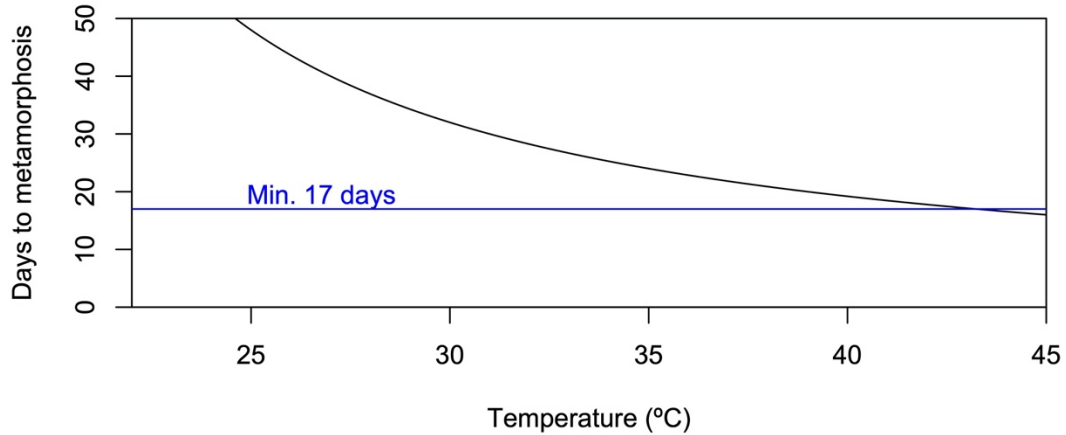
$$\frac{\text{Gosner stages}}{\text{day}} = (0.0958 \cdot T) - 1.437 \quad (2.6)$$

Comparable developmental data does not exist for carnivore morphs. Because Gosner stages describe a fixed number of developmental checkpoints until metamorphosis at stage 46, this equation can be used to predict the number of days until metamorphosis under a range of average temperatures:

$$\text{days to metamorphosis} = \frac{46}{(0.0958 \cdot T) - 1.437} \quad (2.7)$$

The minimum time to metamorphosis for omnivores observed in the field is 17 days (Pomeroy 1981; Pfennig 1990a). This model predicts that omnivore tadpoles will develop in 17 days at 43.2 °C (Fig. 2.4), which is above the critical maximum temperature for the closely-related (but more northerly-distributed) species *Spea hamondii* (Brattstrom 1968).

Figure 2.4. Plot of model predicting number of days to omnivore metamorphosis under different environmental temperatures. The blue line shows the minimum reported time to metamorphosis for omnivores.



Both precipitation and temperature are predicted to change significantly between the near past (1970-2000) and future (2061-2080) across *S. multiplicata*'s range in nearly every month (all p-values < 0.001, except March precipitation: p = 0.0101, May precipitation: p = 0.0813) (Fig. 2.5). The Class A containers fall at the lower end of the size range of breeding pools for *S. multiplicata*. Natural breeding pools range between 5-200 cm deep (mean  $46 \pm 8.2$  cm) with surface area to volume ratios from 1.3-55 (mean  $11.5 \pm 1.9$ ) (Pfennig 1990a). Class A containers are smaller than the mean breeding pool size at 20.32 cm deep, with a surface area to volume ratio of 4.875. The average number of days a filled Class A container needs to empty evaporatively is significantly different between the near past and future climate projections in every month (all p-values < 0.001).

The proportion of raster cells where Class A containers remain filled for each category (under 12 days, 12-17 days, 17-45 days, and above 45 days) was significantly different between the near past and future climatic time frames (all p-

Figure 2.5. Boxplot of average precipitation (top panel) and average daily temperature by month (bottom panel) in 1970-2000 and 2061-2080. Yellow box indicates the six months with the highest rainfall, May-October.

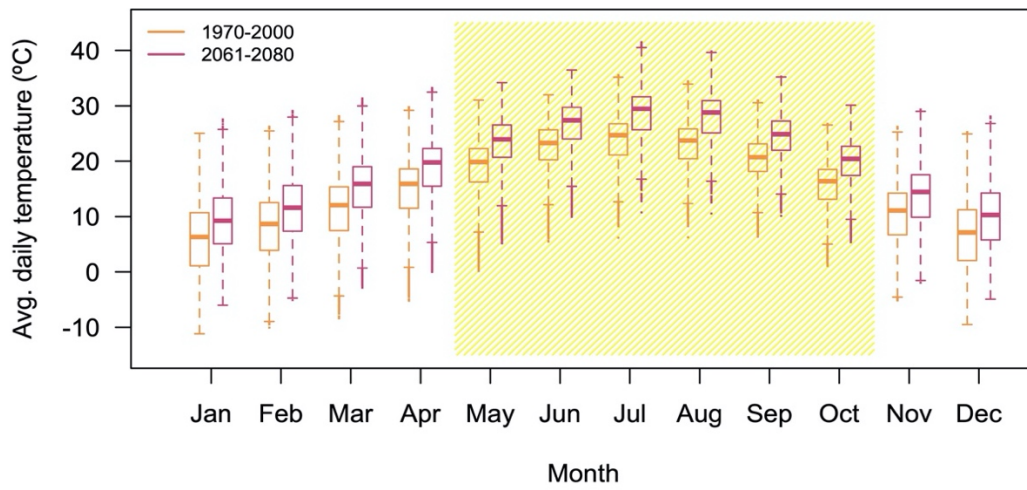
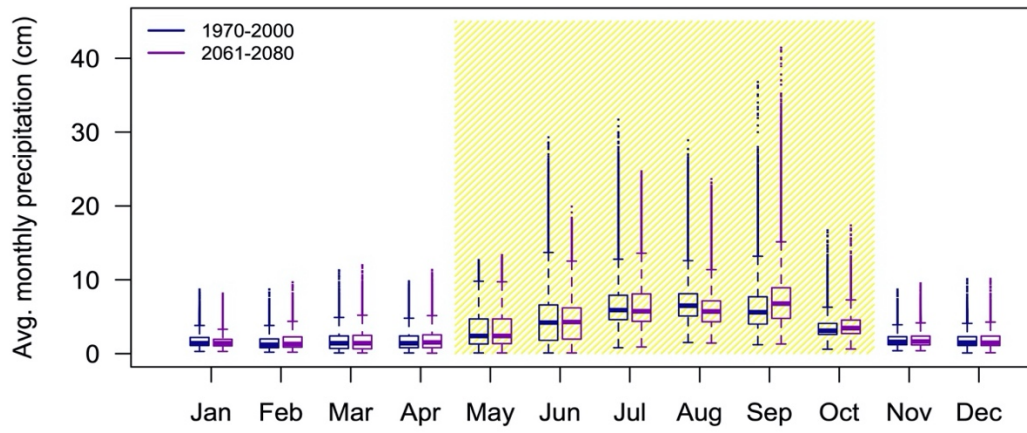
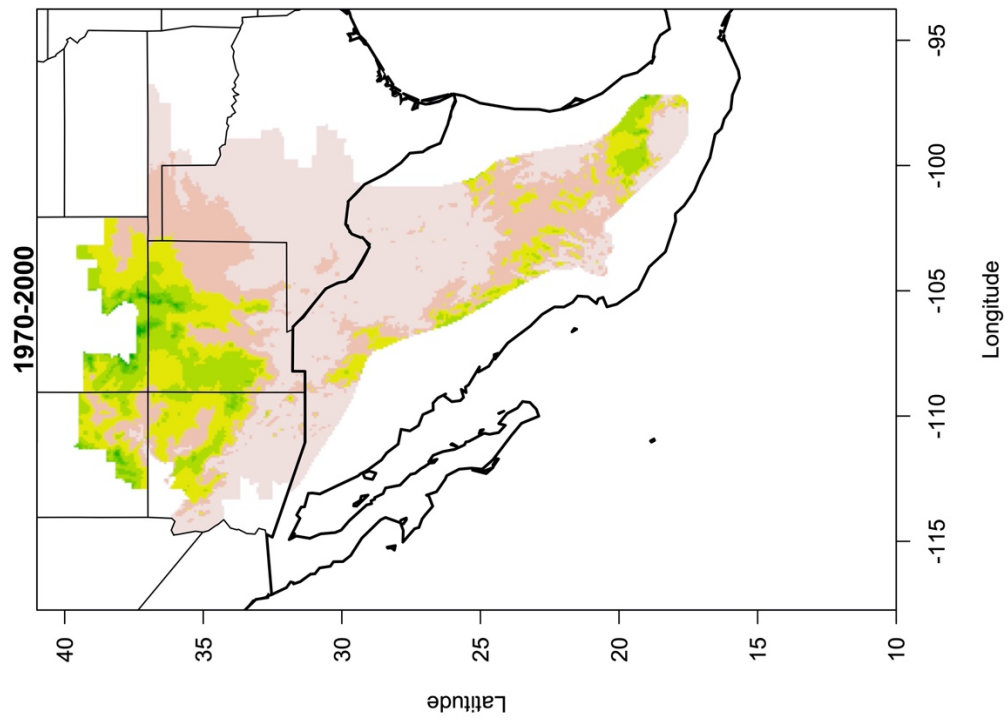
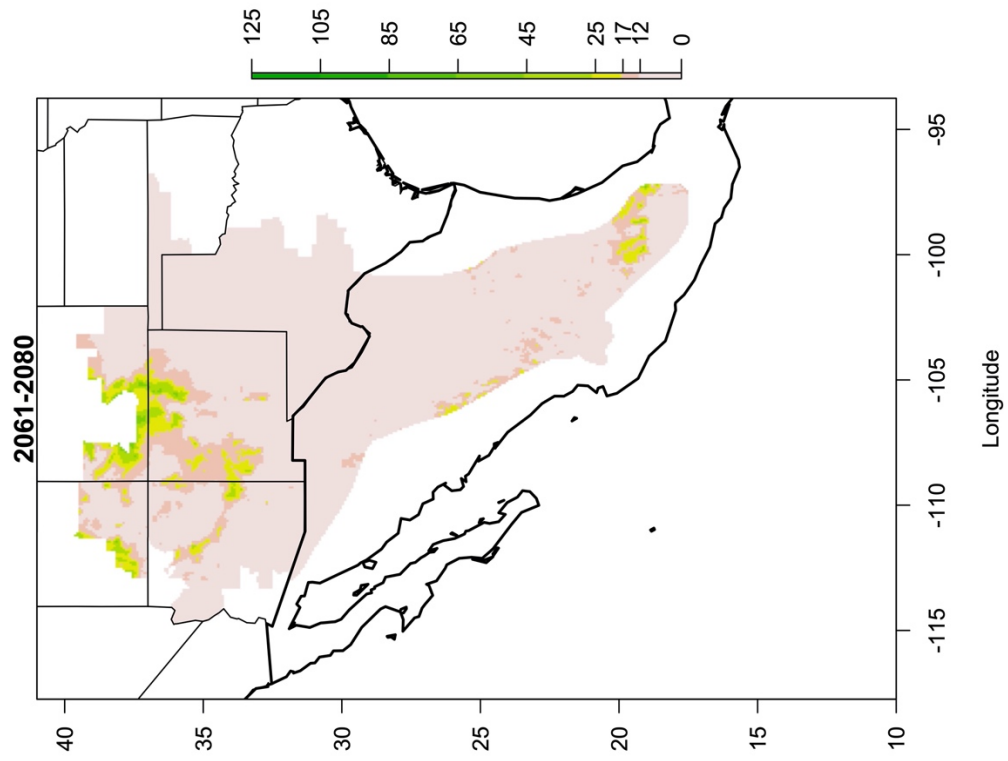


Figure 2.6. Map of average time for Class A containers to empty evaporatively from May-October in 1970-2000 (left panel) and 2061-2080 (right panel), predicted using the Hamon method.



values  $< 0.001$ ). Under future climate projections, Class A containers evaporate in under 12 days over twice as much of *S. multiplicata*'s range than in the near past (1970-2000: 47.71%, 2061-2080: 84.50%), and the proportions of all other duration categories decrease substantially (Fig. 2.6).

## **Discussion**

Polymorphisms can be maintained in an evolutionary stable state (ESS) when the strategies have equal average fitness at equilibrium. It follows that polyphenisms are maintained by a similar evolutionary process: morphs have equal average fitness across all environments, weighted by the frequency of different environments, the Grand Mean (Via 1993). Selection occurring within the environments shapes the reaction norm, which is maintained through gene flow (Crispo 2008). Supporting this view, the lifetime reproductive fitness of polyphenic tiger salamanders is the same for both paedomorphic and metamorphosing adults (Lackey et al. 2019). A major challenge in modeling polyphenisms is that they may not directly affect fecundity but greatly affect survival.

Game theoretic models are able to implicitly capture the effects of a variety of ecological and demographic factors as long as lifetime fitness outcomes are known for all competing strategies. Fitness is typically measured as a combination of survivorship and fecundity. Modeling the effects of environment on morph fitness poses a challenge for *S. multiplicata* because neither fitness component has been quantified for both morphs. The factors influencing morph fitness can still be

modeled mechanistically, however. Because *S. multiplicata* developmental morphs are indistinguishable after metamorphosis, average fecundity per morph is not known, so I focus on factors that influence the survivorship measure of fitness. This requires partitioning fitness into two components: morph determination, and average morph survivorship. The first component, fitness based on morph frequency, depends on resource availability at the pond level and follows many of the same assumptions as the ecological model Ideal Free Distribution (Kennedy et al. 1993). The second component of fitness, survivorship, depends on the proportions of each morph that reach metamorphosis and short-term survivorship after metamorphosis.

The two-strategy game theoretic model I developed gives the equilibrium frequency for a single pond in which morphs have equal average fitness based on resource levels. Because tadpoles develop as omnivores unless carnivory is dietarily triggered, both the payoffs for the omnivore strategy ( $W_{OO}$  and  $W_{OC}$ ) and the payoff for the carnivore strategy in competition with omnivores ( $W_{CO}$ ) depend on the resource levels available to omnivores. By setting the value of  $W_{OO}$  as the intercept of the reaction norm equations for both  $W_{OC}$  and  $W_{CO}$ , these payoffs reflect the relative advantage a carnivorous diet confers compared to omnivory. Because the nutritional value of detritus has never been quantified, the value of  $W_{OO}$  lacks units, but it should scale with the detritus nutritional value-to-tadpole density. Nevertheless, this model is robust and functions at a range of values of  $W_{OO}$  which might reflect the range of values for competition for detritus in nature (Fig 2.3).

Likewise, the tadpole morph reaction norm has not been explicitly described through experiments. To calculate the relationship between the proportion of carnivores in experimental populations and the shrimp-to-tadpole density, I had to make assumptions about tadpole density. If experimental data becomes available, this model can be easily modified to reflect any changes in the reaction norm model slope or curve shape. Finally, we know that a third strategy, switcher, exists in nature (Pfennig 1992*b*), therefore there must be a set of payoffs for switcher that result in a stable three-strategy game. The assumptions I applied to switcher strategy fitness were not sufficient for model stability. It is likely that the switcher strategy arises to correct deviations from the optimal morph frequency within a pond (Pfennig 1992*b*; Friedman and Sinervo 2016). Animals are more likely to exceed their perception limits and deviate from optimality in higher-density populations, where it is harder to assess the competitive environment (Tregenza 1995). Payoffs for the switcher strategy may reflect strong density-dependence. Because errors in morph determination result in lower fitness due to increased competition for fairy shrimp, the switcher strategy would be selected for due to increased switcher survivorship compared to excess carnivores. Therefore, this morph would only be stable in models that account for the impact of resource limitation on morph fitness.

There is less empirical data to parameterize a model for the survivorship component of *S. multiplicata* fitness. Resource levels and tadpole density both impact morph fitness: both omnivores and carnivores will lengthen time to metamorphosis and metamorphose at a smaller body size if resource-limited (Pomeroy 1981), and

omnivore survivorship post-metamorphosis increases with body mass (Pfennig et al. 1991). Carnivores metamorphose at a larger average body length than omnivores, but have smaller average body weight at all sizes (Pomeroy 1981), so the relationship between body size and post-metamorphosis survivorship may differ between omnivores and carnivores. Because the impact of resource levels (particularly detritus) on growth and carnivore survivorship have never been quantified, these aspects of fitness cannot be explicitly modeled. I was able to model the effect of environmental temperature on time to metamorphosis for omnivores and on pond duration.

Higher temperatures result in faster tadpole development (Buchholz and Hayes 2000), however, the model for temperature and minimum time to metamorphosis likely underestimates the maximum developmental. The minimum time to metamorphosis in the wild for omnivores (17 days) is predicted to occur at improbably high average temperatures ( $>40$  °C) under this model (Fig. 2.4). It is possible that the minimum time to metamorphosis for omnivores was experimentally underestimated when tadpoles were fed a diet of rabbit chow, as omnivores in the wild do supplement their detritus and algae diet with fairy shrimp and other high-energy food sources (Pomeroy 1981).

*S. multiplicata*'s breeding season is unlikely to experience dramatic shifts throughout much of range, as rainfall is highest during May-October in both the near past and future climate projections. Precipitation levels are significantly different during most months under the CMIP6 BCC-CSM2-MR ssp585 future climate

scenario, but rainfall is actually predicted to increase during February-April and September-November, which may allow for shifts in breeding season in some regions. Most of *S. multiplicata*'s range is predicted to experience significantly higher temperatures during the breeding season. Class A containers are predicted to evaporatively empty significantly faster under future climate projections than the near past (Fig. 2.6). Across the majority of their range, containers are predicted to dry in less time than the shortest recorded time to metamorphosis for *S. multiplicata* tadpoles (<12 days). This climate scenario strongly favors faster-developing carnivore morphs. However, these measurements should be interpreted with caution, as Class A containers are less than half the size of average *S. multiplicata* breeding ponds (Pfennig 1990a). It is possible to improve these estimates through modification of the Hamon equation using measured pan coefficients to predict evaporation from specific bodies of water.

Although it is not possible to fully model both fitness based on morph frequency and fitness based on survivorship due to lack of appropriate data for some fitness parameters, I have addressed the main questions regarding the ecological impact of plasticity in *S. multiplicata*: time lag between environmental conditions and plastic response, reversibility of plastic response, and the shape of the reaction norm (Miner et al. 2005). I have identified areas where more study can fill in the knowledge gaps. The reaction norm for this species can be quantified more explicitly through experiments which control for shrimp-to-tadpole density. Likewise, the effect of resource limitation, particularly detritus, on time to metamorphosis and

survivorship shortly after metamorphosis need to be quantified. Finally, the conditions under which the switcher strategy appears in the wild have never been studied.

Plasticity in *Spea* becomes even more complicated when interspecies competition is considered. *S. multiplicata* has two sympatric congeners, *S. bombifrons* and *Scaphiopus couchii*. *S. bombifrons* has both omnivore and carnivore developmental morphs, while *Sc. couchii* tadpoles are all omnivorous. In ponds where *S. bombifrons* and *S. multiplicata* co-occur, *S. bombifrons* is more likely to develop carnivorous morphs while *S. multiplicata* remain omnivorous (Levis and Pfennig 2019). In fact, *S. bombifrons* tadpoles frequently become carnivores, regardless of diet (Levis et al. 2018). *S. bombifrons* and *S. multiplicata* have evolved different reaction norms (*S. bombifrons* would have a steeper slope), shifting the mean phenotypes of each population (Via 1993). On the other extreme, *S. multiplicata* develop more carnivorous morphs when in sympatry with *Sc. couchii* (Buchholz and Hayes 2000). *Sc. couchii* omnivores outcompete *S. multiplicata* omnivores; they metamorphose more quickly at a smaller body size than *S. multiplicata* (Buchholz and Hayes 2000). Equilibrium morph frequencies can be calculated in ponds with multiple species as long as the reaction norms of both species have been described by using a two-population game theory model (Friedman and Sinervo 2016). Competition between two species with different reaction norms results in character displacement in the expressed polyphenisms between species. Thus plasticity may maintain species coexistence by reducing direct competition between similar morphs

(Miner et al. 2005; Levis and Pfennig 2019). Climate change may alter these species interactions, if faster-drying ponds favor carnivore morphs in *S. multiplicata*, even in sympatry.

Plasticity in *S. multiplicata* could alternately be modeled using a Lefkovich matrix to explicitly incorporate transitions between morph types (Friedman and Sinervo 2016). This approach would merge the morph frequency and survivorship components of fitness. However, this approach would require more data on transitions between all three strategies and the effects of resource levels, density, and temperature on time to metamorphosis for each strategy. It appears likely that climate change will alter the selective pressure on this species' morphs, and understanding how the various ecological factors affect fitness of each polyphenism will allow us to test hypotheses about evolution of plasticity and reaction norms. Given the debate about mechanisms of evolution in plastic systems, working towards a complete understanding of fitness in *S. multiplicata* may help clarify the mechanisms of selection on plastic traits.

## Citations

- Angilletta, M. J., P. H. Niewiarowski, and C. A. Navas. 2002. The evolution of thermal physiology in ectotherms. *Journal of Thermal Biology* 27:249–268 Invited.
- Bomze, I. M. 1983. Lotka-Volterra equation and replicator dynamics: A two-dimensional classification. *Biological Cybernetics* 48:201–211.
- Brattstrom, B. H. 1968. Thermal acclimation in Anuran amphibians as a function of latitude and altitude. *Comparative Biochemistry And Physiology* 24:93–111.
- Buchholz, D. R., and T. B. Hayes. 2000. Larval period comparison for the spadefoot toads *Scaphiopus couchii* and *Spea multiplicata* (Pelobatidae: Anura). *Herpetologica* 56:455–468.
- Caetano, G., J. Santos, and B. Sinervo. 2019. Mappinguari: Process-Based Biogeographical Analysis. R package.
- Charnov, E. 1982. Alternative life-histories in protogynous fishes: A general evolutionary theory. *Marine Ecology Progress Series* 9:305–307.
- Creusere, F. M., and W. G. Whitford. 1976. Ecological relationships in a desert Anuran community. *Herpetology* 32:7–18.
- Crispo, E. 2008. Modifying effects of phenotypic plasticity on interactions among natural selection, adaptation and gene flow. *Journal of Evolutionary Biology* 21:1460–1469.
- de Jong, G. 2005. Evolution of phenotypic plasticity: Patterns of plasticity and the emergence of ecotypes. *New Phytologist* 166:101–118.
- Friedman, D., and B. Sinervo. 2016. Evolutionary Games in Natural, Social, and Virtual Worlds. *Evolutionary Games in Natural, Social, and Virtual Worlds*.
- Gosner, K. L. 1960. A simplified table for staging anuran embryos and larvae with notes on identification. *Herpetologica* 16:183–190.
- Hamon, W. R. 1960. *Estimating potential evapotranspiration*.
- Harwell, G. R. 2012. Estimation of evaporation from open water—A review of selected studies, summary of U.S. Army Corps of Engineers data collection and methods, and evaluation of two methods for estimation of evaporation from five reservoirs in Texas. U.S. Geological Survey Scientific Investigations Report 2012–5202 96.

- Kennedy, M., R. D. Gray, M. Kennedy, and R. D. Gray. 1993. Can ecological theory predict the distribution of foraging animals? A critical analysis of experiments on the Ideal Free Distribution. *Oikos* 68:158–166.
- Lackey, A. C. R., M. P. Moore, J. Doyle, N. Gerlanc, A. Hagan, M. Geile, C. Eden, et al. 2019. Lifetime fitness, sex-specific life history, and the maintenance of a polyphenism. *American Naturalist* 194:230–245.
- Levis, N. A., S. de la Serna Buzón, and D. W. Pfennig. 2015. An inducible offense: Carnivore morph tadpoles induced by tadpole carnivory. *Ecology and Evolution* 5:1405–1411.
- Levis, N. A., A. J. Isdaner, and D. W. Pfennig. 2018. Morphological novelty emerges from pre-existing phenotypic plasticity. *Nature Ecology and Evolution* 2:1289–1297.
- Levis, N. A., and D. W. Pfennig. 2019. How stabilizing selection and nongenetic inheritance combine to shape the evolution of phenotypic plasticity. *Journal of Evolutionary Biology* 32:706–716.
- Miner, B. G., S. E. Sultan, S. G. Morgan, D. K. Padilla, and R. A. Relyea. 2005. Ecological consequences of phenotypic plasticity. *Trends in Ecology and Evolution* 20:685–692.
- Padilla, D. K., and M. M. Savedo. 2013. A systematic review of phenotypic plasticity in marine invertebrate and plant systems. *Advances in Marine Biology* 65:67–94.
- Pfennig, D. 1990a. The adaptive significance of an environmentally-cued developmental switch in an anuran tadpole. *Oecologia* 85:101–107.
- Pfennig, D. W. 1990b. “Kin recognition” among spadefoot toad tadpoles: a side-effect of habitat selection?” *Evolution* 44:785–798.
- . 1992a. Proximate and functional causes of polyphenism in an anuran tadpole. *Functional Ecology* 6:167–174.
- Pfennig, D. W. 1992b. Polyphenism in spadefoot toad tadpoles as a locally adjusted stable strategy. *Evolution* 46:1408–1420.
- Pfennig, D. W., and W. A. Frankino. 1997. Kin-mediated morphogenesis in facultatively cannibalistic tadpoles. *Evolution* 51:1993.
- Pfennig, D. W., A. Mabry, and D. Orange. 1991. Environmental causes of correlations between age and size at metamorphosis in *Scaphiopus multiplicatus*. *Ecology* 72:2240–2248.

- Pigliucci, M., C. J. Murren, and C. D. Schlichting. 2006. Phenotypic plasticity and evolution by genetic assimilation. *Journal of Experimental Biology* 209:2362–2367.
- Policansky, D. 1982. Sex change in plants and animals. *Annual review of ecology and systematics*. Volume 13 471–495.
- Pomeroy, L. v. 1981. Developmental polymorphism in the tadpoles of the spadefoot toad *Scaphiopus multiplicatus*.
- Pyke, C. R. 2004. Simulating vernal pool hydrologic regimes for two locations in California, USA. *Ecological Modelling* 173:109–127.
- R Core Team. 2014. R: A language and environment for statistical computing. R Foundation for Statistical Computing, Vienna, Austria. URL <http://www.R-project.org/>.
- Rohatgi, A. 2020. WebPlotDigitizer. Pacifica, CA, USA.
- Sabziparvar, A. A., H. Tabari, A. Aeini, and M. Ghafouri. 2010. Evaluation of class a pan coefficient models for estimation of reference crop evapotranspiration in cold semi-arid and warm arid climates. *Water Resources Management* 24:909–920.
- Santos-Barrera, G., G. Hammerson, and P. Ponce-Campos. 2010. *Spea multiplicata*. The IUCN Red List of Threatened Species 2010: e.T59047A11875070.
- Schlichting, C. D. 1986. The evolution of phenotypic plasticity in plants. *Annual Review of Ecology and Systematics* 17:667–693.
- Stebbins, R. C. 2003. *A Field Guide to Western Reptiles and Amphibians* (Peterson Field Guides). Peterson Field Guides.
- Taborsky, M., R. F. Oliveira, and H. J. Brockmann. 2008. The evolution of alternative reproductive tactics. *Alternative Reproductive Tactics: An Integrative Approach*.
- Tregenza, T. 1995. Building on the Ideal Free Distribution. *Advances in Ecological Research* 26:253–307.
- van Tienderen, P. H. 1991. Evolution of generalists and specialists in spatially heterogeneous environments. *Evolution* 45:1317–1331.
- Via, S. 1993. Adaptive phenotypic plasticity: target or by-product of selection in a variable environment? *The American Naturalist* 142:352–365.
- West-Eberhard, M. 1989. Phenotypic plasticity and the origins of diversity. *Annual Review of Ecology and Systematics* 20:249–278.

Yang, C. H., and J. A. Pospisilik. 2019. Polyphenism – A window into gene-environment interactions and phenotypic plasticity. *Frontiers in Genetics* 10:132.

## **Thermal ecology and extinction risk of New World day geckos (Sphaerodactylidae, Squamata) under climate change**

### **Introduction**

Anthropogenic climate change will have devastating effects on global biodiversity (Thomas et al. 2004; Sekercioglu et al. 2008; Sinervo et al. 2010; Bellard et al. 2012; Pinsky et al. 2019). Tropical ectotherms are considered at particular risk (Deutsch et al. 2008; Tewksbury et al. 2008; Huey et al. 2009; Sinervo et al. 2010; Laurance et al. 2011). Potentially 20% of all lizard species may go extinct globally, with a much higher rate projected for the tropics (Thomas et al. 2004; Huey et al. 2009; Sinervo et al. 2010). The New World tropics are a major center of biodiversity for reptiles and amphibians (Gaston et al. 1995). Together, these factors paint a bleak outlook for New World tropical lizards. However, compared to other latitudes and other taxa, few thermal ecology studies have been performed on reptiles in tropical latitudes (Sunday et al. 2011), making specific predictions for these regions difficult. Due to fundamental climatic and ecosystem differences between temperate and tropical regions, it is crucial to develop models of climate vulnerability of tropical species in the tropics, rather than apply temperate-based models in tropical regions (Zuk 2016).

Tropical ectotherms are broadly expected to be adapted to narrower ranges of temperatures (Tewksbury et al. 2008), because the tropics experience lower seasonal temperature variation than temperate regions (Janzen 1967; Ghalambor et al. 2006).

Most tropical species regularly experience temperatures close to the upper limit of the range of temperatures they can tolerate (Sunday et al. 2014). Therefore the thermoregulatory priority for tropical lizards in many habitats is to avoid high temperatures, rather than to seek heat, as temperate species do (Kearney et al. 2009). Tropical species of lizard are more likely to be thermoconformers, as opposed to basking heliotherms (Tewksbury et al. 2008), though even lizards deep in the Amazon rainforest are able to utilize light gaps in the canopy to bask (Diele-Viegas et al. 2018). Generalized predictions about tropical species neglect to account for the impact of microhabitat on the thermal landscape available to lizards (Sears et al. 2011, 2016).

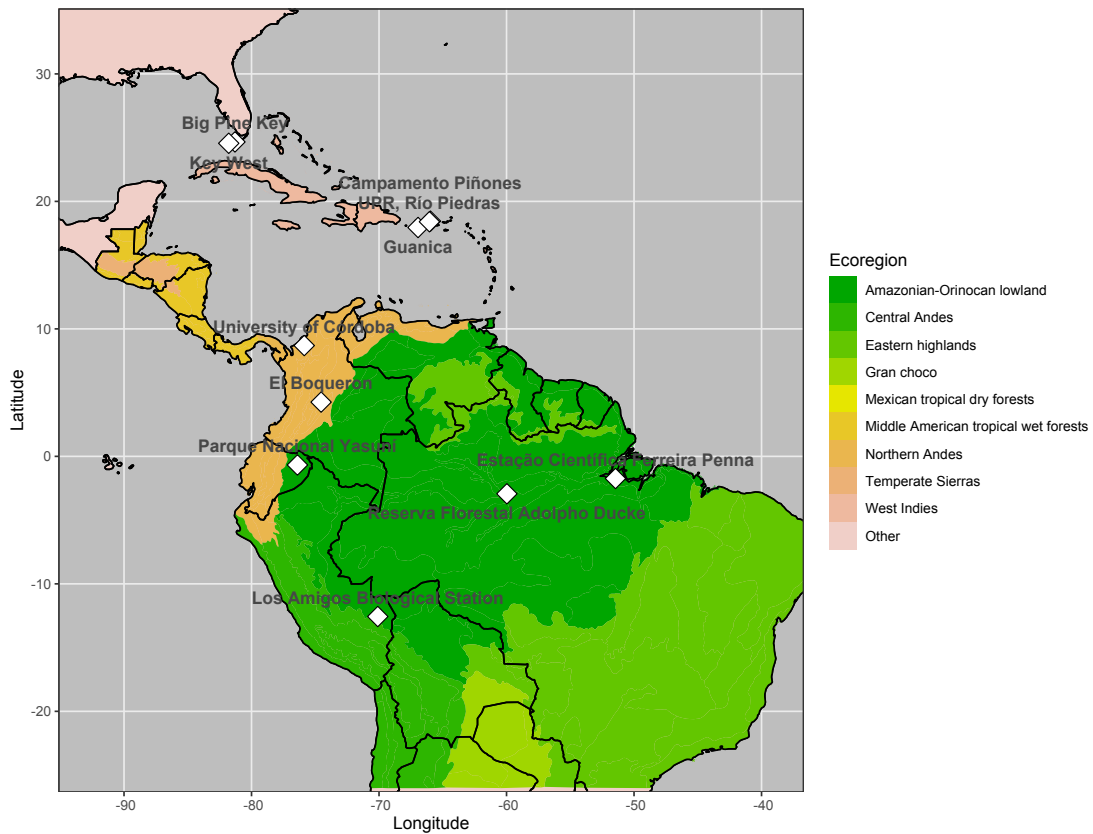
The thermal physiology of ectotherms evolves slowly in response to changes in environmental temperature (Huey and Kingsolver 1993; Etterson and Shaw 2001) and is subject to phylogenetic constraint (Huey and Kingsolver 1989), leaving lizards unable to keep pace with a rapidly warming climate. Sinervo et al. (2010) shows that latitude has a bigger impact on extinction risk than thermoregulatory mode. The tropics are predicted to experience a more rapid increase in seasonal mean temperature than temperate latitudes (Kirtman and Power 2020). By 2100 summer temperatures will surpass the hottest recorded temperatures, challenging organisms with a novel thermal environment (Battisti and Naylor 2009). Amazonian temperatures are predicted to rise 3.3°C this century, however deforestation could account for an additional 3–8°C of warming if habitat loss results in changes to the biophysical properties of the region (Foley et al. 2007; Malhi et al. 2008; Prevedello

et al. 2019). This means that tropical species in particular will likely face a shift in thermal environment that will outpace their ability to adapt, putting them at particular risk of extinction.

Because tropical species face different challenges than temperate species, tropical species require models developed with their particular biology in mind. Day geckos in the family Sphaerodactylidae (Squamata) are an excellent clade with which to study extinction risk in tropical lowland regions, as they have diversified across a broad range of habitats across the New World tropics (24°S–24°N), from Mexico to Brazil and across the Caribbean, in dry (xeric) scrub to wet tropical forest habitats, and across a broad elevational range (0 – 1,600 m) (Rivero-Blanco and Dixon 1979; Álvarez-Pérez 1992; Schargel 2008). The subfamily Sphaerodactylinae consists of six speciose New World genera *Aristelliger* (8), *Coleodactylus* (5), *Gonatodes* (25), *Lepidoblepharis* (21), *Pseudogonatodes* (7), and *Sphaerodactylus* (96) (via VertNet.org). The clade consists primarily of diurnal small-bodied thermoconformers (Álvarez-Pérez 1992; Vitt et al. 2005; Diele-Viegas et al. 2018). Despite the high risk of climate-driven extinction expected for tropical species, Sinervo et al. (2010) included a generalized analysis of this clade and concluded that no populations were predicted at risk of climate-driven extinction. In contrast, a study on *Gonatodes concinnatus* using methods derived from Sinervo et al. (2010) found that this species is at high risk of extinction by 2070 (Altamirano-Benavides et al. 2019). Because this group encompasses a large number of species across a variety of microhabitats,

detailed ecophysiological models are needed to explore species-level differences that might impact persistence across this clade.

Figure 3.1. Localities where sphaerodactyline thermal physiology measurements were taken in South America and the Caribbean during 2013-15.



I used an ecophysiology-based model to predict climate-driven extinctions of the sub-family Sphaerodactylinae in the New World tropics (Sinervo et al. 2010, 2019; Caetano et al. 2019). I measured thermal physiology properties of seven different species of sphaerodactyline lizards, including widespread mainland species and island species, leaf litter-dwelling and arboreal species, and species from wet forest and xeric habitats. Because lizards are able to take advantage of variation in

temperature across microhabitats, capturing fine-scale habitat variation is crucial to estimating the temperatures available (Sears et al. 2011; Kearney 2013; Clusella-Trullas and Chown 2014). The laboratory measurements of lizards' thermal physiological parameters were used to calculate the number of hours lizards are able to be active in the environment and their physical performance based on the microhabitat temperatures they would experience. Microhabitat temperatures were obtained from a dataset of high-resolution hourly estimates of microclimatic temperatures under specific altitude, shade, and substrate conditions (Kearney et al. 2014). Future climate predictions only report projected air temperatures, therefore near past air temperatures were then used to predict active hours in the environment and physical performance calculated under the microhabitat conditions. I used projected future air temperatures to assess habitat suitability in 2070 under future climate projections. Finally, species distribution models were used to assess habitat suitability under future climate conditions, and to identify species at risk from climate change.

## **Methods**

### *Thermal physiology data collection*

I measured thermal physiology parameters in seven species of sphaerodactylid lizards in South America and the Caribbean during 2013-15 at sites in Brazil, Colombia, Peru, Ecuador, and the United States (Fig. 3.1, Table 3.1).

Lizards were held in the lab for 3 days and fasted during the duration of trials. Due to

time constraints in the field, I was unable to measure  $CT_{min}$ ,  $CT_{max}$ , and performance parameters for three species: *G. albogularis*, *S. argus*, *S. elegans*. I obtained species records and additional thermal physiology data from literature (Álvarez-Pérez 1992; Vitt et al. 2000, 2005; Bruschi et al. 2016; Diele-Viegas et al. 2018).

Thermal preference ( $T_{pref}$ ) was measured on at least 10 males and 10 females of each species. Lizards were placed in a laboratory temperature gradient (20–40°C) and allowed to acclimate for 15 min. After the acclimation period, lizards were allowed to move freely in gradient for 1 hr 45 min. Body temperature was recorded with a thermocouple taped to each lizard's venter every 1 minute or by thermal gun (Transcat Amprobe IR-750) every 5 minutes. For small-bodied squamates such as these, surface and internal body temperature readings are indistinguishable (Luna and Font 2013). Thermal preference ( $T_{pref}$ ) was calculated as the average body temperature across all individuals during the recorded time frame (Paranjpe et al. 2012).

Critical thermal temperatures,  $CT_{min}$  and  $CT_{max}$ , are defined as the minimum and maximum body temperatures at which the righting response is lost. After  $T_{pref}$  trials were performed, I measured these values in five males and five females of each species. Lizards were placed in a container over an ice bath or hot water bath. Lizards' body temperature was monitored as the temperature of the water bath was regulated to increase or decrease body temperature by 1°C every 1 min (Herrando-Pérez et al. 2019). I tested lizards' righting reflex periodically by flipping them on

their backs and poking them to stimulate a righting response. The trial was stopped when the critical thermal limit was reached and the righting reflex was lost.

Afterwards, lizards were returned to ambient temperature.

Table 3.1. List of sphaerodactyline species included in this study, localities where thermal physiology measurements were taken, types of data collected, and habitat preference.

Species	Field sampling localities	Data	Habitat
<i>C. amazonicus</i>	<ul style="list-style-type: none"> <li>Reserva Florestal Adolpho Ducke, Amazonas, Brazil</li> <li>Estação Científica Ferreira Penna, Pará, Brazil</li> </ul>	$T_{pref}$ , TPC, $CT_{min}$ , $CT_{max}$	Leaf litter, heavy shade
<i>G. albogularis</i>	<ul style="list-style-type: none"> <li>El Boqueron (roadside), Cundinamarca, Colombia</li> <li>University of Córdoba, Monteria, Colombia</li> </ul>	$T_{pref}$	Arboreal, partial shade
<i>G. humeralis</i>	<ul style="list-style-type: none"> <li>Reserva Florestal Adolpho Ducke, Amazonas, Brazil</li> <li>Estação Científica Ferreira Penna, Pará, Brazil</li> <li>Parque Nacional Yasuní, Ecuador</li> <li>Los Amigos Biological Station, Peru</li> </ul>	$T_{pref}$ , TPC, $CT_{min}$ , $CT_{max}$	Arboreal, partial shade
<i>S. argus</i>	<ul style="list-style-type: none"> <li>Key West (roadside), Florida, United States</li> </ul>	$T_{pref}$	Ground and arboreal
<i>S. elegans</i>	<ul style="list-style-type: none"> <li>Bahia Honda State Park and Key Deer Reserve, Florida, United States</li> <li>Big Pine Key, Florida, United States</li> </ul>	$T_{pref}$	Leaf litter and debris
<i>S. macrolepis</i>	<ul style="list-style-type: none"> <li>University of Puerto Rico (UPR), Río Piedras, Puerto Rico, United States</li> <li>Campamento Piñones, Puerto Rico, United States</li> </ul>	$T_{pref}$ , TPC, $CT_{min}$ , $CT_{max}$	Leaf litter, heavy shade
<i>S. nicholsi</i>	<ul style="list-style-type: none"> <li>Guanica (roadside), Puerto Rico, United States</li> </ul>	$T_{pref}$ , TPC, $CT_{min}$ , $CT_{max}$	Leaf litter, partial shade

Because all the species in this study are related phylogenetically, I used an ANOVA followed by Tukey's multiple comparisons of means to compare  $T_{pref}$ ,  $CT_{min}$ , and  $CT_{max}$  values between species. For *C. amazonicus*, *G. albogularis*, and *S. macrodactylus*, I compared  $T_{pref}$ ,  $CT_{min}$ , and  $CT_{max}$  values between two study sites by using Student's T-test to compare sites, and for *G. humeralis* I used an ANOVA

followed by Tukey multiple comparisons of means because  $T_{\text{pref}}$  data was collected at four sites. I used linear models with phylogenetic independent contrasts (PIC) to compare whether  $T_{\text{pref}}$  is predicted by either average body size (snout-to-vent length) or average sampling Latitude, and to compare whether thermal tolerance breadth is predicted by maximum performance (number of body lengths run until exhaustion),  $CT_{\text{max}}$ , or average sampling latitude. The phylogeny from (Zheng and Wiens 2016) and R package Ape (Paradis and Schliep 2019) were used to perform the PICs.

I quantified how lizards' motor function responds to changes in environmental temperature by performing performance trials at different temperatures, then fitting thermal performance curves (TPC). These trials were performed after  $T_{\text{pref}}$  trials, using different individuals than used in CT trials. At least five male and five female lizards of each species had their body temperature raised or lowered to set temperatures ( $T_c$ ) of 20, 25, 30, 33 or 35°C, depending on species. Lizards were then placed in a circular track with a 1 or 2 m circumference, and poked as stimulus to run (Bennett 1980). Lizards were run until exhaustion and the distance and time run were recorded. Each lizard was subjected to three trials at three different temperatures a minimum of 12 hours apart, unless prevented by death. The maximum number of body lengths run was used as the performance parameter at each temperature, calculated as the maximum distance run divided by the individual's snout-to-vent body length. A Kumaraswamy curve (equation below), Gaussian curve, quadratic curve, and cubic curve were fitted to the performance data for every trial. Fitted curves were compared using AIC values (Angilletta 2006; Sinervo et al. 2019).

$$TPC(T_e) = ab\left(\frac{(T_{e,i}-CT_{min})}{(CT_{max}-CT_{min})^{(a-1)}}\right)\left(1 - \frac{(T_{e,i}-CT_{min})}{(CT_{max}-CT_{min})^a}\right)^{(b-1)c} \quad 3.1$$

The optimal temperature ( $T_{opt}$ ) allowing for maximum performance was calculated from the fitted curve. Thermal range was calculated as  $CT_{max} - CT_{min}$ , as well as the  $B_{80}$ , the thermal range for the central 80% of the performance curve. Additionally, a generalized sphaerodactylid TPC was imputed from the combined data from all species measured for use in analyses for species lacking TPC measurements but having  $T_{pref}$  (Sinervo et al. 2010, 2018, 2019). The average values of  $CT_{min}$  ( $10.97^{\circ}C$ ) and  $CT_{max}$  ( $37.78^{\circ}C$ ) across all specimens were used for the generalized model.

### *Ecophysiology models*

I used the ecophysiological model of climate-driven extinction developed in Sinervo et al. (2010 and 2019) and Caetano et al. (2020). Lizard's thermal limitations were used to calculate the number of hours lizards are able to be active in the environment, hours of activity ( $h_a$ ), and the number of hours that the environment is too hot for activity, hours of restriction ( $h_r$ ), to parameterize these models. I used microclim raster data (20x20 km, 10 arcmin resolution) (Kearney et al. 2014) to quantify ecophysiological parameters under present-day temperatures in the microhabitats where target species are found, then fitted WorldClim air temperatures to predict these parameter estimates. I used species distribution models to compare changes in habitat suitability between the near past (WorldClim v2.1 1970-2000) and the 2070 future projections (WorldClim v1.4 2070) (downscaled to 1x1 km, 30 arcsec resolution) (Fick and Hijmans 2017; Sinervo et al. 2019). WorldClim and microclim

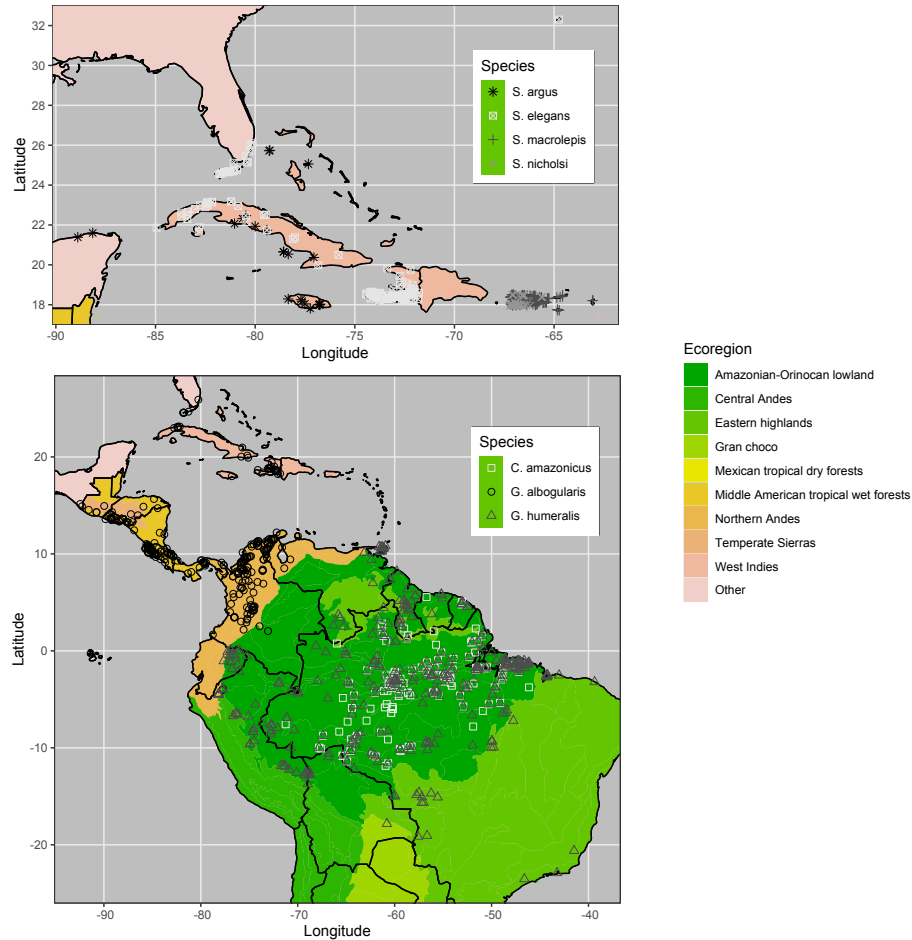
datasets treat coastal cells differently - microclim lacks temperature data for some coastal cells, as these cells are treated as sea rather than land, while WorldClim rasters contain land temperature data (New et al. 2002; Kearney et al. 2014). Coastal occurrence records in microclim rasters were relocated up to 20 km to the nearest “land” cell. Because of this non-standard treatment of coastlines, small islands including sampling localities in the Florida Keys are not represented in microclim data, but can be recovered in the WorldClim analytical steps. Thus, these sampling localities were recovered in later modeling steps using WorldClim.

Species occurrence records were obtained from VertNet.org, the herpetological collections of the University of Brasília and the Universidad Nacional de Colombia Bogotá, field sites, and publications (Álvarez-Pérez 1992; Vitt et al. 1997, 2000, 2005; Miranda et al. 2010; Allen and Powell 2014; Dominguez-Lopez et al. 2015). Occurrence records were trimmed to include only localities above 1 km apart using the *cleanpoints* function in the R package Mappinguari (Caetano et al. 2019) (Fig. 3.2).

I used the average temperatures for the 0%, 50%, and 100% shade microclim temperature rasters for soil substrates. *G. albogularis* and *G. humeralis* are frequently found on tree trunks (Vitt et al. 2000; Dominguez-Lopez et al. 2015), so for these species I averaged the temperatures from 0 cm and 100 cm altitude microclim datasets. For all other species, which are found on the forest floor and under leaf litter, I averaged the 0 cm and 1 cm altitude datasets. These temperatures were used to calculate  $h_a$  and  $h_r$  for each month of the year at all sites in the cleaned occurrence

records following Sinervo et al. 2019.  $H_a$  is defined as the number of hours per day when environmental temperature ( $T_e$ ) is above the minimum active body temperature for sphaerodactyline lizards:  $T_e > T_{b,min \text{ active}}$ . I used the lowest reported minimum active temperature ( $T_{b,min \text{ activity}}$ ) for Sphaerodactylidae, 20.3°C, measured in *S. klauberi* (Álvarez-Pérez 1992).  $H_r$  is defined as the numbers of hours per day when environmental temperature is above the thermal preference of a given species, as lizards will not be active at high temperatures:  $T_e > T_{pref}$ .

Figure 3.2. Occurrence records for seven species of sphaerodactyline gecko: *Chattogecko amazonicus*, *Gonatodes albogularis*, *G. humeralis*, *Sphaerodactylus argus*, *S. elegans*, *S. macrolepis*, and *S. nicholsi*.



I calculated the Riemann integral for both  $h_a$  and  $h_r$  by fitting polygons to the hourly temperatures at each locality to measure the numbers of hours lizards can remain active. Any negative values were replaced with 0.

$$h_{a,m} = \int_{t=\text{sunrise}}^{\text{sunset}} f(T_{Min,m} - T_{b,min \text{ active}}) dt \quad 3.2$$

$$h_{r,m} = \int_{t=\text{sunrise}}^{\text{sunset}} f(T_{Max,m} - T_{pref}) dt \quad 3.3$$

All  $h_a$  and  $h_r$  calculated from  $T_e$  at each locality for soil substrate (I) and each shade %'s (i,  $N_e$ ) are averaged to calculate the average conditions at each locality. This reflects a lizard's ability to select among available sun/shade microhabitats and substrates.

$$\bar{h}_{a,m} = \sum_{i=1}^{N_e} \sum_{h=\text{sunrise}}^{\text{sunset}} \frac{I(h_a(T_{e,i}(m,h) > T_{min \text{ active}}))}{N_e} \quad 3.4$$

$$\bar{h}_{r,m} = \sum_{i=1}^{N_e} \sum_{h=\text{sunrise}}^{\text{sunset}} \frac{I(h_r(T_{e,i}(m,h) > T_{pref}))}{N_e} \quad 3.5$$

I calculated average hourly performance based on Kumaraswamy function TPCs and microclim environmental temperature data. TPCs were calculated during daylight hours, when  $T_e > T_{b, \text{min active}}$ , otherwise performance is 0. Similar to  $h_a$  and  $h_r$ , TPCs are then averaged among all shade environments ( $N_e$ ).

$$\overline{TPC}_m = \sum_{i=1}^{N_e} \sum_{h=\text{sunrise}}^{\text{sunset}} \frac{(TPC_{h,m}(T_{e,i}) | T_{e,i} > T_{b,min \text{ active}})}{N_e} \quad 3.6$$

Because microclim data only reflects present climate and future climate predictions present future air temperatures only, I generated predictive fits for microclim-based calculations of  $h_a$ ,  $h_r$ , and  $\overline{TPC}_m$  for Worldclim v2.1 CMIP6 near past air temperature rasters (1970-2000), 30 arcsec resolution (worldclim.org). I used JMP statistical software to fit to a 4-parameter Richard's function using non-linear

regression for  $h_a$  and  $h_r$  (Kirchhof et al. 2017; Sinervo et al. 2018; Caetano et al. 2020). This also downscaled the lower-resolution microclim data to Worldclim's 1x1 km resolution.

$$h_{a,m}(T_{Min,m} - T_{b,min act.}) = \tau_{a,1}/(1 + \tau_{a,2}e^{[-\tau_{a,3}(T_{Min,m}-T_{b,min act.})]})^{(1/\tau_{a,4})} \quad 3.7$$

$$h_{r,m}(T_{Max,m} - T_{pref}) = \tau_{r,1}/(1 + \tau_{r,2}e^{[-\tau_{r,3}(T_{Max,m}-T_{pref})]})^{(1/\tau_{r,4})} \quad 3.8$$

$\overline{TPC}_m$  values for each occurrence record were fit as a linear function of  $T_{Min}$  and  $T_{Max}$ , quadratic terms  $T_{Min}^2$  and  $T_{Max}^2$ , as well as an interaction term  $T_{Min} \times T_{Max}$ .

$$\overline{TPC}_m(T_{Min}, T_{Max}) = u + vT_{Min} + wT_{Max} + xT_{Min}^2 + yT_{Max}^2 + zT_{Min}T_{Max} \quad 3.9$$

These same equations were subsequently used to downscale  $h_a$  and  $h_r$  from Worldclim v1.4 rpc-85 2070, 30 arcsec resolution future climate projections (worldclim.org). I used the deprecated v1.4 instead of the newer v2.1, because future projections at 30 arcsec resolution have not yet been published. To improve model accuracy, I averaged the three v1.4 climate models which received the highest skill scores for terrestrial temperature and precipitation in tropical latitudes (20°S–20°N): BCC-CSMI4, HadGem2-ES, and MPI-ESM-LR (Anav et al. 2013).

Finally, I used the R package biomod2 (Thuiller et al. 2009, 2020) to perform species distribution modeling for each of the seven sphaeodactyline species. Monthly  $h_a$ ,  $h_r$ , and  $\overline{TPC}_m$  values were calculated for each occurrence record site. I used a quadratic GLM in biomod2 with first-level interaction terms to determine the significant ecophysiological and environmental predictors of species range with the factors: winter and summer precipitation levels,  $h_a$ ,  $h_r$ , and  $\overline{TPC}_m$ . Pseudo-absences were generated by biomod2 using the “disk” routine, which bounds pseudo-absences

Table 3.2. Thermal physiology parameters for seven species of sphaerodactyline geckos. Average values are calculated across all study sites for each species. Site averages are also listed. (\* Data from Bruschi et al. 2016.)

Species	Collection site	N (T <sub>pref</sub> )	SVL (mm)	Avg. T <sub>pref</sub> ± SD	T <sub>opt</sub>	N (CT <sub>min</sub> )	Avg. CT <sub>min</sub> ± SD	N (CT <sub>max</sub> )	Avg. CT <sub>max</sub> ± SD	Range	B <sub>80</sub>
<i>C. amazonicus</i>	Average among sites	83	17.09	23.48 ± 2.49	27.80	24	8.233 ± 4.28	22	36.29 ± 2.99	28.06	10.95
	Reserva Florestal Adolpho Ducke	37	17.77	22.80 ± 2.95		14	7.414 ± 3.74	12	36.40 ± 3.69	28.99	
	Estação Científica Ferreira Penna	46	16.59	24.03 ± 1.90		10	9.380 ± 4.90	10	36.16 ± 2.05	26.78	
<i>G. albogularis</i>	Average among sites	65	38.62	31.76 ± 2.46				20*	37.55 ± 0.24*		
	El Boqueron	21	37.74	32.77 ± 1.76							
	University of Córdoba	44	39.00	31.28 ± 2.61							
<i>G. humeralis</i>	Average among sites	190	33.74	25.34 ± 2.68	25.25	22	10.97 ± 3.42	22	37.78 ± 4.98	26.81	18.00
	Reserva Florestal Adolpho Ducke	98	33.48	25.81 ± 3.17							
	Estação Científica Ferreira Penna	52	32.12	24.95 ± 2.17	25.25	22	10.97 ± 3.42	22	37.78 ± 4.98	26.81	18.00
	Parque Nacional Yasuni	18	35.71	23.37 ± 0.90							
	Los Amigos Biological Station	22	37.42	25.79 ± 1.05							
<i>S. argus</i>	Key West	21	26.56	27.40 ± 0.87							
<i>S. elegans</i>	Big Pine Key	11	31.91	29.00 ± 0.88							
<i>S. macrolepis</i>	Average among sites	28	25.26	24.35 ± 2.82	26.80	6	6.700 ± 1.44	7	38.94 ± 3.97	32.24	14.25
	UPR, Río Piedras	16	25.62	25.56 ± 2.76		2	8.050 ± 0.919	3	38.40 ± 1.65	33.32	
	Campamento Piñones	12	24.73	22.74 ± 2.05		4	6.025 ± 1.17	4	39.35 ± 5.41	30.35	
<i>S. nicholsi</i>	Guamica	35	17.49	29.28 ± 5.32	31.75	6	8.383 ± 2.22	6	43.83 ± 1.35	35.45	20.60

by a minimum (10 km) and maximum distance (600 km) from existing sampling points. For species with more than 50 occurrence records, five times the number of pseudo-absence points than the number of occurrence records were used, for species with fewer than 50 occurrence records (*S. argus* and *S. nicholsi*), ten times the number of pseudo-absence points were used (Barbet-Massin et al. 2012). Populations in 2070 whose occupancy probability was above the critical probability of persistence ( $P_{critical}$ ), defined as the 0.05 quantile for the recent past (1970-2000), were considered safe from climate-driven extinction (Sinervo et al. 2010).

## Results

### *Thermal physiology parameters*

I measured thermal physiology parameters in 476 specimens across seven species of sphaerodactylid lizards at 11 field sites in South America and the Caribbean (Table 3.2).  $T_{pref}$  is significantly different across all species ( $p < 0.01$ ). The Tukey multiple comparisons of means shows that all pairs of species are significantly different, except five pairs (*C. amazonicus* & *S. macrolepis*, *G. humeralis* & *S. macrolepis*, *S. argus* & *S. elegans*, *S. argus* & *S. nicholsi*, *S. elegans* & *S. nicholsi*) (Table 3.3). Within the same species,  $T_{pref}$  measurements are significantly different at different sites (*C. amazonicus*:  $t = -2.19$ ,  $df = 58.90$ ,  $p = 0.032$ ; *G. albogularis*:  $t = 2.71$ ,  $df = 55.68$ ,  $p = 0.0090$ , *S. macrolepis*:  $t = -3.10$ ,  $df = 26$ ,  $p = 0.0046$ ). The four sites where *G. humeralis* were sampled are also significantly different ( $p = 0.0019$ ); the post hoc test shows that *G. humeralis* at Parque Nacional Yasuní in Ecuador is

significantly different from those at Los Amigos Biological Station in Peru ( $p = 0.019$ ) and Reserva Florestal Adolpho Ducke in Brazil ( $p = 0.0018$ ). With phylogenetic contrasts controlled for, neither the average snout-vent length measured, the average Latitude of sampling, nor both factors together significantly predict average  $T_{pref}$  of these species.

$CT_{min}$  is significantly different among the species measured ( $p = 0.024$ ), as is  $CT_{max}$  ( $p = 0.0014$ ). Post hoc tests show that no two species have significantly different  $CT_{min}$  when tested pairwise, but *S. nicholsi* has a significantly different  $CT_{max}$  than *C. amazonicus* and *G. humeralis* (Table 3.4).  $CT_{min}$  and  $CT_{max}$  were measured at two different sites for both *C. amazonicus* and *S. macrolepis*, but neither ecophysiological parameter differs significantly between sites: *C. amazonicus* ( $CT_{min}$ :  $t = -1.07$ ,  $df = 16.11$ ,  $p = 0.30$ ;  $CT_{max}$ :  $t = 0.19$ ,  $df = 17.68$ ,  $p = 0.85$ ) and *S. macrolepis* ( $CT_{min}$ :  $t = -2.32$ ,  $df = 2.69$ ,  $p = 0.11$ ;  $CT_{max}$ :  $t = 0.33$ ,  $df = 3.71$ ,  $p = 0.76$ ).

### *Ecophysiology models*

To find the best-fit thermal performance curve, I compared Gaussian, cubic, quadratic, and Kumaraswamy curves TPC model fits for *C. amazonicus*, *G. humeralis*, *S. macrolepis*, *S. nicholsi*, and a generalized sphaerodactylid. Kumaraswamy curve AIC value were lower than Gaussian, cubic, and quadratic curves (Table 3.5). Therefore Kumaraswamy curve fits were used in all subsequent analyses. The optimal body temperature for maximum performance ( $T_{opt}$ ) was calculated for each TPC curve (Table 3.2). Thermal range and  $B_{80}$  are also reported in

Table 3.2.  $T_{pref}$  is lower than  $T_{opt}$  in *C. amazonicus*, *S. macrolepis*, and *S. nicholsi*, but not in *G. humeralis*. The  $T_{opt}$  calculated for *C. amazonicus* is near the reported field active temperature ( $T_b$ ) of 27.4 (Vitt et al. 2005), approximately one degree cooler in *S. nicholsi*,  $T_b$ : 32.8 (Álvarez-Pérez 1992), and several degrees cooler than the observed  $T_b$  for *G. humeralis*,  $T_b$ : 30.3 (Vitt et al. 2000) and *S. macrolepis*,  $T_b$ : 30.4 (Powell 1999) (Fig. 3.3).

Figure 3.3. Thermal performance curves for sphaerodactyline geckos. Fitted Kumaraswamy curve in gray. Shaded area shows the  $B_{80}$ . Yellow, single-dashed line at preferred temperature ( $T_{pref}$ ), red, double-dashed line at optimal temperature ( $T_{opt}$ ), and purple, short-dashed line at published field active temperature ( $T_b$ ).

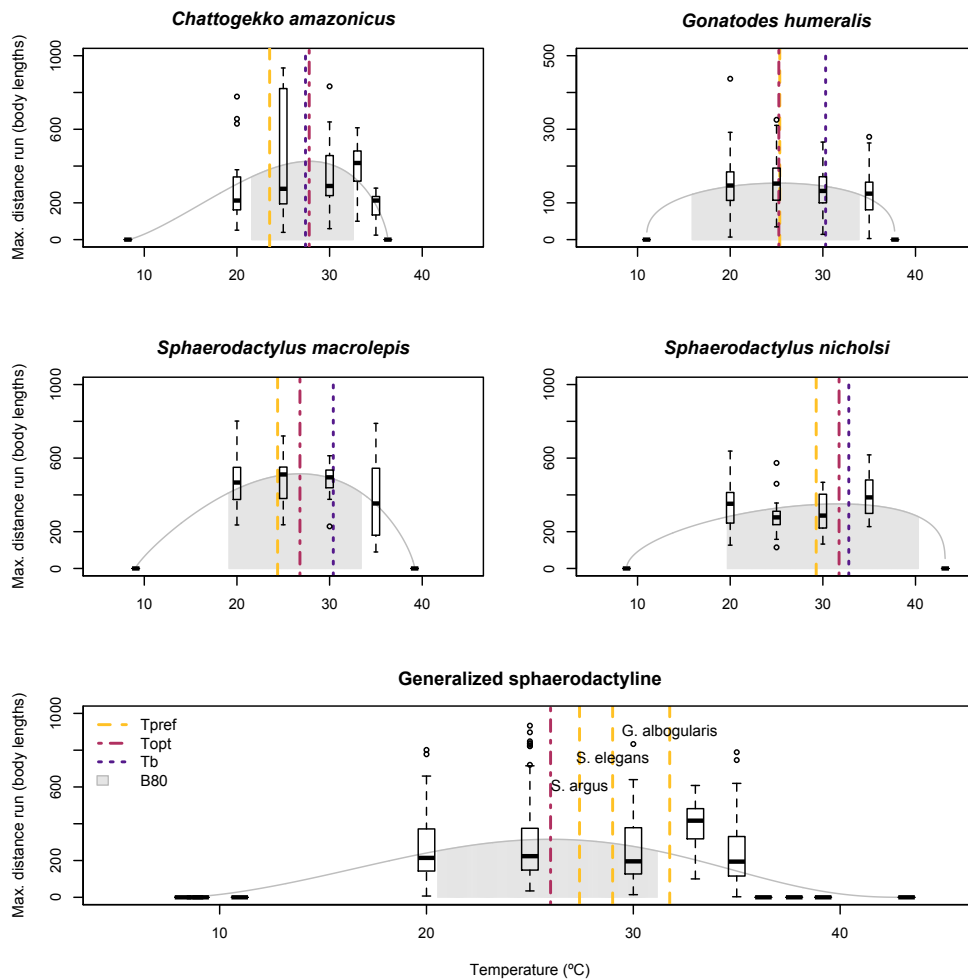
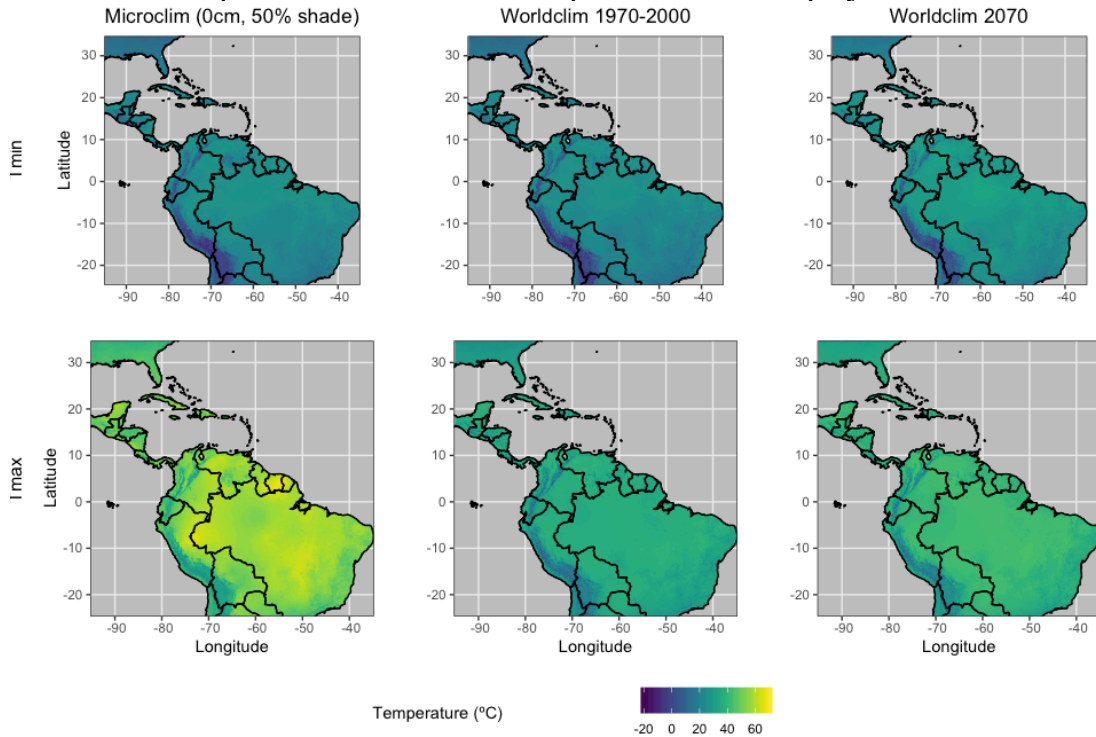


Figure 3.4. Yearly average monthly minimum ( $T_{\min}$ , top row) and maximum ( $T_{\max}$ , bottom row) temperatures from microclim (0 cm altitude, 50% shade), WorldClim v2.1 1970-2000 near past, and WorldClim v1.4 rpc-85 2070 future projections.



The coefficients for models 3.1, 3.7, 3.8, and 3.9 are found in Table 3.6. The average yearly  $T_{\min}$ , calculated from monthly Worldclim rasters increased between 2.7-4.6° C across occurrence records for all species; yearly  $T_{\max}$  increased between 2.6-4.8° C (Fig. 3.4, Table 3.7). *C. amazonicus*, *G. albogularis*, *G. humeralis*, and *S. elegans* had fewer populations below the  $P_{\text{critical}}$  (critical probability of persistence: 0.05 quantile for the recent past) in 2070 than in the recent past (0.3-2% of populations) (Fig. 3.5-3.7, 3.9). On the other hand, the majority of populations for *S. argus* (66%), *S. macrolepis* (89%), and *S. nicholsi* (100%) are below the  $P_{\text{critical}}$  (Fig. 3.8, 3.10, 3.11). Across all seven species, extirpated sites are projected to experience

a significantly larger drop (-3.3 cm) in average monthly precipitation than persistent sites (-1.49 cm) ( $t = -12.60$ ,  $df = 482.35$ ,  $p\text{-value} < 0.0001$ ), though *S. macrolepis* is the only species with lower average precipitation across a large number of extirpated sites (Table 3.7). Extirpated sites also have a significantly larger decrease in time of activity between 2070 and the near past ( $\Delta \text{Avg. } h_a\text{-}h_r$ ) than persistent sites ( $t = -8.23$ ,  $df = 581.81$ ,  $p\text{-value} = <0.0001$ ) (Table 3.7).

## Discussion

Sphaerodactyline lizards epitomize small-bodied tropical thermoconformers. Many sphaerodactylines thermoregulate to avoid high heat (Heatwole 1966; Álvarez-Pérez 1992) as expected of tropical lizards (Kearney et al. 2009). Their body temperatures are strongly predicted by air and substrate temperatures (Vitt et al. 1997; Miranda et al. 2010). The species included in this study demonstrate different thermal ecology, tied to their microhabitat preference and range.

*Chattogekko amazonicus*, *Sphaerodactylus elegans*, *S. macrolepis*, and *S. nicholsi* are all leaf litter specialists. *C. amazonicus* and *S. nicholsi* are among the smallest lizards in the world (Meiri 2008). However, *C. amazonicus* prefers cool, moist environments and deep shade (da Cunha et al. 1985; Vitt et al. 2005), while *S. nicholsi* is found in more open, xeric microhabitats (Álvarez-Pérez 1992; Rivero 2006). *S. elegans* is found on the ground, under complex litter and debris and can be found near human habitations (Thomas et al. 1998), while *S. macrolepis* inhabits humid habitats of dense grass and leaf litter in both sand and soil substrates (Nava

2004; Allen and Powell 2014). I collected *S. nicholsi* in the xeric Guanica region of Puerto Rico from both dry, sparsely shaded leaf litter and moist, densely matted litter.

The thermal performance curves show that *C. amazonicus* and *S. macrolepis* both have characteristics associated with thermal specialists (Huey and Kingsolver 1989; Angilletta 2009). The tall, peaked thermal performance curves and small  $B_{80}$  ranges, although their thermal ranges are not narrow compared to other species in this study (Fig. 3.3, Table 3.2). Likewise, *C. amazonicus* and *S. macrolepis* have the lowest  $T_{pref}$  values and are better adapted to cool temperatures, reflected in their microhabitat preferences. In both these species,  $T_{pref} < T_{opt}$ . Despite their similarities, *C. amazonicus* is predicted to persist across most of its range, while *S. macrolepis* is predicted to experience widespread extirpations (Fig. 3.5, 3.10). This is potentially related to the fact that *C. amazonicus* is active at temperatures ( $T_b$ ) near its  $T_{opt}$ , and *S. macrolepis* is frequently active above its  $T_{opt}$ . *S. macrolepis* may already be experiencing thermal stress, though its  $T_b$  still falls within the breadth of its  $B_{80}$ . In contrast, *S. nicholsi* has a shorter, broader thermal performance curve and large  $B_{80}$ , indicative of a thermal generalist (Huey and Kingsolver 1989; Angilletta 2009). It is clearly the most hot-adapted species in this study, having the highest  $T_{pref}$  and  $CT_{Max}$ . In *S. nicholsi*,  $T_{pref} < T_{opt} < T_b$ , and it is also at high risk of extinction (Fig. 3.3, 3.11). I was unable to measure performance and critical temperatures in *S. elegans*, but based on  $T_{pref}$ , it also appears to be hot-adapted. *S. elegans* is the only island species and only *Spherodactylus* species at low risk from climate change (Fig. 3.9), however the generalized sphaerodactyline thermal performance curve and average critical

temperatures were used in the species distribution model, so predictions may be less accurate than if a species-specific model were used.

*Gonatodes albogularis* and *G. humeralis* are both frequently found on high perches in trees, near human disturbance, and on human structures (Rivero-Blanco and Dixon 1979; Vitt et al. 1997; Dominguez-Lopez et al. 2015). *G. albogularis* inhabits deciduous and dry forests and has been observed active on surfaces up to 35.8 °C (Heatwole 1966; Rivero-Blanco and Dixon 1979). Like *S. elegans* and *S. nicholsi*, it is hot adapted. It is predicted to be at low risk from climate change (Fig. 3.6), however the species distribution model used the generalized sphaerodactyline thermal performance curve and average critical temperatures. In contrast to *G. albogularis*, *G. humeralis* prefers shaded, wet forests and cooler temperatures (Rivero-Blanco and Dixon 1979). The thermal range for *G. humeralis* is not particularly large compared to other species, however its  $B_{80}$  is relatively large. Its thermal performance curve suggests that *G. humeralis* is also a thermal generalist, whose thermal traits fall between the hot- and cold-adapted species. *G. humeralis* is predicted to persist across most of its range (Fig. 3.7), unlike *S. macrolepis* and *S. nicholsi*, although its  $T_{\text{pref}} \sim T_{\text{opt}} < T_b$  (Table 3.2). Finally, *S. argus* is found on the ground, under complex litter and debris and near human habitations, but also in dry bromeliads up in trees (Thomas et al. 1998; Krysko and Sheehy 2005). Like other *Spherodactylus* island species, it is at high risk from climate change (Fig. 3.8), though the generalize model was also used here. *S. argus*'s  $T_{\text{pref}}$  is intermediate compared to

other species in this study, but is statistically indistinguishable from *S. elegans* and *S. nicholsi*.

When thermal performance curves are left-skewed as exemplified by *C. amazonicus*, the fitness cost of being active at temperatures above  $T_{opt}$  is greater than the cost of being active at lower temperatures (Martin and Huey 2008). We would therefore expect  $T_{pref}$  to fall below  $T_{opt}$ , particularly when the performance curve is heavily skewed. This relationship can be seen in *C. amazonicus*, *S. macrolepis*, and *S. nicholsi*, but not *G. humeralis*. However, a wide performance breadth reduces selection on  $T_{opt}$  (Huey and Kingsolver 1993; Angilletta et al. 2002), and species with symmetrical performance curves like *G. humeralis* need less of a buffer between  $T_{pref}$  and  $T_{opt}$ . Broad thermal performance curves, as seen in *G. humeralis* and *S. nicholsi* reflect selection due to large variability in body temperatures (van Berkum 1988). This may reflect the different microhabitats where *S. nicholsi* was collected, and also explain why *G. humeralis* has one of the largest geographic ranges of any gecko species (Pinto et al. 2019).

Field active body temperature ( $T_b$ ) and  $T_{pref}$  are typically correlated (Huey 1982; Sinervo et al. 2010). Consistent with other studies,  $T_{pref}$  is not predicted by either collection latitude or body size, when phylogenetic relatedness is accounted for (Clusella-Trullas and Chown 2014). However, only a small number of species are included in this study, compared to the size of this clade.  $T_{pref}$  was measured in multiple populations of *C. amazonicus*, *G. albogularis*, *G. humeralis*, and *S. macrolepis*, and differs significantly across sites for all those species. This suggests

that populations acclimate to local conditions (Huey and Kingsolver 1989; Angilletta et al. 2002). For instance, many Amazonian species, including *G. humeralis*, demonstrate a biogeographic split between the Eastern and Western Amazon (Avila-Pires 1995; Gamble et al. 2008; Pinto et al. 2019). However,  $T_{\text{pref}}$  in *G. humeralis* differs significantly between the two western field sites, but only one western site differs from either eastern site, suggesting that climate, not descent, is driving variation in  $T_{\text{pref}}$ . Local adaptation may impact species distribution models, as models are based on measurements from small numbers of populations, and may be missing within-species variation that contributes to species persistence (Herrando-Pérez et al. 2019).

Extreme environmental temperatures drive the evolution of  $CT_{\text{Min}}$  and  $CT_{\text{Max}}$  (Sunday et al. 2014, 2019). The xeric species, *S. nicholsi* was the most obvious example of this, with a considerably higher  $CT_{\text{Max}}$  than the other species in this study.  $CT_{\text{Min}}$  and  $CT_{\text{Max}}$  were measured at two sites for *C. amazonicus* or *S. macrolepis*, but unlike  $T_{\text{pref}}$ , neither differs between sites. Also, thermal tolerance breadth is not significantly predicted by average sampling latitude. The average monthly maximum temperature across occurrence records for each species (Table 3.7) is lower than their  $CT_{\text{Max}}$  (or the generalized  $CT_{\text{Max}}$ ) both in the near past and 2070 climate projections. This means these species are not likely to experience temperatures regularly above their thermal safety margins (Huey and Kingsolver 1989; Sunday et al. 2014), however, average maximum temperature does not rule out extreme heat events. There is no evidence of a potential tradeoff between optimal performance and thermal

breadth (Huey and Kingsolver 1989; Altamirano-Benavides et al. 2019) among the four species in this study with TPCs; average maximum performance was not predicted by either  $CT_{Max}$  or thermal tolerance breadth.

Contrary to expectation, more than half of the species in this study are at minimal risk from climate change. The mainland species, *C. amazonicus*, *G. albogularis*, and *G. humeralis* are all predicted to experience minimal future extirpations, while the island species *S. argus*, *S. macrolepis*, and *S. nicholsi* are predicted to experience significant population losses, and in the case of *S. nicholsi*, extinction. Although *S. elegans* is an island species and more closely related to the others, it is predicted to experience few extirpations, conversely the mainland species *G. concinnatus* is predicted to lose 82.5% of its populations by 2070 (Altamirano-Benavides et al. 2019). This model may not be as accurate predicting extirpations in *G. albogularis*, *S. argus*, and *S. elegans*, because only generalized spherodactylid TPCs and CTs were available. For all these species,  $T_{pref}$  falls above the generalized  $T_{opt}$ , which may indicate thermal stress or a mismatched curve.

It is clear that different ecophysiological factors influence the ranges of these species. Species with highest predicted extirpations neither experience the hottest future  $T_{Min}$  and  $T_{Max}$ , nor the largest increase in  $T_{Min}$  and  $T_{Max}$  across occurrence records. Net time of activity (Avg.  $h_a-h_r$ ) decreases more in 2070 than at extirpated sites than persistent sites (Table 3.7), consistent with predicted mechanisms of climate-driven extinctions (Sinervo et al. 2010; Caetano et al. 2020), though this is not true of *S. elegans* and *S. macrolepis*. Precipitation is another consistent factor in

species persistence. Across all species, sites that are predicted to be extirpated by 2070 have a larger projected drop in precipitation than persistent sites. This pattern is not seen in *S. macrolepis*, though extirpated *S. macrolepis* sites do have lower average monthly precipitation than persistent sites. Due to their small size and relatively higher surface-to-volume ratio, sphaerodactyline lizards are particularly susceptible to evaporative water loss (Snyder 1975; Leclair Jr. 1978; Dunson and Bramham 1981; MacLean 1985). Microhabitat choice for *S. macrolepis* and other Puerto Rican *Sphaerodactylus* is primarily driven by humidity (Nava 2004), though this may not be universal as *G. albogularis* shows no preference for humidity in an experimental gradient (Heatwole 1966). The newer Worldclim v2.1 30-second rasters should give us more accurate future forecasts of environmental factors.

Species facing threat from climate change have three general options: evolution/plasticity, migration, or extinction (Parmesan 2006). Sphaerodactyline lizards are largely cathemeral, and may adjust their activity period as long as there is available light (Rivero-Blanco and Dixon 1979; Hoogmoed and de Avila-Pires 1989), which means that species that are tolerant of human presence may be able to extend their time of activity. Although mainland species were not predicted to be at high risk by this study, habitat loss may pose a large threat to even human-tolerant species, such as *G. humeralis*. Deforestation decreases abundance of *G. humeralis*, and *C. amazonicus* will avoid even single treefalls (Vitt et al. 1998; Carvalho et al. 2008). Beyond simple habitat degradation, deforestation may accelerate Amazonian warming (Foley et al. 2007; Malhi et al. 2008). Future iterations of this model will

utilize deforestation data to improve predictions (Prevedello et al. 2019). Extinction risk is particularly concerning in the Caribbean, due to limited migration opportunities for island species. The Caribbean islands are designated as a biodiversity hotspot, home to 2.9% of endemic vertebrates globally (Myers et al. 2000). Both *macrolepis*, and *S. nicholsi* are endemic to the island of Puerto Rico, along with several other *Spherodactylus* species (Álvarez-Pérez 1992; Rivero 2006). There is reason to be cautiously optimistic about Amazonian sphaerodactylines, but species in the Caribbean may require conservation intervention to save them from extinction.

Figure 3.5. Species distribution model for *C. amazonicus*. Top panel shows distribution of occupancy probability for 144 sites; yellow dashed line shows  $P_{\text{critical}}$  (0.05 quantile for 1975) and red double-dashed line shows mean occupancy probability for time frame. Lower panel: larger grey squares show extirpation sites below  $P_{\text{critical}}$  and black squares show sites above  $P_{\text{critical}}$ .

Figure 3.6. Species distribution model for *G. albogularis*. Top panel shows distribution of occupancy probability for 297 sites; yellow dashed line shows  $P_{\text{critical}}$  (0.05 quantile for 1975) and red double-dashed line shows mean occupancy probability for time frame. Lower panel: larger grey circles show extirpation sites below  $P_{\text{critical}}$  and black circles show sites above  $P_{\text{critical}}$ .

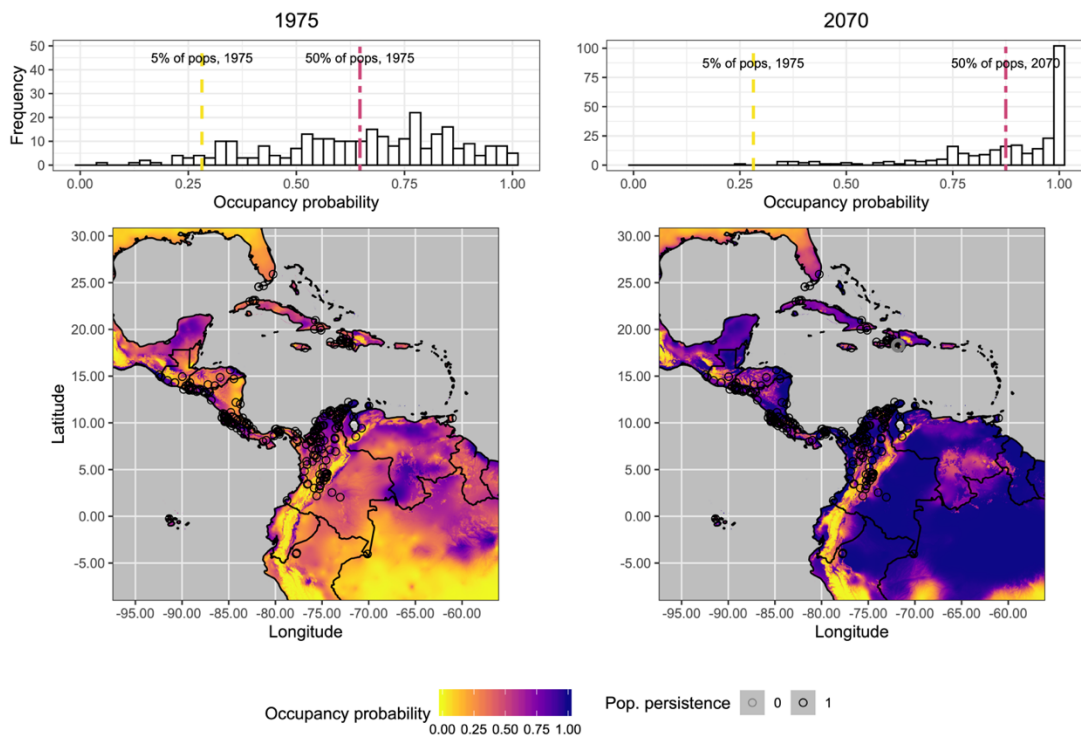
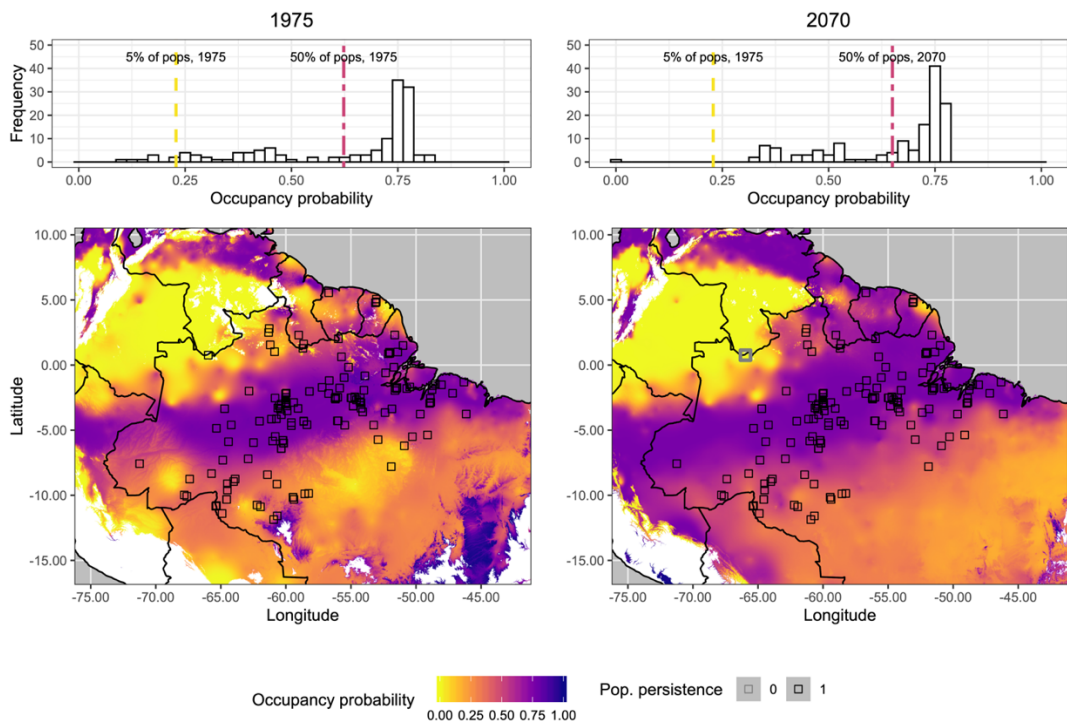


Figure 3.7. Species distribution model for *G. humeralis*. Top panel shows distribution of occupancy probability for 359 sites; yellow dashed line shows  $P_{\text{critical}}$  (0.05 quantile for 1975) and red double-dashed line shows mean occupancy probability for time frame. Lower panel: larger grey triangles show extirpation sites below  $P_{\text{critical}}$  and black triangles show sites above  $P_{\text{critical}}$ .

Figure 3.8. Species distribution model for *S. argus*. Top panel shows distribution of occupancy probability for 29 sites; yellow dashed line shows  $P_{\text{critical}}$  (0.05 quantile for 1975) and red double-dashed line shows mean occupancy probability for time frame. Lower panel: larger grey stars show extirpation sites below  $P_{\text{critical}}$  and black stars show sites above  $P_{\text{critical}}$ .

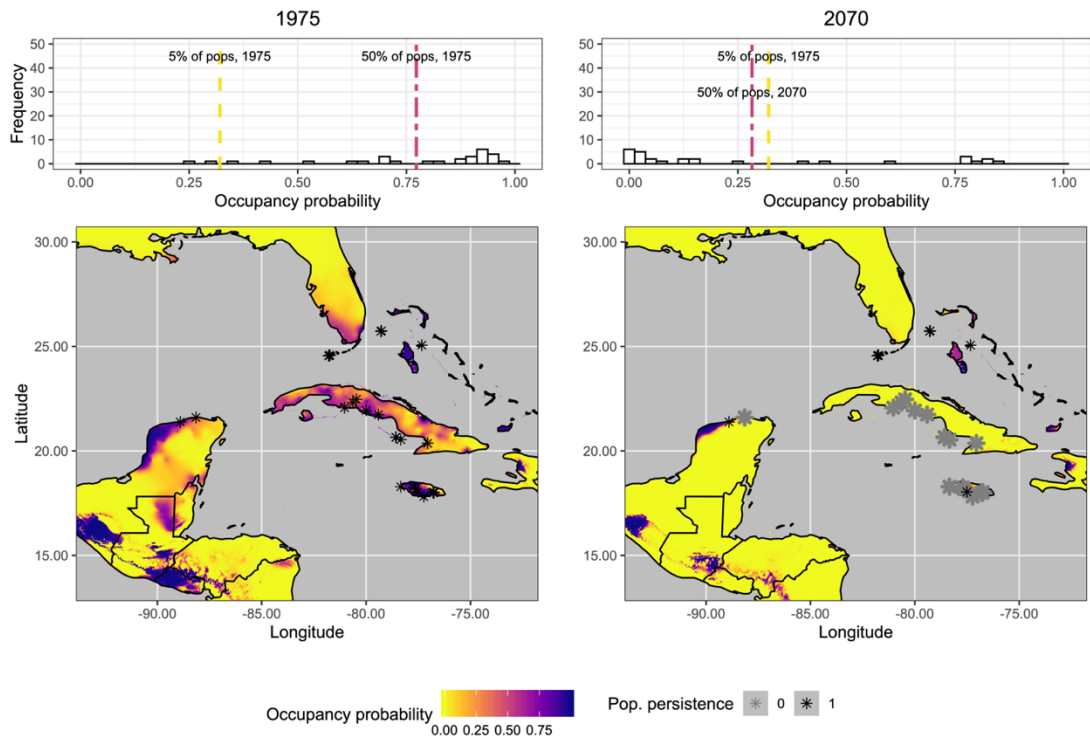
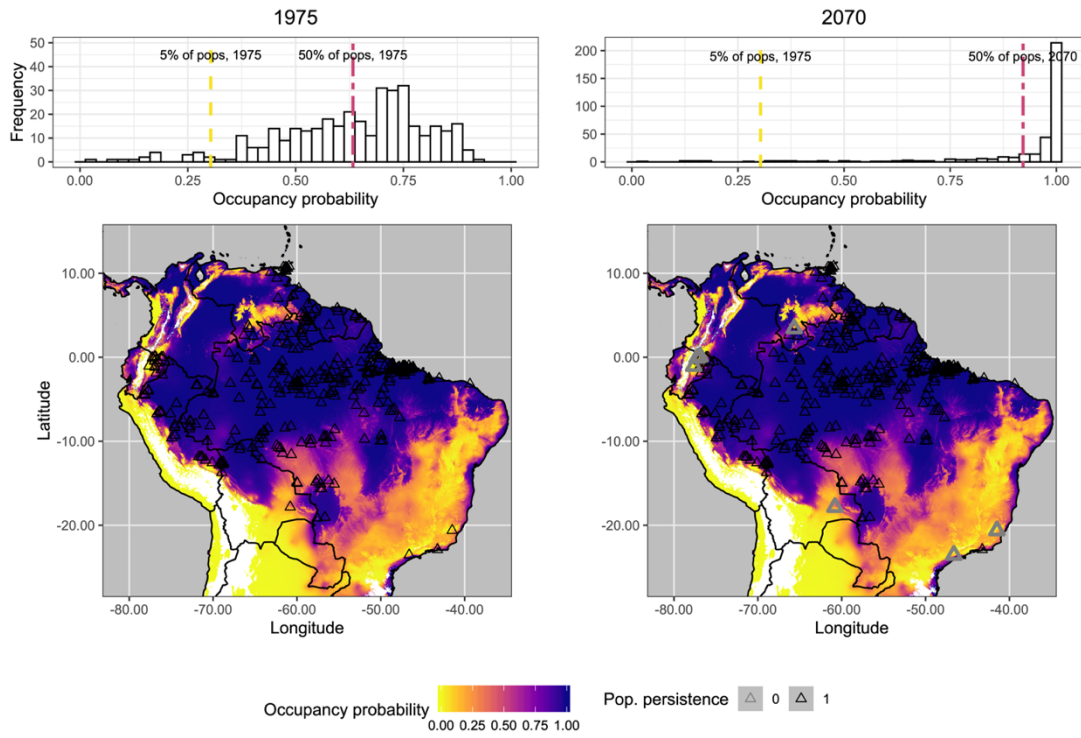


Figure 3.9. Species distribution model for *S. elegans*. Top panel shows distribution of occupancy probability for 133 sites; yellow dashed line shows  $P_{\text{critical}}$  (0.05 quantile for 1975) and red double-dashed line shows mean occupancy probability for time frame. Lower panel: larger grey inverted triangles show extirpation sites below  $P_{\text{critical}}$  and black inverted triangles show sites above  $P_{\text{critical}}$ .

Figure 3.10. Species distribution model for *S. macrodactylus*. Top panel shows distribution of occupancy probability for 81 sites; yellow dashed line shows  $P_{\text{critical}}$  (0.05 quantile for 1975) and red double-dashed line shows mean occupancy probability for time frame. Lower panel: larger grey plusses show extirpation sites below  $P_{\text{critical}}$  and black plusses show sites above  $P_{\text{critical}}$ .

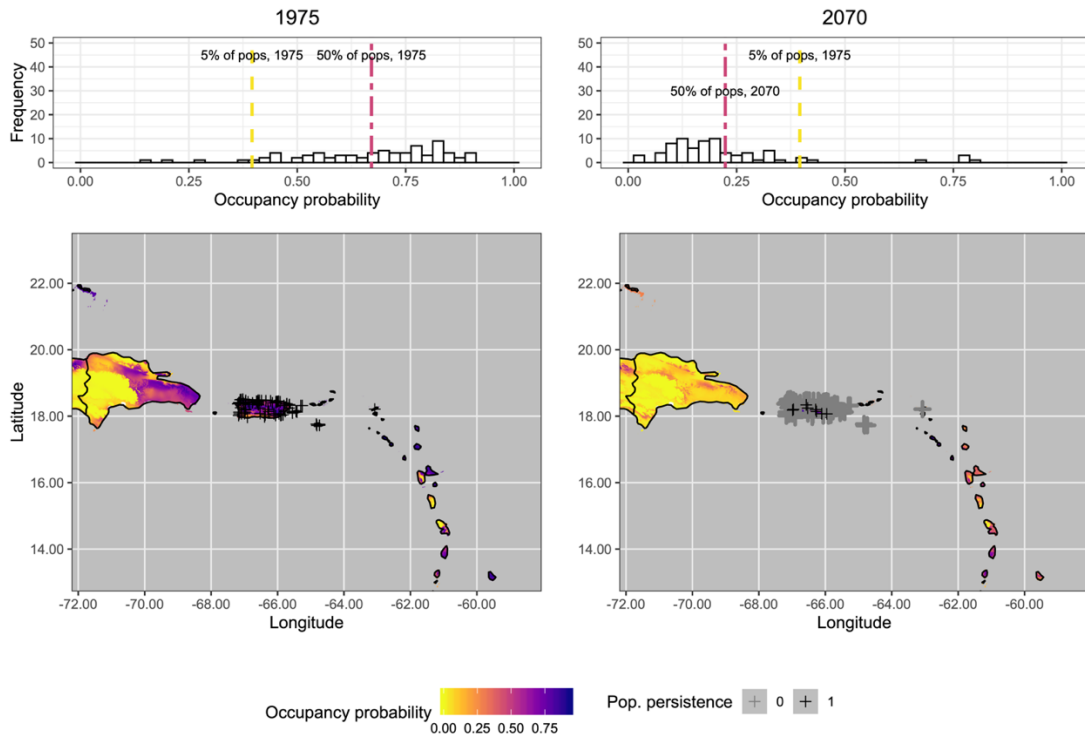
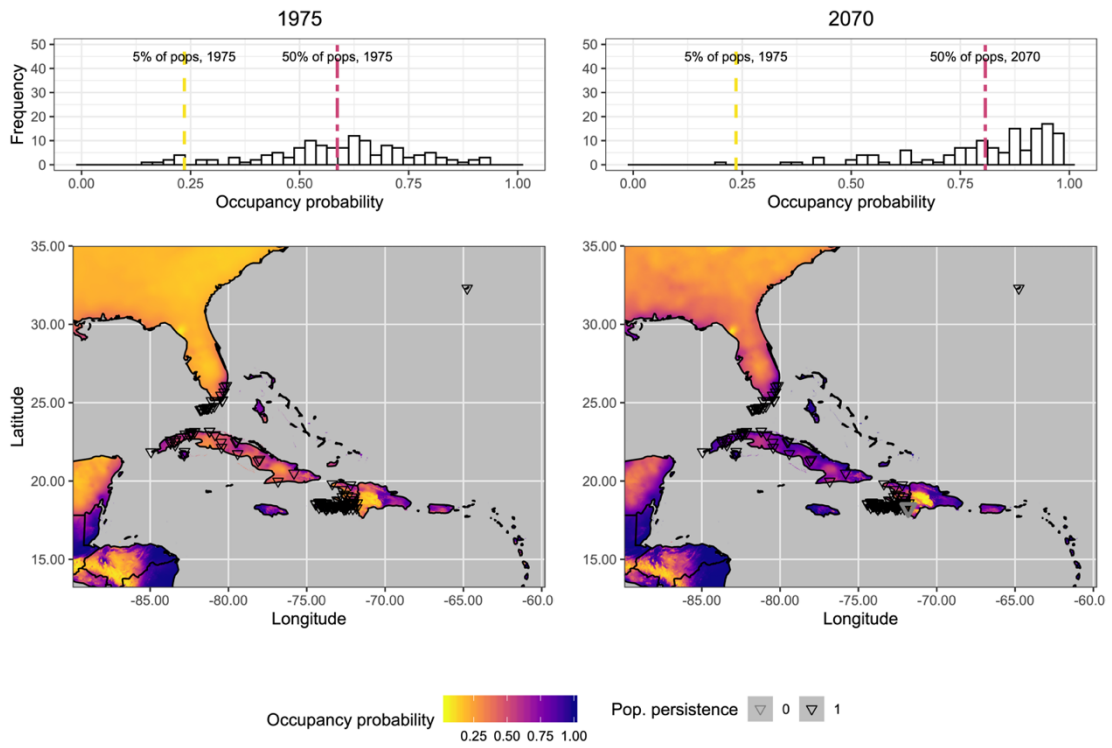


Figure 3.11. Species distribution model for *S. nicholsi*. Top panel shows distribution of occupancy probability for 40 sites; yellow dashed line shows  $P_{\text{critical}}$  (0.05 quantile for 1975) and red double-dashed line shows mean occupancy probability for time frame. Lower panel: larger grey x's show extirpation sites below  $P_{\text{critical}}$  and black x's show sites above  $P_{\text{critical}}$ .

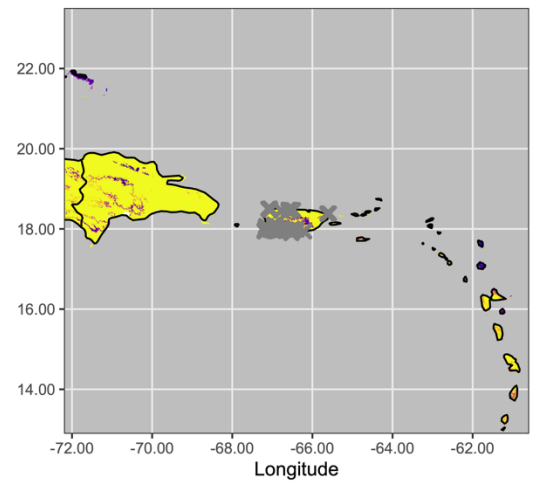
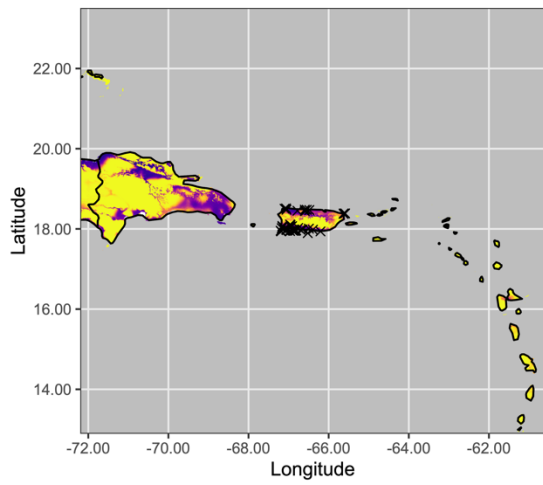
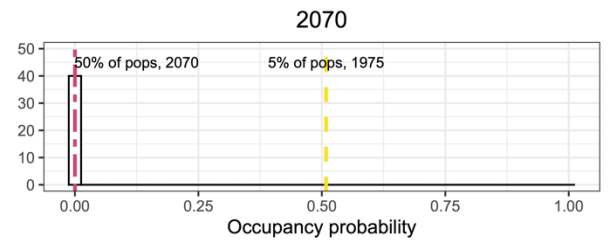
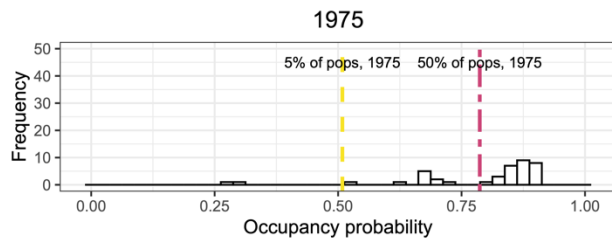


Table 3.3. P-values for Tukey multiple comparisons of means for  $T_{\text{pref}}$ .

Table 3.4. P-values for Tukey multiple comparisons of means for  $CT_{\text{min}}$  and  $CT_{\text{max}}$ .

Table 3.5. AIC values for Gaussian, quadratic, cubic, and Kumarswamy thermal performance curve (TPC) model fits.

	<i>G. albogularis</i>	<i>G. humeralis</i>	<i>S. argus</i>	<i>S. elegans</i>	<i>S. macrolepis</i>	<i>S. nicholsi</i>
<i>C. amazonicus</i>	<0.0001	<0.0001	<0.0001	<0.0001	0.80	<0.0001
<i>G. albogularis</i>		<0.0001	<0.0001	0.05	<0.0001	0.0008
<i>G. humeralis</i>			0.029	0.0008	0.60	<0.0001
<i>S. argus</i>				0.74	0.0044	0.20
<i>S. elegans</i>					0.0001	1.00
<i>S. macrolepis</i>						<0.0001

P (T<sub>pref</sub>)

	<i>C. amazonicus</i>	<i>G. humeralis</i>	<i>S. macrolepis</i>	<i>S. nicholsi</i>
<i>C. amazonicus</i>		0.060	0.79	1.00
<i>G. humeralis</i>	0.59		0.060	0.41
<i>S. macrolepis</i>	0.41	0.90		0.85
<i>S. nicholsi</i>	0.0006	0.0077	0.12	

P (CT<sub>min</sub>)

P (CT<sub>max</sub>)

TPC model	<i>C. amazonicus</i>	<i>G. humeralis</i>	<i>S. macodactylus</i>	<i>S. nicholsi</i>	generalized
Guassian	2313.98	3302.24	1456.63	1283.55	8965.99
quadratic	2321.17	3257.99	1429.78	1260.15	8971.63
cubic	2297.86	3256.50	1424.06	1256.01	8973.36
Kumaraswamy	2297.80	3227.93	1420.67	1242.85	8951.22

Table 3.6. Coefficients for Kumaraswamy thermal performance curve (TPC) model (Eqn. 3.1), and downscaled Worldclim  $h_a$ ,  $h_r$ , and quadratic  $\overline{TPC}_m$  model fits (Eqns. 3.7, 3.8, 3.9).

Species	Kumaraswamy curve			$h_{a,m}$				$h_{r,m}$				$\overline{TPC}_m$					
	<i>a</i>	<i>b</i>	<i>c</i>	$\tau_{a,1}$	$\tau_{a,2}$	$\tau_{a,3}$	$\tau_{a,4}$	$\tau_{r,1}$	$\tau_{r,2}$	$\tau_{r,3}$	$\tau_{r,4}$	<i>u</i>	<i>v</i>	<i>w</i>	<i>x</i>	<i>y</i>	<i>z</i>
<i>C. amazonicus</i>	2.278	1.712	261.3	24	0.8686	3.610	31.28	24	-1.040	0.0104	-6.714	3905.	212.3	-206.4	18.14	-22.86	-20.48
<i>G. albogularis</i>	2.549	3.803	160.8	24	0.5542	0.9936	5.814	24	0.5542	0.9936	5.8139	4086.	139.9	-77.72	-18.35	38.24	-47.59
<i>G. humeralis</i>	1.357	1.355	127.2	24	193.4	8.005	92.98	24	-0.1461	0.3811	-0.0166	4123.	-47.60	-4.497	-8.275	-1.806	-0.4232
<i>S. argus</i>	2.549	3.803	160.8	24	6.778	1.289	8.083	24	932.8	0.3283	5.182	3716.	-33.47	-158.75	-139.0	-102.3	157.0
<i>S. elegans</i>	2.549	3.803	160.8	24	108251.	5.468	73.05	24	3.346	0.0990	1.101	7385.	-87.39	126.6	7.147	96.70	-47.53
<i>S. macrolepis</i>	1.833	1.743	356.6	24	0.0809	1.509	4.105	24	0.4432	0.2224	0.1507	12680.	-98.74	-2.918	-237.5	-342.4	480.9
<i>S. nicholsi</i>	1.532	1.300	275.3	24	4.836	2.355	13.06	24	-0.1645	0.0838	-0.0947	42965.	-1100.	1946.	-333.9	-711.1	1180.

Table 3.7. Yearly average thermal physiological parameters across all occurrence sites for predicted persistent populations (white column background) and extirpated populations (grey column background).

	<i>C. amazonicus</i>		<i>G. albogularis</i>		<i>G. humeralis</i>		<i>S. argus</i>		<i>S. elegans</i>		<i>S. macrolepis</i>		<i>S. nicholsi</i>	
	# Pops.	143	1	296	1	351	8	10	19	132	1	8	73	40
1970-2000	Avg. Precip (cm)	18.2	26.0	15.3	17.0	18.5	21.6	9.2	11.1	11.9	17.0	16.6	15.4	9.9
	T <sub>Min</sub>	21.5	17.9	21.0	10.6	21.3	17.4	21.4	20.6	20.0	10.6	17.6	20.5	20.5
	T <sub>Max</sub>	31.2	28.0	31.0	22.7	31.1	28.0	28.3	29.7	29.6	22.7	27.7	30.0	31.0
	Avg. h <sub>a</sub>	23.5	18.3	21.9	5.1	23.2	18.1	21.0	19.2	20.2	9.9	15.7	22.7	21.2
	Avg. h <sub>r</sub>	14.8	11.4	20.4	5.7	9.1	2.9	6.8	7.4	6.6	4.0	6.8	10.8	4.8
2070	Avg. Precip	14.8	25.0	15.0	13.0	16.2	23.9	8.7	9.7	10.2	13.0	12.6	11.5	7.6
	Δ Avg. Precip	-3.3	-1.0	-0.4	-4.0	-2.2	2.3	-0.5	-1.3	-1.6	-4.0	-4.0	-3.9	-2.3
	T <sub>Min</sub>	26.1	22.4	24.2	13.6	25.5	21.1	24.1	23.4	22.8	13.6	20.2	23.1	23.1
	T <sub>Max</sub>	36.0	32.7	34.2	25.6	35.5	31.7	31.0	32.4	32.4	25.6	30.3	32.6	33.6
	Avg. h <sub>a</sub>	24.0	24.0	23.5	8.4	24.0	22.1	23.4	23.3	23.2	12.4	23.2	23.9	23.9
	Δ Avg. h <sub>a</sub>	0.5	5.7	1.6	3.3	0.8	4.0	2.5	4.0	3.1	2.5	7.5	1.2	2.7
	Avg. h <sub>r</sub>	16.7	15.5	23.1	9.2	19.5	11.2	8.1	8.8	8.0	4.9	11.3	15.1	6.6
	Δ Avg. h <sub>r</sub>	1.9	4.2	2.8	3.5	10.4	8.3	1.3	1.4	1.3	1.0	4.5	4.2	1.9
Δ Avg. h <sub>a-hr</sub>	-1.3	1.5	-0.7	-0.2	-9.7	-4.2	1.2	2.6	1.8	1.5	3.0	-1.4	0.8	

## Citations

- Allen, K. E., and R. Powell. 2014. Thermal biology and microhabitat use in Puerto Rican eyespot geckos (*Sphaerodactylus macrolepis macrolepis*). *Herpetological Conservation and Biology* 9:590–600.
- Altamirano-Benavides, M. A., S. F. Domínguez-Guerrero, F. J. Muñoz-Nolasco, D. M. Arenas-Moreno, R. Santos-Bibiano, R. G. T. Pérez, L. E. Lozano-Aguilar, et al. 2019. Thermal ecology and extinction risk due to climate change of *Gonatodes concinnatus* (Squamata: Sphaerodactylidae), an endemic lizard from western Amazonia. *Revista Mexicana de Biodiversidad* 90.
- Álvarez-Pérez, H. J. 1992. *Thermal characteristics of Sphaerodactylus species in Puerto Rico and their implications for the distribution of species in Puerto Rico*. San Juan, PR: University of Puerto Rico.
- Anav, A., P. Friedlingstein, M. Kidston, L. Bopp, P. Ciais, P. Cox, C. Jones, et al. 2013. Evaluating the land and ocean components of the global carbon cycle in the CMIP5 earth system models. *Journal of Climate* 26:6801–6843.
- Angilletta, M. 2009. *Thermal adaptation: a theoretical and empirical synthesis*. Oxford University Press, Oxford, England.
- Angilletta, M. J. 2006. Estimating and comparing thermal performance curves. *Journal of Thermal Biology* 31:541–545.
- Angilletta, M. J., P. H. Niewiarowski, and C. A. Navas. 2002. The evolution of thermal physiology in ectotherms. *Journal of Thermal Biology* 27:249–268 Invited.
- Avila-Pires, T. C. S. de. 1995. *Lizards of Brazilian Amazonia*. Zoologische Verhandelingen (Vol. 299).
- Barbet-Massin, M., F. Jiguet, C. H. Albert, and W. Thuiller. 2012. Selecting pseudo-absences for species distribution models: How, where and how many? *Methods in Ecology and Evolution* 3:327–338.
- Battisti, David. S., and R. L. Naylor. 2009. Historical warnings of future food insecurity with unprecedented seasonal heat. *Science* 323:240–244.
- Bellard, C., C. Bertelsmeier, P. Leadley, W. Thuiller, and F. Courchamp. 2012. Impacts of climate change on the future of biodiversity. *Ecology Letters* 15:365–377.
- Bennett, A. F. 1980. The thermal dependence of lizard behaviour. *Animal Behaviour* 28:752–762.

- Brusch, G. A., E. N. Taylor, and S. M. Whitfield. 2016. Turn up the heat: thermal tolerances of lizards at La Selva, Costa Rica. *Oecologia* 180:325–334.
- Caetano, G. H. O., J. C. Santos, L. B. Godinho, V. H. G. L. Cavalcante, L. M. Diele-Viegas, P. H. Campelo, L. F. Martins, et al. 2020. Time of activity is a better predictor of the distribution of a tropical lizard than pure environmental temperatures. *Oikos* 1–11.
- Caetano, G., J. Santos, and B. Sinervo. 2019. Mapeamento: Process-Based Biogeographical Analysis. R package.
- Carvalho, E. A. R., A. P. Lima, W. E. Magnusson, and A. L. K. M. Albernaz. 2008. Long-term effect of forest fragmentation on the Amazonian gekkonid lizards, *Coleodactylus amazonicus* and *Gonatodes humeralis*. *Austral Ecology* 33:723–729.
- Clusella-Trullas, S., and S. L. Chown. 2014. Lizard thermal trait variation at multiple scales: A review. *Journal of Comparative Physiology B: Biochemical, Systemic, and Environmental Physiology* 184:5–21.
- da Cunha, O. R., F. P. do Nascimento, and T. C. S. Ávila-Pires. 1985. Os reptéis da área de Carajás, Pará, Brasil (testudines e Squamata). I. Publicações Avulsas do Museu Paraense Emilio Goeldi, Belém 40:9–92.
- Deutsch, C. A., J. J. Tewksbury, R. B. Huey, K. S. Sheldon, C. K. Ghalambor, D. C. Haak, and P. R. Martin. 2008. Impacts of climate warming on terrestrial ectotherms across latitude. *Proceedings of the National Academy of Sciences of the United States of America* 105:6668–6672.
- Diele-Viegas, L. M., L. J. Vitt, B. Sinervo, G. R. Colli, F. P. Werneck, D. B. Miles, W. E. Magnusson, et al. 2018. Thermal physiology of Amazonian lizards (Reptilia: Squamata). *PLoS ONE* 13:1–23.
- Dominguez-Lopez, M. E., F. P. Kacoliris, and A. M. Ortega-Leon. 2015. Effects of microhabitat temperature on escape behavior in the diurnal gecko, *Gonatodes albogularis* (DUMERIL & BRIBON, 1836). *Herpetozoa* 28:49–54.
- Dunson, W. A., and C. R. Bramham. 1981. Evaporative water loss and oxygen consumption of three small lizards from the Florida Keys: *Sphaerodactylus cinereus*, *S. notatus*, and *Anolis sagrei*. *Physiological Zoology* 54:253–259.
- Etterson, J. R., and R. G. Shaw. 2001. Constraint to adaptive evolution in response to global warming. *Science* 294:151–154.

- Fick, S. E., and R. J. Hijmans. 2017. WorldClim 2: new 1-km spatial resolution climate surfaces for global land areas. *International Journal of Climatology* 37:4302–4315.
- Foley, J. A., G. P. Asner, M. H. Costa, M. T. Coe, R. DeFries, H. K. Gibbs, E. A. Howard, et al. 2007. Amazonia revealed: Forest degradation and loss of ecosystem goods and services in the Amazon Basin. *Frontiers in Ecology and the Environment* 5:25–32.
- Gamble, T., A. M. Simons, G. R. Colli, and L. J. Vitt. 2008. Tertiary climate change and the diversification of the Amazonian gecko genus *Gonatodes* (Sphaerodactylidae, Squamata). *Molecular Phylogenetics and Evolution* 46:269–277.
- Gaston, K. J., P. H. Williams, P. Eggleton, and C. J. Humphries. 1995. Large scale patterns of biodiversity: Spatial variation in family richness. *Proceedings of the Royal Society B: Biological Sciences* 260:149–154.
- Ghalambor, C. K., R. B. Huey, P. R. Martin, J. J. Tewksbury, and G. Wang. 2006. Are mountain passes higher in the tropics? Janzen’s hypothesis revisited. *Integrative and Comparative Biology* 46:5–17.
- Heatwole, H. 1966. Factors affecting orientation and habitat selection in some geckos. *Zeitschrift für Tierpsychologie* 23:303–314.
- Herrando-Pérez, S., F. Ferri-Yáñez, C. Monasterio, W. Beukema, V. Gomes, J. Belliure, S. L. Chown, et al. 2019. Intraspecific variation in lizard heat tolerance alters estimates of climate impact. *Journal of Animal Ecology* 88:247–257.
- Hoogmoed, M. S., and T. C. S. de Avila-Pires. 1989. Observations on the nocturnal activity of lizards in a marshy area in Serra do Navio, Brazil. *Tropical Zoology* 2:165–173.
- Huey, R. B. 1982. Temperature, physiology, and the ecology of reptiles. *Biology of the Reptilia* 12:25–91.
- Huey, R. B., C. A. Deutsch, J. J. Tewksbury, L. J. Vitt, P. E. Hertz, H. J. Á. Pérez, and T. Garland. 2009. Why tropical forest lizards are vulnerable to climate warming. *Proceedings of the Royal Society B: Biological Sciences* 276:1939–1948.
- Huey, R. B., and J. G. Kingsolver. 1989. Evolution of thermal sensitivity of ectotherm performance. *Trends in Ecology and Evolution* 4:131–135.
- Huey, R. B., and J. G. Kingsolver. 1993. Evolution of resistance to high temperature in ectotherms. *American Naturalist* 142.

- Janzen, D. H. 1967. Why mountain passes are higher in the tropics. *The American Naturalist* 101:233–249.
- Kearney, M. R., A. P. Isaac, and W. P. Porter. 2014. microclim: Global estimates of hourly microclimate based on long-term monthly climate averages. *Scientific Data* 1:1–9.
- Kearney, M., R. Shine, and W. P. Porter. 2009. The potential for behavioral thermoregulation to buffer “cold-blooded” animals against climate warming. *Proceedings of the National Academy of Sciences of the United States of America* 106:3835–3840.
- Kearney, R. M. 2013. Activity restriction and the mechanistic basis for extinctions under climate warming. *Ecology Letters* 16:1470–1479.
- Kirchhof, S., R. S. Hetem, H. M. Lease, D. B. Miles, D. Mitchel, J. McUller, M. O. Rcodei, et al. 2017. Thermoregulatory behavior and high thermal preference buffer impact of climate change in a Namib Desert lizard. *Ecosphere* 8.
- Kirtman, B., and S. B. Power. 2020. Near-term Climate Change: Projections and Predictability. Pages 953–1028 *in* Climate Change 2013: The Physical Science Basis. The Intergovernmental Panel on Climate Change.
- Krysko, K. L., and C. M. Sheehy. 2005. Ecological status of the ocellated gecko, *Sphaerodactylus argus argus* Gosse 1850, in Florida, with additional herpetological notes from the Florida Keys. *Caribbean Journal of Science* 41:169–172.
- Laurance, W. F., D. Carolina Useche, L. P. Shoo, S. K. Herzog, M. Kessler, F. Escobar, G. Brehm, et al. 2011. Global warming, elevational ranges and the vulnerability of tropical biota. *Biological Conservation* 144:548–557.
- Leclair Jr., R. 1978. Water loss and microhabitats in three sympatric species of lizards (Reptilia, Lacertilia) from Martinique, West Indies. *Journal of Herpetology* 12:177–182.
- Luna, S., and E. Font. 2013. Use of an infrared thermographic camera to measure field body temperatures of small lacertid lizards. *Herpetological Review* 44:59–62.
- MacLean, W. P. 1985. Water-loss rates of *Sphaerodactylus parthenopion* (Reptilia: Gekkonidae), the smallest amniote vertebrate. *Comparative Biochemistry and Physiology -- Part A: Physiology* 82:759–761.
- Malhi, Y., J. T. Roberts, R. A. Betts, T. J. Killeen, W. Li, and C. A. Nobre. 2008. Climate change, deforestation, and the fate of the Amazon. *Science* 319:169–172.

- Martin, T. L., and R. B. Huey. 2008. Why “suboptimal” is optimal: Jensen’s inequality and ectotherm thermal preferences. *American Naturalist* 171:102–118.
- Meiri, S. 2008. Evolution and ecology of lizard body sizes. *Global Ecology and Biogeography* 17:724–734.
- Miranda, J. P., A. Ricci-Lobão, and C. F. D. Rocha. 2010. Influence of structural habitat use on the thermal ecology of *Gonatodes humeralis* (Squamata: Gekkonidae) from a transitional forest in Maranhão, Brazil. *Zoologia* 27:35–39.
- Myers, N., R. A. Mittermeyer, C. G. Mittermeyer, G. A. B. da Fonseca, and J. Kent. 2000. Biodiversity hotspots for conservation priorities. *Nature* 403:853–858.
- Nava, S. S. 2004. *Microhabitat selection, resource partitioning, and evaporative water loss by dwarf geckos, (Sphaerodactylus), on Puerto Rico.*
- New, M., D. Lister, M. Hulme, and I. Makin. 2002. A high-resolution data set of surface climate over global land areas. *Climate Research* 21:1–25.
- Paradis, E., and K. Schliep. 2019. Ape 5.0: An environment for modern phylogenetics and evolutionary analyses in R. *Bioinformatics* 35:526–528.
- Paranjpe, D. A., R. D. Cooper, A. Patten, and B. Sinervo. 2012. Measuring thermal profile of reptiles in laboratory and field. *Proceedings of Measuring Behaviour* 2012:460–462.
- Parmesan, C. 2006. Ecological and evolutionary responses to recent climate change. *Annual Review of Ecology, Evolution, and Systematics* 37:637–669.
- Pinsky, M. L., A. M. Eikeset, D. J. McCauley, J. L. Payne, and J. M. Sunday. 2019. Greater vulnerability to warming of marine versus terrestrial ectotherms. *Nature*.
- Pinto, B. J., G. R. Colli, T. E. Higham, A. P. Russell, D. P. Scantlebury, L. J. Vitt, and T. Gamble. 2019. Population genetic structure and species delimitation of a widespread, Neotropical dwarf gecko. *Molecular Phylogenetics and Evolution* 133:54–66.
- Powell, R. 1999. Herpetology of Navassa Island, West Indies R. *Caribbean Journal of Science* 35:1–13.
- Prevedello, J. A., G. R. Winck, M. M. Weber, E. Nichols, and B. Sinervo. 2019. Impacts of forestation and deforestation on local temperature across the globe. *PLoS ONE* 14:1–18.
- Rivero, J. A. 2006. *Guiá para la identificación de lagartos y culebras de Puerto Rico.* La Editorial Universidad de Puerto Rico, San Juan, Puerto Rico.

- Rivero-Blanco, C., and J. R. Dixon. 1979. *The neotropical lizard genus Gonatodes Fitzinger (Sauria: Sphaerodactylidae)*.
- Schargel, W. E. 2008. *Species limits and phylogenetic systematics of the genus Gonatodes (Squamata: Sphaerodactylidae)*.
- Sears, M. W., M. J. Angilletta, M. S. Schuler, J. Borchert, K. F. Dilliplane, M. Stegman, T. W. Rusch, et al. 2016. Configuration of the thermal landscape determines thermoregulatory performance of ectotherms. *Proceedings of the National Academy of Sciences of the United States of America* 113:10595–10600.
- Sears, M. W., E. Raskin, and M. J. Angilletta. 2011. The world is not flat: Defining relevant thermal landscapes in the context of climate change. *Integrative and Comparative Biology* 51:666–675.
- Sekercioglu, C. H., S. H. Schneider, J. P. Fay, and S. R. Loarie. 2008. Climate change, elevational range shifts, and bird extinctions. *Conservation Biology* 22:140–150.
- Sinervo, B., R. Bertrand, E. Darnet, H. le Chevalier, A. Trochet, A. Dupoué, J. Souchet, et al. 2019. *Ecophysiological Species Distribution Models for Pyrenean Ectotherms under Climate Change*. Moulis, France.
- Sinervo, B., F. Méndez-de-la-Cruz, D. B. Miles, B. Heulin, E. Bastiaans, M. V. S. Cruz, R. Lara-Resendiz, et al. 2010. Erosion of lizard diversity by climate change and altered thermal niches. *Science* 328:894–899.
- Sinervo, B., D. B. Miles, W. U. Yayong, F. R. Méndez-De La Cruz, S. Kirchhof, and Q. I. Yin. 2018. Climate change, thermal niches, extinction risk and maternal-effect rescue of toad-headed lizards, *Phrynocephalus*, in thermal extremes of the Arabian Peninsula to the Qinghai-Tibetan Plateau. *Integrative Zoology* 13:450–470.
- Snyder, G. K. 1975. Respiratory metabolism and evaporative water loss in a small tropical lizard. *Journal of Comparative Physiology B* 104:13–18.
- Sunday, J., J. M. Bennett, P. Calosi, S. Clusella-Trullas, S. Gravel, A. L. Hargreaves, F. P. Leiva, et al. 2019. Thermal tolerance patterns across latitude and elevation. *Philosophical Transactions of the Royal Society B: Biological Sciences* 374.
- Sunday, J. M., A. E. Bates, and N. K. Dulvy. 2011. Global analysis of thermal tolerance and latitude in ectotherms. *Proceedings of the Royal Society B: Biological Sciences* 278:1823–1830.

- Sunday, J. M., A. E. Bates, M. R. Kearney, R. K. Colwell, N. K. Dulvy, J. T. Longino, and R. B. Huey. 2014. Thermal-safety margins and the necessity of thermoregulatory behavior across latitude and elevation. *Proceedings of the National Academy of Sciences of the United States of America* 111:5610–5615.
- Tewksbury, J. J., R. B. Huey, and C. A. Deutsch. 2008. Ecology: Putting the heat on tropical animals. *Science* 320:1296–1297.
- Thomas, C. D., A. Cameron, R. E. Green, M. Bakkenes, L. J. Beaumont, Y. C. Collingham, B. F. N. Erasmus, et al. 2004. Extinction risk from climate change. *Nature* 427:145–148.
- Thomas, R., S. B. Hedges, and O. Garrido. 1998. A New Gecko (*Sphaerodactylus*) from the Sierra Maestra of Cuba. *Journal of Herpetology* 32:66–69.
- Thuiller, W., D. Georges, R. Engler, and F. Breiner. 2020. biomod2: Ensemble Platform for Species Distribution Modeling. R package.
- Thuiller, W., B. Lafourcade, R. Engler, and M. B. Araújo. 2009. BIOMOD - A platform for ensemble forecasting of species distributions. *Ecography* 32:369–373.
- van Berkum, F. H. . 1988. Latitudinal patterns of the thermal sensitivity of sprint speed in lizards. *The American Naturalist* 132:327–343.
- Vitt, L. J., S. S. Sartorius, T. C. S. Avila-Pires, P. A. Zani, and M. C. Espósito. 2005. Small in a big world: ecology of leaf-litter geckos in New World tropical forests. *Herpetological Monographs* 19:137.
- Vitt, L. J., R. A. Souza, S. S. Sartorius, T. C. S. Avila-pires, M. C. Espósito, and M. Cristina. 2000. Comparative ecology of sympatric *Gonatodes* (Squamata: Gekkonidae) in the western Amazon of Brazil. *Copeia* 2000:83–95.
- Vitt, L. J., P. A. Zani, A. A. M. de Barros, and A. A. M. de Barros. 1997. Ecological variation among populations of the Gekkonid lizard *Gonatodes humeralis* in the Amazon basin. *Copeia* 1997:32.
- Vitt, L., C. Teresa, S. Avila-Pires, J. P. Caldwell, and V. R. L. Oliveira. 1998. The impact of individual tree harvesting on thermal environments of lizards in Amazonian rain forest. *Conservation Biology* 12:654–664.
- Zheng, Y., and J. J. Wiens. 2016. Combining phylogenomic and supermatrix approaches, and a time-calibrated phylogeny for squamate reptiles (lizards and snakes) based on 52 genes and 4162 species. *Molecular Phylogenetics and Evolution* 94:537–547.

Zuk, M. 2016. Temperate assumptions: How where we work influences how we think. *The American naturalist* 188:S1–S7.

## GENERAL SYNTHESIS

The three chapters of this thesis describe the persistence of biological variation under selective pressure at different ecological and evolutionary scales. In **Chapter 2**, plastic polyphenisms arose from a single genotype; in **Chapter 1**, variation was genetically fixed and could reflect polymorphisms within a species or difference between species; and in **Chapter 3**, ecophysiology and habitat differed across species. These studies collectively identify and evaluate major forces that stabilize systems of competitors: intransitivity, apostasis, fluctuating environmental conditions, climate.

Although competitive intransitivity (cyclical hierarchy of competitors) and apostasis (rare advantage or negative frequency-dependence) both contribute to stability in competitive systems, neither is essential nor sufficient for stability. Many biological studies focus on these factors, particularly intransitivity, as the basis of stability (Laird and Schamp 2009; Allesina and Levine 2011). In **Chapter 1**, I showed that apostasis is not necessary in stable competitive systems, but that these systems can in fact support a small degree of anti-apostasis (advantage when common). This is important as many alternative strategies include a cooperative morph, which would experience a fitness advantage at high frequencies (Sinervo and Calsbeek 2006; Friedman and Sinervo 2016). I also showed that models that assume that intransitivity is necessary for stability underestimate the capacity for stability, particularly larger, even-numbered systems of competitors (Allesina and Levine

2011). Systems of alternative strategies that are not intransitive (Shuster and Wade 1991; Sinervo and Calsbeek 2006) and lack apostasis (Cameron et al. 2009; Friedman and Sinervo 2016) exist in nature. Notably, *Scaphiopus multiplicata*'s omnivore and carnivore morphs, explored in **Chapter 2**, are not strictly under intransitive or apostatic conditions, as both are maintained under varying resource abundance, resulting in a range of values describing competitive interactions.

Environmental variation also plays a large role in the maintenance of biological variation. In **Chapter 2**, I showed that *S. multiplicata*'s polyphenisms are maintained by environmental variation, and that the environmental conditions leading to differential morph survivorship are likely to shift under climate change projections. However, further studies are needed to describe the relative strength of biotic and abiotic factors on morph selection. In **Chapter 3**, I described how extinction risk in sphaerodactyline geckos varies under future climate predictions. Although many of the species included in this had similar thermal ecological traits, predictions of their persistence differed greatly. The capacity to withstand climatic changes is not purely a function of an organism' biology, but also of where it occurs.

Sphaerodactyline geckos present a potentially rich model system for studying alternative strategies. Many species have multiple male morphs, particularly in the genus *Gonatodes*. Sphaerodactyline species may have two recognized male morphs (Quesnel 1957; Rivero-Blanco and Dixon 1979; Regalado 2003; Cole and Kok 2006; Schargel 2008; Sturaro and Avila-Pires 2013), or three male morphs (Rivero-Blanco and Dixon 1979). *Gonatodes rozei* is highly unusual as it has four male morphs

(Rivero-Blanco and Schargel 2012), which could make it one of the largest known systems of alternative strategies. This species is particularly interesting, as four-strategy systems have never been explicitly studied in an ecological context, and there has been speculation that they should be less stable than three or five-strategy systems (Allesina and Levine 2011). Unfortunately, none of these species were easily accessible to study alternative male reproductive strategies during my PhD work, however they present a new potentially rich study system for alternative strategies.

All of the models in this thesis can be extended to also encompass species interactions. The game theory framework in **Chapter 1** can be extended to the web of species interactions that comprise an ecosystem. An interesting question which arises from this chapter is whether ecosystems are stabilized by weak interactions among subsets of organisms, which are in turn stabilized by stronger interactions in species “blocks,” similar to faces of larger systems of strategies. Future work could apply the game theory model in **Chapter 2** to sympatric congeners of *S. multiplicata* which have similar polyphenisms. Combining models for morph determination of multiple toad species can illustrate how trait displacement occurs under multi-species competition. Furthermore, with more empirical studies, it is possible to more fully describe morph determination and morph fitness to model the selective mechanisms acting on plasticity in this system. Finally, though ecophysiological traits are largely phylogenetically conserved (Huey and Kingsolver 1989), variation in thermal properties among parapatric congeners can result in competitive exclusion of one species (Sinervo et al. 2010). The ecophysiological model in **Chapter 3** can be

extended to include the possibility of range shifts and competitive exclusion of species. This is particularly relevant for island species that have limited potential to migrate to cooler habitats.

These studies highlight the importance of incorporating empirical data in modeling. More empirical studies and experimental manipulations are needed to understand the mechanisms that maintain complex systems of interactions, such as species interactions (Schluter 1994; Sinervo and Basolo 1996). These models and their potential extensions are important to expanding the scale at which we apply models in ecology. Given the rapid changes to climate and habitat availability driven by human expansion, ecosystem resilience to perturbation is of particular concern. We need tools to predict how species losses will affect eventual equilibrium outcomes – whether ecosystems will survive in a recognizable state, or whether the loss of key species can affect larger-scale stability.

## ADDITIONAL CITATIONS

- Allesina, S., and J. M. Levine. 2011. A competitive network theory of species diversity. *Proceedings of the National Academy of Sciences of the United States of America* 108:5638–5642.
- Bourne, G. R., F. Breden, and T. C. Allen. 2003. Females prefer carotenoid colored males as mates in the pentamorphic livebearing fish, *Poecilia parae*. *Naturwissenschaften* 90:402–405.
- Brown, J. H., J. F. Gillooly, A. P. Allen, V. M. Savage, and G. B. West. 2004. Toward a metabolic theory of ecology. *Ecology* 85:1771–1789.
- Cameron, D. D., A. White, and J. Antonovics. 2009. Parasite-grass-forb interactions and rock-paper-scissor dynamics: Predicting the effects of the parasitic plant *Rhinanthus minor* on host plant communities. *Journal of Ecology* 97:1311–1319.
- Cole, C. J., and P. J. R. Kok. 2006. A new species of gekkonid lizard (Sphaerodactylinae: Gonatodes) from Guyana, South America. *American Museum Novitates* 3524:1.
- Darwin, C., and A. Wallace. 1858. On The Tendency of Species to Form Varieties. *London Society* 1–8.
- Friedman, D., and B. Sinervo. 2016. Evolutionary Games in Natural, Social, and Virtual Worlds. *Evolutionary Games in Natural, Social, and Virtual Worlds*.
- Huey, R. B., C. A. Deutsch, J. J. Tewksbury, L. J. Vitt, P. E. Hertz, H. J. Á. Pérez, and T. Garland. 2009. Why tropical forest lizards are vulnerable to climate warming. *Proceedings of the Royal Society B: Biological Sciences* 276:1939–1948.
- Huey, R. B., and J. G. Kingsolver. 1989. Evolution of thermal sensitivity of ectotherm performance. *Trends in Ecology and Evolution* 4:131–135.
- Laird, R. A., and B. S. Schamp. 2009. Species coexistence, intransitivity, and topological variation in competitive tournaments. *Journal of Theoretical Biology* 256:90–95.
- May, R. M. 1972. Will a large complex system be stable? *Nature* 238:413–414.
- McCann, K. S. 2000. The diversity–stability debate. *Nature* 405:228–233.
- Parmesan, C. 2006. Ecological and evolutionary responses to recent climate change. *Annual Review of Ecology, Evolution, and Systematics* 37:637–669.

- Pielou, E. C. 1981. The usefulness of ecological models: A stock-taking. *The Quarterly Review of Biology* 56:17–31.
- Pinsky, M. L., A. M. Eikeset, D. J. McCauley, J. L. Payne, and J. M. Sunday. 2019. Greater vulnerability to warming of marine versus terrestrial ectotherms. *Nature*.
- Quesnel, V. C. 1957. Life history of the Streak Lizard, *Gonatodes vittatus*. *Living World, Journal of the Trinidad and Tobago Field Naturalists' Club* 5–14.
- Regalado, R. 2003. Social behavior and sex recognition in the Puerto Rican dwarf gecko *Sphaerodactylus nicholsi*. *Caribbean Journal of Science* 39:77–93.
- Rivero-Blanco, C., and J. R. Dixon. 1979. *The neotropical lizard genus Gonatodes Fitzinger (Sauria: Sphaerodactylidae)*.
- Rivero-Blanco, C., and W. E. Schargel. 2012. A strikingly polychromatic new species of *Gonatodes* (Squamata: Sphaerodactylidae) from northern Venezuela. *Zootaxa* 66–78.
- Schargel, W. E. 2008. *Species limits and phylogenetic systematics of the genus Gonatodes (Squamata: Sphaerodactylidae)*.
- Schluter, D. 1994. Experimental evidence that competition promotes divergence in adaptive radiation. *Science* 266:798–801.
- Shuster, S. M., and M. J. Wade. 1991. Equal mating success among male reproductive strategies in a marine isopod. *Nature* 350:608–610.
- Sinervo, B., and A. L. Basolo. 1996. Testing Adaptation Using Phenotypic Manipulations. Pages 149–185 *in* *Adaptation*. Academic Press.
- Sinervo, B., and R. Calsbeek. 2006. The developmental, physiological, neural, and genetical causes and consequences of frequency-dependent selection in the wild. *Annual Review of Ecology, Evolution, and Systematics* 37:581–610.
- Sinervo, B., F. Méndez-de-la-Cruz, D. B. Miles, B. Heulin, E. Bastiaans, M. V. S. Cruz, R. Lara-Resendiz, et al. 2010. Erosion of lizard diversity by climate change and altered thermal niches. *Science* 328:894–899.
- Sturaro, M. J., and T. C. S. Avila-Pires. 2013. Redescription of the gecko *Gonatodes caudiscutatus* (Günther, 1859) (Squamata: Sphaerodactylidae). *South American Journal of Herpetology* 8:132–145.
- Tewksbury, J. J., R. B. Huey, and C. A. Deutsch. 2008. Ecology: Putting the heat on tropical animals. *Science* 320:1296–1297.